

A Box Model Study of the Greenland Sea, Norwegian Sea, and Arctic Ocean

by

Daniel Y. Robitaille

**A Thesis submitted to
the Faculty of Graduate Studies and Research
in partial fulfilment of
the requirements of the degree of**

MASTER OF SCIENCE

**Department of Atmospheric and Oceanic Sciences
McGill University
Montréal, Québec**

Copyright (c) Daniel Robitaille, July 1993

Short version of the title:

A box model study of the Greenland Sea, Norwegian Sea and Arctic Ocean

PERMISSION REQUEST

We hereby grant you permission to reprint the material specified in your letter (see recto) for the purpose you have indicated therein, at no charge, provided that:

1. The material to be used has appeared in our publication without credit or acknowledgement to another source.

2. Suitable acknowledgement to the source is given as follows:

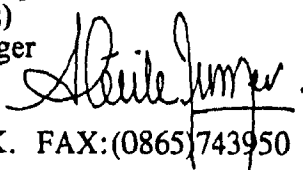
For Books: "Reprinted from (Author/Title), Copyright (Year), Pages No., with kind permission from Pergamon Press Ltd, Headington Hill Hall, Oxford OX3 0BW, UK"

For Journals: "Reprinted from Journal title, Volume number, Author(s), Title of article, Pages No., Copyright (Year), with kind permission from Pergamon Press Ltd, Headington Hill Hall, Oxford OX3 0BW, UK."

3. Reproduction of this material is confined to the purpose for which permission is hereby given.

For Future Permissions please contact:

Anne-Cecile Junger (Ms)
Subsidiary Rights Manager
Pergamon Press Ltd
Headington Hill Hall
Oxford OX3 0BW, U.K. FAX: (0865) 743950



This permission is granted from non-exclusive world **English** rights only. For other languages please reapply separately for each one required.

Abstract

A simple box model of a high-latitude two-layer ocean, first developed by Martinson *et al.*, 1981, is applied to four Arctic regions connected together: the Greenland Sea, the Norwegian Sea, the Arctic Ocean, and the Greenland Gyre. The latter, in fact, is a small convective region embedded in the northwest corner of the Norwegian Sea region. The model for each region consists of a thermodynamic ice layer that covers two layers of salty water which can, under specific conditions, become statically unstable and hence create a state of active overturning. The system is forced by monthly mean atmospheric temperatures in the four regions, as well as by continental runoffs and by inflows from adjacent oceans.

The model predicts the ice thickness, and the temperature and salinity of the water in the upper layer for the four regions. Also determined are the water temperature and salinity for the lower layer in the Arctic Ocean box. The convective state of any given region, i.e., whether it is in an active overturning mode or not, is also obtained continuously.

The different output variables of the model, which are the response to climatological forcing conditions, compare favourably with observed data. In this control run, the Arctic Ocean region is characterized by continuous ice cover, the Greenland Sea and Greenland Gyre have ice cover only during winter, and the Norwegian Sea region never forms an ice cover. Another feature of the model is the winter time occurrence of convective overturning in the upper 200 m in the Greenland Gyre region.

The model is also used for different anomaly experiments: a positive air temperature anomaly which represents a global warming of the earth, a negative salt anomaly in the Norwegian Sea which simulates the Great Salinity Anomaly of the 1960s and 1970s, and an increase in the ice flux through Fram Strait which parameterizes anomalous ice production in the Arctic.

Résumé

Un modèle en boîte simple à deux couches pour les latitudes nordiques, développé en premier lieu par Martinson *et al.*, 1981, est appliqué à quatre régions arctiques connectées ensemble: la mer du Groenland, la mer de Norvège, l'océan Arctique, et le courant giratoire du Groenland. Ce dernier est en fait une petite région de convection située au nord-ouest de la région de la mer de Norvège. Le modèle consiste pour chaque région en une couche de glace thermodynamique recouvrant deux couches d'eau salée qui peuvent, sous des conditions spécifiques, devenir instable et créer un état de renversement actif de l'eau. Le système est contrôlé par les températures atmosphériques mensuelles moyennes dans les quatre régions, ainsi que par le débit d'eau des continents et par le flot venant des océans adjacents.

Le modèle prédit l'épaisseur de la glace, la température et la salinité de l'eau dans la couche supérieure, et ce dans les quatre régions. La température et la salinité de l'eau pour la couche inférieure dans l'océan Arctique sont aussi déterminées. L'état de convection d'une région, i.e., si la région est ou n'est pas dans un état de renversement actif, est aussi obtenu continuellement.

Les variables de sortie du modèle, qui sont contrôlées par des conditions climatiques moyennes, se comparent favorablement avec les observations. Dans cette simulation de contrôle, l'océan Arctique est caractérisé par une couche de glace continue, la mer et le courant giratoire du Groenland ont une couche de glace en hiver seulement, et il n'y a jamais de glace dans la mer de Norvège. Un autre élément du modèle est la présence en hiver d'une région de renversement actif de l'eau dans le premier 200 m en profondeur dans la région du courant giratoire du Groenland.

Le modèle est aussi utilisé pour différentes expériences: une anomalie positive de la température de l'air qui représente un réchauffement global de la terre, une anomalie saline négative dans la mer de Norvège pour simuler la Grande Anomalie Saline des décennies 1960 et 1970, et une augmentation du flux de glace traversant le détroit de Fram pour simuler une production anormale de glace dans l'Arctique.

Acknowledgements

I would like to thank my supervisor Dr. Lawrence Mysak for his help, guidance, and financial support during the course of my thesis research. I would also like to thank Dr. Mark Darby for his help, ideas, and discussions during his stay at McGill, Dave Holland for some atmospheric data, Jean-François Gallant for helping me with some of the figures in this thesis, and lastly my parents, for constant moral and financial support throughout the course of my studies.

Figures 2.2, 3.6 and 3.7 are reprinted from: Deep-Sea Research, Vol. 37, No. 9, R.A. Clarke, J.H. Swift, J. L. Reid, and K.P. Koltermann, The Formation of Greenland Sea Deep-Water: Double Diffusion or Deep Convection?, pp. 1385-1424, Copyright (1990), with the kind permission from Pergamon Press Ltd, Headington Hill Hall, Oxford OX3 0BW, UK.

Table of Contents

Abstract.....	ii
Résumé.....	iii
Acknowledgements.....	iv
Table of Contents.....	v
List of Tables.....	vi
List of Figures.....	vii
1. Introduction.....	1
2. Description of the Model.....	5
2.1 Geographic regions included in the model.....	5
2.2 Overview of the model	10
2.3 The governing equations.....	32
3. First Experiment: The control run	43
3.1 Results in the four regions.	43
3.2 Scale Analysis of the different terms in the governing equations.	56
4. Anomaly Experiments	65
4.1 Effect of warmer temperatures in each region.	65
4.2 Great Salinity Anomaly Experiment.	73
4.3 Effect of more ice advection through Fram Strait.	78
5. Summary and Conclusions	85
Appendix	89
References	106

List of Tables

Table 2.1 Values of parameters used in the model for the links between the four regions and the rest of the world oceans	19
Table 2.2 Parameters used in the model	24
Table 2.3 Physical constants used in the model.....	27
Table 2.4 Heat and salt exchange coefficients used in the model.....	27
Table 3.1 Monthly mean air temperatures used in the model (in degrees Celsius).....	44
Table 3.2 Initial conditions used in the control run.....	44
Table 3.3 Numerical estimate of the terms for the Greenland Sea (State 2).....	57
Table 3.4 Numerical estimate of the terms for the Greenland Sea (State 4).....	58
Table 3.5 Numerical estimate of the terms for the Norwegian Sea (State 2).....	59
Table 3.6 Numerical estimate of the terms for the Arctic Ocean (State 4).....	61
Table 3.7 Numerical estimate of the terms for the Greenland Gyre (State 2).....	62
Table 3.8 Numerical estimate of the terms for the Greenland Gyre (State 3).....	62
Table 3.9 Numerical estimate of the terms for the Greenland Gyre (State 4).....	64

List of Figures

Fig. 1.1. Negative (or reversing) feedback loop linking northern Canadian river runoff, Arctic sea-ice extent, Greenland-Iceland Sea ice extent, and salinity, convection and cyclogenesis around Iceland. (from Mysak and Power, 1992).....	3
Fig. 2.1. Positions of the four boxes used in the model, where region 1 is the Greenland Sea, 2 is the Norwegian Sea, 3 is the Arctic Ocean, and 4 is the Greenland Gyre.	5
Fig. 2.2. Salinity in the upper 20 meters (From Clarke <i>et al.</i> , 1990). The 'X' marks the approximate location of the Greenland Gyre region in the model.	8
Fig. 2.3. Temperature and salinity sections across Fram Strait, at approximately 79°N (from Jónsson <i>et al.</i> , 1992).	9
Fig. 2.4. The four different states in which each region can find itself (adapted from Martinson <i>et al.</i> , 1981).....	10
Fig. 2.5. The links between the four regions in the model and the rest of the world oceans.	18
Fig. 2.6. A sketch of an east-west section of the upper layer of the Norwegian Sea and Greenland Gyre.	31
Fig. 3.1. Results from the control run for the Greenland Sea region.....	45
Fig. 3.2. Results from the control run for the Norwegian Sea region.....	46
Fig. 3.3. Results from the control for the Arctic Ocean region.	47
Fig. 3.4. Results from the control run for the Greenland Gyre region.....	48

Fig. 3.5. States for the four regions in the control run.....	51
Fig. 3.6. Potential temperature in the Norwegian and Greenland basins (from Clarke <i>et al.</i> , 1990).	54
Fig. 3.7. Salinity in the Norwegian and Greenland basins (from Clarke <i>et al.</i> , 1990).....	54
Fig. 4.1. Greenland Sea results for the temperature increase experiment.	68
Fig. 4.2. Norwegian Sea results for the temperature increase experiment.	69
Fig. 4.3. Arctic Ocean results for the temperature increase experiment.	70
Fig. 4.4. Greenland Gyre results for the temperature increase experiment.	71
Fig. 4.5. States of the system in the temperature increase experiment.....	72
Fig. 4.6. Salinity of the upper layer in the Norwegian Sea for the 0.25 salinity anomaly experiment.	74
Fig. 4.7. Results for the Greenland Gyre for the 0.25 salinity anomaly experiment.	75
Fig. 4.8. Salinity of the upper layer in the Norwegian Sea for the 0.6 salinity anomaly experiment.	76
Fig. 4.9. Results for the Greenland Gyre for the 0.6 salinity anomaly experiment.	77
Fig. 4.10. Results for the Arctic Ocean in the ice advection experiment.	80
Fig. 4.11. Results for the Greenland Sea in the ice advection experiment.	81
Fig. 4.12. Results for the Norwegian Sea in the ice advection experiment.	82
Fig. 4.13. Results for the Greenland Gyre in the ice advection experiment.	83

Fig. 4.14. States of the system for the ice advection experiment.....	84
Fig. A-1. Numerical estimate of the temperature terms in the Greenland Sea (State 2). ..	89
Fig. A-2. Numerical estimate of the salinity terms in the Greenland Sea (State 2).....	90
Fig. A-3. Numerical estimate of the temperature terms in the Greenland Sea (State 4). ..	91
Fig. A-4. Numerical estimate of the salinity terms in the Greenland Sea (State 4).....	92
Fig. A-5. Numerical estimate of the ice thickness terms in the Greenland Sea (State 4).....	93
Fig. A-6. Numerical estimate of the temperature terms in the Norwegian Sea (State 2).....	94
Fig. A-7. Numerical estimate of the salinity terms in the Norwegian Sea (State 2).	95
Fig. A-8. Numerical estimate of the temperature terms in the Arctic Ocean (State 4)... ..	96
Fig. A-9. Numerical estimate of the salinity terms in the Arctic Ocean (State 4).....	97
Fig. A-10. Numerical estimate of the ice thickness terms in the Arctic Ocean (State 4).....	98
Fig. A-11. Numerical estimate of the temperature terms in the Greenland Gyre (State 2).....	99
Fig. A-12. Numerical estimate of the salinity terms in the Greenland Gyre (State 2).....	99
Fig. A-13. Numerical estimate of the temperature terms in the Greenland Gyre (State 3).....	100
Fig. A-14. Numerical estimate of the salinity terms in the Greenland Gyre (State 3).....	101
Fig. A-15. Numerical estimate of the ice thickness terms in the Greenland Gyre (State 3).....	102

Fig. A-16. Numerical estimate of the temperature terms in the Greenland Gyre (State 4).....	103
Fig. A-17. Numerical estimate of the salinity terms in the Greenland Gyre (State 4).....	104
Fig. A-18. Numerical estimate of the ice thickness terms in the Greenland Gyre (State 4).....	105

1. Introduction

The Greenland and Norwegian Seas constitute a region of considerable climatic interest because of their location between the Arctic Ocean, a region of year-round sea-ice cover with relatively cold and fresh water, and the North Atlantic Ocean, a region of relatively warm and salty water. The Arctic and Atlantic Oceans have very different water properties, and if either of the two oceans undergoes a change in its characteristics, this variation will be transmitted to the other ocean through the Greenland and Norwegian Seas. One of the best known perturbations of this kind in recent years was the northern North Atlantic "Great Salinity Anomaly" or GSA (Dickson *et al.*, 1988). This anomaly manifested itself in the late 1960's and the beginning of the 1970's with the occurrence of fresher-than-normal water in the upper layer of the sea north of Iceland. It has been suggested that this salinity anomaly was related to variations in other climate components through a negative feedback loop (Mysak *et al.*, 1990), which implies the existence of an interdecadal Arctic climatic oscillation. Being part of a cycle, the Great Salinity Anomaly becomes only one episode in a continuous series of negative salinity anomalies, recurring every 15 to 20 years or so.

In Aagaard and Carmack (1989), we can find a very nice discussion of the processes occurring in the Greenland, Iceland, and Norwegian Seas (also referred as the GIN Sea). They describe the convective gyres of the Greenland and Iceland Seas as the major windows the surface has on the deep ocean in the GIN Sea region, and they are also the main paths used to transmit the properties at the surface to the subsurface. The paths of convection in these two gyre regions are maintained in part by a local precipitation excess and also by a lateral influx of freshwater from the East

Greenland Current. The authors also declare that the present-day Greenland and Iceland Seas are rather delicately poised with respect to their ability to sustain convection.

In this thesis a simple dynamical model of the upper layers of the Arctic Ocean and GIN Sea is developed and used to study, among other things, convection in latter region. The governing equations for this model are derived for seasonal and interannual time scales. The model consists of four boxes, with one of them representing the Greenland Gyre region. The model in each box is a variant of the Weddell Sea polynya model due to Martinson *et al.* (1981). Using physical considerations and observed data, we attempt to create a zone of shallow convection in the upper 200 m in the Greenland Gyre region. We shall also find that this zone of shallow convection will be related to other elements and events in the Arctic Climate system, such as the Great Salinity Anomaly. This small zone of convection near the surface will help us look at the parameters that influence the delicate balance described in Aagaard and Carmack (1989), at least in the depths range covered by this model.

The multi-box model, as defined in this thesis, has its limitations and, as with any model, can be seen as a simplification of reality. But this simplification has its appeal because the results of a simple box model can be interpreted more easily, and some processes can be identified more readily than in more complex (e.g., general circulation) models.

This model can also be used easily for some experiments, for example the propagation of the GSA from one region to another (section 4.2). Mysak and Power

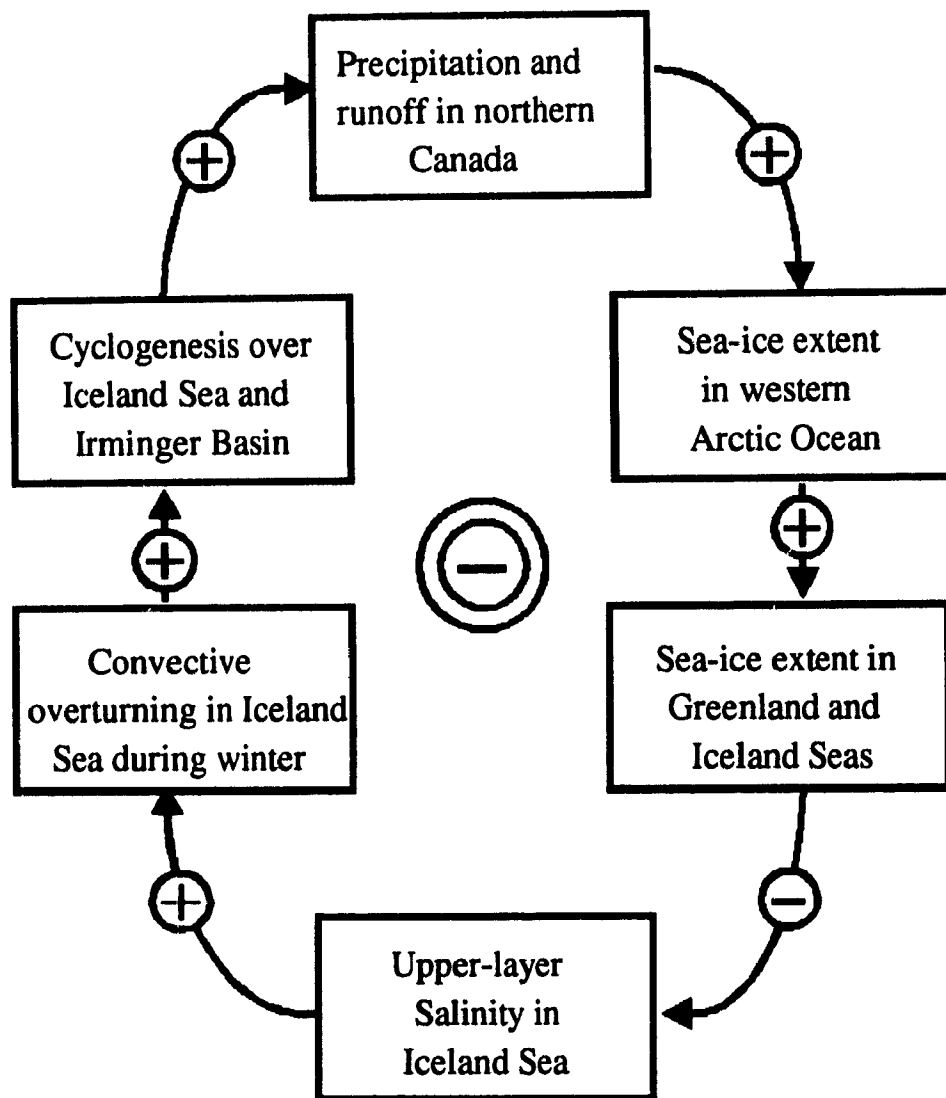


Fig. 1.1. Negative (or reversing) feedback loop linking northern Canadian river runoff, Arctic sea-ice extent, Greenland-Iceland Sea ice extent, and salinity, convection and cyclogenesis around Iceland. (from Mysak and Power, 1992).

(1992) have attempted to incorporate the GSA into an interdecadal climate cycle, as described by a negative feedback loop (Fig. 1.1). For a further discussion of this feedback loop, the reader is referred to Mysak and Power (1992). The model in this thesis can be seen as an attempt to crudely simulate a part of this loop, mainly those components involving the ice-ocean system. Thus in this thesis, the atmosphere is 'specified' in a rather simple and crude way, and so this loop cannot be modelled in its entirety by the ice-ocean box model presented here. The model in this thesis can be seen as a first step toward simulating the complete feedback loop of Mysak and Power using a simple dynamical model. A model simulating the complete feedback loop could then be used to look at possible interdecadal climate cycles.

The structure of this thesis is as follows: In section 2, a complete description of the model will be given. In section 3, the results of the numerical simulation using a set of control parameters will be given and analyzed. In section 4, the model response to several types of imposed anomalies will be examined. Finally in section 5, the results will be summarized and discussed.

2. Description of the Model

2.1 Geographic regions included in the model

The multi-box model developed in this thesis represents the upper-ocean part of four different but connected geographic locations: The Arctic Ocean, the (west) Greenland and Norwegian Seas, and the Greenland Gyre. The approximate geographic position of the boxes for each region is shown in figure 2.1.

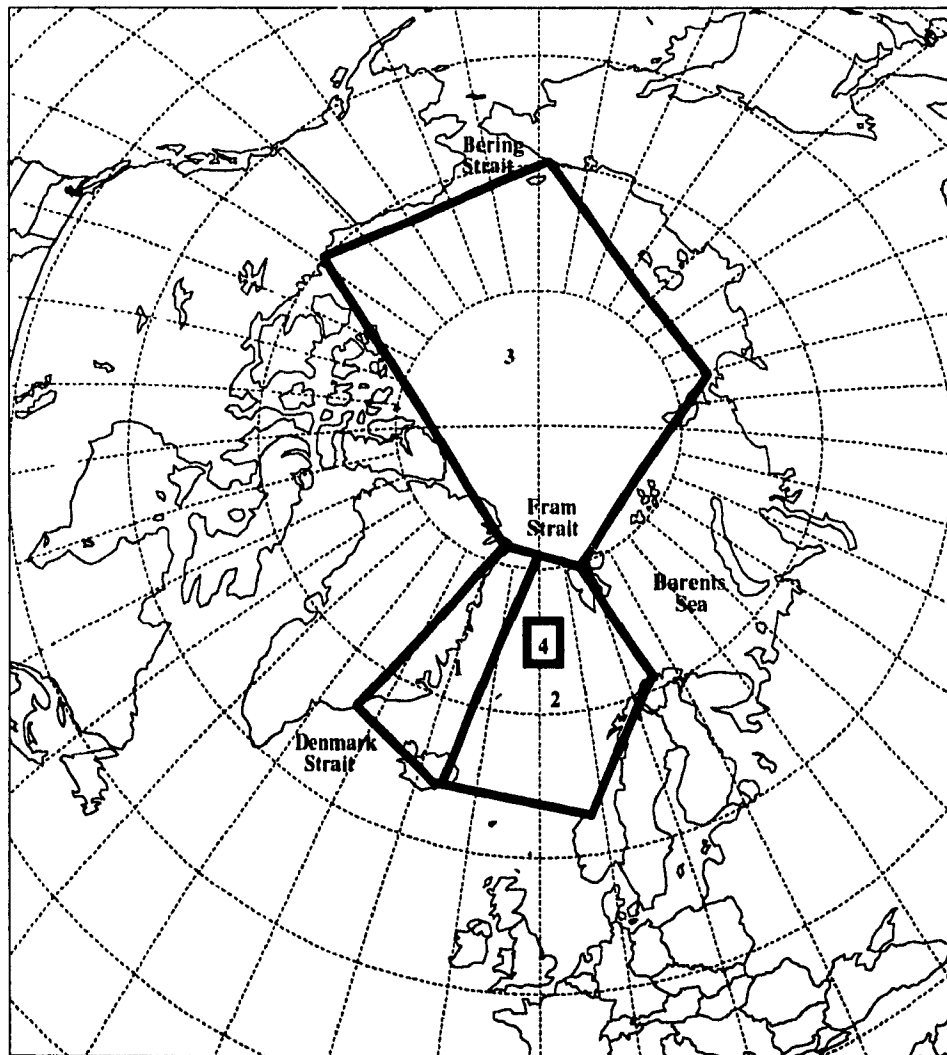


Fig. 2.1. Positions of the four boxes used in the model, where region 1 is the west Greenland Sea, 2 is the Norwegian Sea, 3 is the Arctic Ocean, and 4 is the Greenland Gyre.

Trying to represent the high-latitude ocean area in Fig. 2.1 with a limited number of regions in a simple box model is not an easy task. One must walk on a thin line between a model with too many boxes in which simple interpretations of the regions under study are lost in the equations, and a model with not enough boxes that doesn't really represent the physics of the area.

The Arctic Ocean can be represented with one box that should represent relatively well the average values of upper-ocean temperature, salinity, and ice thickness in that large area. The area south of Fram Strait is a more complex region. While looking at the interactions between the North Atlantic and the Arctic Ocean, we can recognize a couple of important features that can be incorporated in a simple multi-box model: in the upper 100-200 m there is a southward current, the East Greenland Current, which bring relatively fresh and cold water from the Arctic through the west side of Fram Strait; on the eastern side of the Strait there is a relatively warm and salty water coming from the North Atlantic and entering the Arctic. To represent these two features, Box #1 and Box #2 were defined (Fig. 2.1).

The upper-ocean salinity field south of Fram Strait is partially shown in Fig. 2.2. That figure shows the difference in the surface salinity field between Box #1 and Box #2. On the western side of the region, Box #1 (because of the East Greenland Current) corresponds to a region of relatively low salinities, generally between 34.0 and 34.8 (at least for the areas with some data). Box #2, on the east side of the area, feels the effect of the North Atlantic by having relatively higher salinities (in the 34.8 to 35.2 range). Box #1 is named 'Greenland Sea region' to recognize the fact that this region includes part of the Greenland Sea, (as defined in Fig. 1 of Aagaard and Carmack, 1989), the East Greenland Current, and is situated on the east coast of

Greenland. Box #2 is named 'Norwegian Sea region' because it includes the Norwegian Sea and is situated on the west coast of Norway.

To gain some insight into some of the smaller-scale phenomena which cannot be represented by these large boxes, a smaller one was centered at 75°N , 0° . This smaller box is approximately located where the Greenland Gyre is centered (Fig. 1 of Carmack and Aagaard, 1973), and thus is named 'Greenland Gyre region'. The area of this fourth box is $1/10$ the area of the Greenland Sea region, and $1/20$ the area of the Norwegian Sea region.

Separating the surface waters passing through the Fram Strait region (a southward current of cold and fresh water on the west side, and a northward current of warm and saline water on the east side) into two boxes can be justified by looking at the observations in Fig. 2.3. In that figure, the temperature and salinity field at the surface is seen as being very different if we look at the east or west part of the Strait.

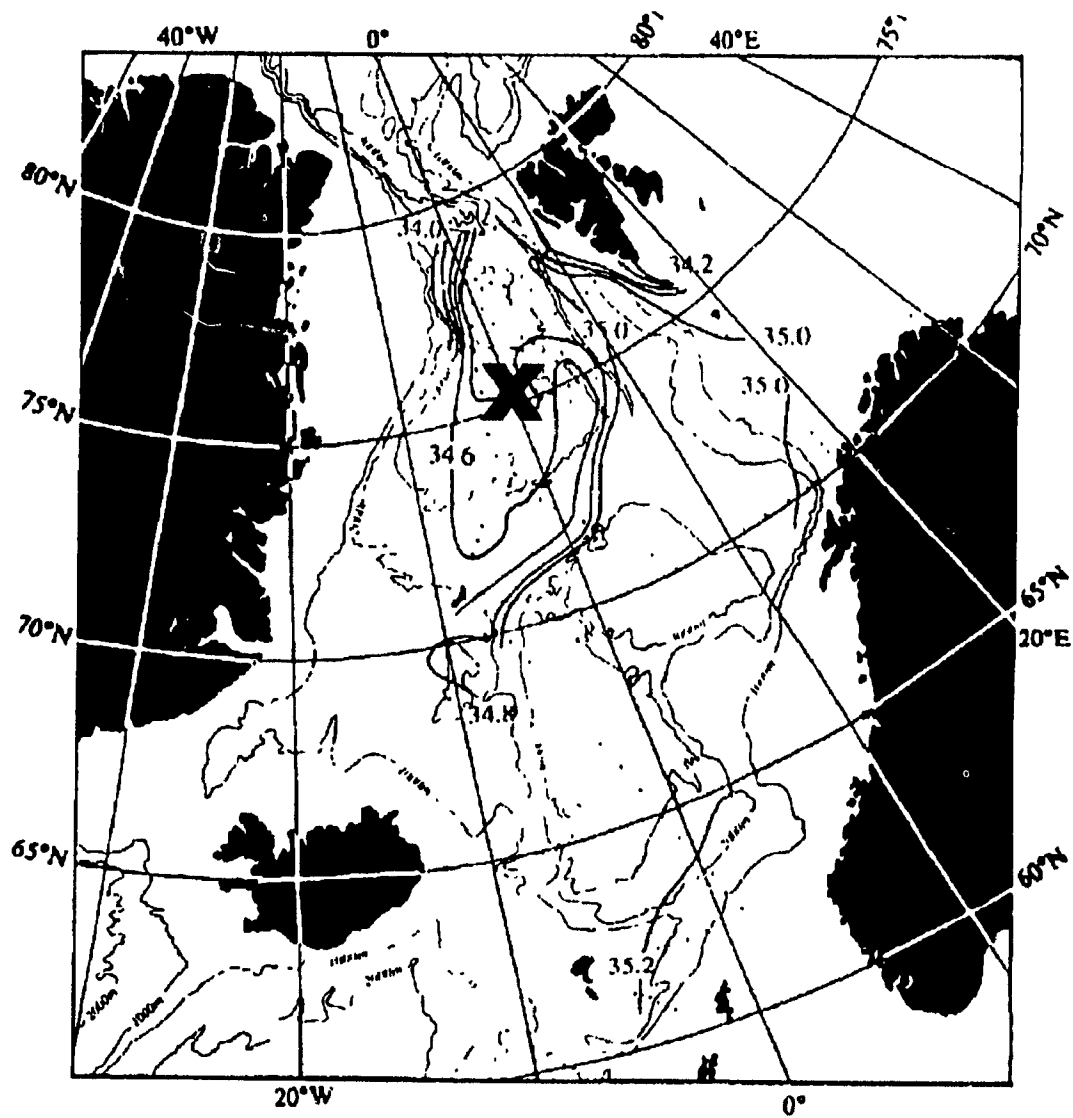


Fig. 2.2. Salinity in the upper 20 meters (From Clarke *et al.*, 1990). The 'X' marks the approximate location of the Greenland Gyre region in the model.

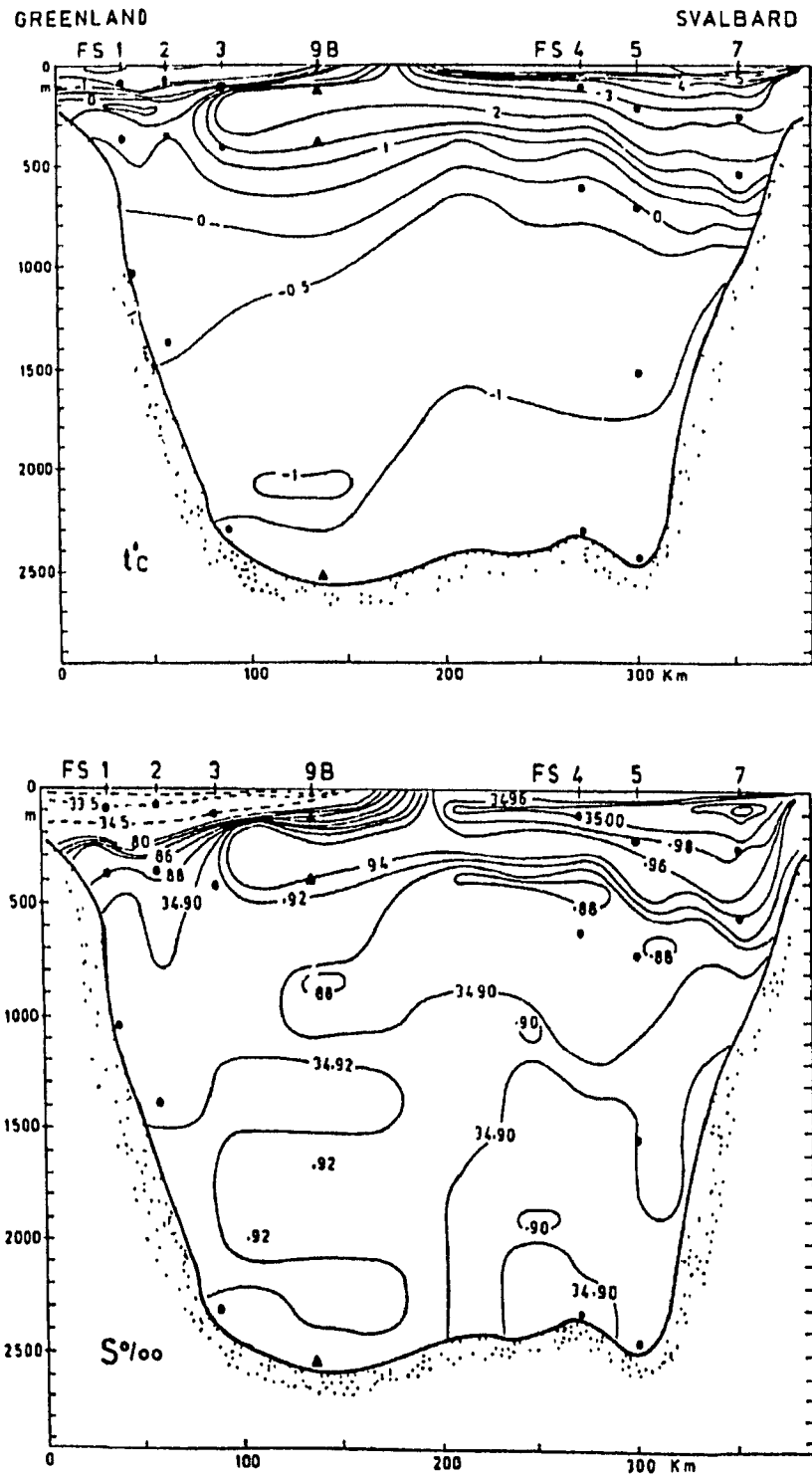


Fig. 2.3. Temperature and salinity sections across Fram Strait, at approximately 79°N (from Jónsson *et al.*, 1992).

2.2 Overview of the model

In each of the four regions a simple two-layer model is used to represent the upper ocean in the Arctic and upper 2000 m in the GIN Sea. This model is based on the Weddell Polynya model developed by Martinson *et al.* (1981). In that model, the ice-ocean system, at a given time, can be in one of four different states (see fig 2.4). The system can have no ice (States 1 and 2), or have an ice cover (States 3 and 4). In States 2 and 4 the system is statically stable, with the density of the upper (mixed) layer being less than the density of the lower layer. In States 1 and 3 the system is in an actively overturning mode with the density uniform everywhere in the box. As will be shown later, the boxes for the different regions will be connected to represent various horizontal inflows and outflows.

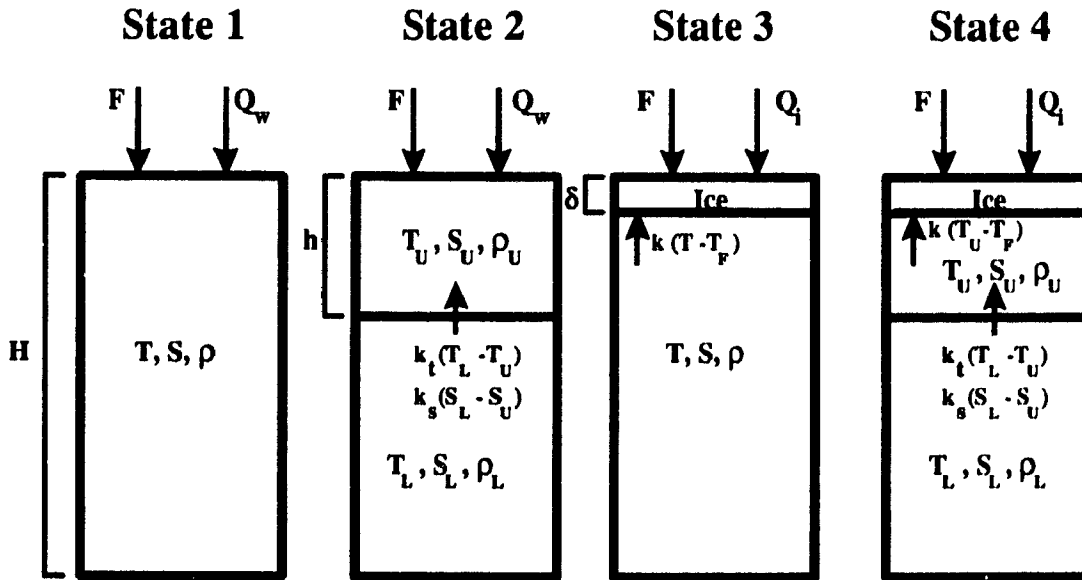


Fig. 2.4. The four different states in which each region can find itself (adapted from Martinson *et al.*, 1981).

In the two ice-free states, the system is heated or cooled by the heat flux Q_w , which becomes Q_i in the two states with ice. We adopt the convention that when

$Q_w > 0$, there is a heat transfer from the atmosphere to the ocean, and similarly from the atmosphere to the ice when $Q_i > 0$. In Martinson *et al.* (1981) the values used for Q_w and Q_i were based on observed data. In this thesis Q_w and Q_i are parameterized in terms of observed temperature data; the relations between the temperatures and heat fluxes are given by the following two equations:

$$Q_w = K_{wa} (T_{\text{atmosphere}} - T_{\text{water}}) , \quad (2.1)$$

$$Q_i = K_{ia} (T_{\text{atmosphere}} - T_{\text{ice}}) , \quad (2.2)$$

where K_{wa} and K_{ia} are heat exchange coefficients, $T_{\text{atmosphere}}$ is the air temperature obtained from observations, T_{water} is the temperature of sea water, which will be given by the model itself, and T_{ice} is the model-predicted temperature at the surface of the ice. This relatively simple heat flux formulation has been used in a similar way in numerous models (for example R ed, 1984; Willmott and Mysak, 1989; Wood and Mysak, 1989; and Darby and Willmott, 1993) for different time scales ranging from a few days to over a century, with or without a seasonal cycle. In the future, this heat flux formulation will need further testing and verification to see if it is precise enough to be used in the simulation of a seasonal cycle. Following Welander and Bauer (1977), T_{ice} is obtained by equating the ice-to-air heat flux to the heat flux upward through the ice:

$$K_{ia} (T_{\text{ice}} - T_{\text{atmosphere}}) = \frac{\kappa_i (T_F - T_{\text{ice}})}{\delta} , \quad (2.3)$$

where κ_i is the conductivity of the ice, δ is the thickness of the ice and T_F is the temperature of the water just under the ice cover, which is equal to the freezing temperature of the water; it is also the temperature at the bottom of the ice. The

steady-state equation (2.3) applies because there is no melting or freezing at the ice surface. From eq. (2.3) we obtain the temperature at the surface of the ice, namely,

$$T_{ice} = \frac{\frac{\kappa_i T_F}{\delta} + K_{ia} T_{atmosphere}}{K_{ia} + \frac{\kappa_i}{\delta}} . \quad (2.4)$$

The quantity F in figure 2.4 is the fresh water input into the system, which includes continental runoff from sources surrounding the region under study, freshwater input due to excess precipitation over evaporation, ice transport into minus the ice transport out of the region. This term will be described in greater detail later.

The different ρ 's in figure 2.4 are the densities averaged over each box, each of which can be calculated in terms of the box temperature T and salinity S , by the linear equation of state:

$$\frac{(\rho - \rho_0)}{\rho_0} = -\alpha(T - T_0) + \beta(S - S_0) , \quad (2.5)$$

where T_0 denotes the mean temperature, S_0 denotes the means salinity and ρ_0 is the mean density of sea water. The constants α and β are the coefficient of thermal expansion and the coefficient of haline contraction. In the temperature range (-2°C to $+3^\circ\text{C}$) and the salinity range (32-35‰) the following values of the coefficients may be used: $\alpha=5.5 \times 10^{-5} \text{ K}^{-1}$ and $\beta=8 \times 10^{-4}$ (Stigebrandt, 1981). The use of a linear equation of state (as was done in the original model of Martinson *et al.*, 1981) can be justified by the fact that the model uses only one or two layers, and the density calculated from eq. 2.5 is compared with the density at an interface between two layers of water which is never deeper than 200 m.

The quantity H is the total depth of the box while h is the depth of the upper (mixed) layer in States 2 and 4. These two values will generally be different for each region. δ is the thickness of the ice. Between the two layers in States 2 and 4, transfers of heat and salt are allowed according to the fluxes $k_t(T_L - T_U)$ and $k_s(S_L - S_U)$, where k_t and k_s are exchange coefficients. We also have an exchange of heat between the water and ice which is given by $k(T_L - T_U)$, where k is the water-ice exchange coefficient. As the ice cover forms or melts, the salinity of the layer below also changes in a manner which will be described in section 2.3.

At a given time, the system in one region must be in one of the four states. The system will change its state according to the following rules (criteria):

State 2 \rightarrow State 1

From (2.5), the difference in the density between the lower and upper layer is found to be

$$\rho_L - \rho_U = \rho_0 [-\alpha(T_L - T_U) + \beta(S_L - S_U)] . \quad (2.6)$$

The system will go from State 2 to State 1 when the density of the upper layer (ρ_U) is greater than the density of the lower layer (ρ_L). According to (2.6) this will happen when

$$-\alpha(T_L - T_U) + \beta(S_L - S_U) < 0 . \quad (2.7)$$

When this condition holds, the system enters State 1 in which the two layers are mixed into one deep uniform layer of depth H with temperature T and salinity S given by the depth-weighted averages:

$$T = \frac{[hT_U + (H - h)T_L]}{H} , \quad (2.8)$$

$$S = \frac{[hS_U + (H - h)S_L]}{H} \quad (2.9)$$

State 2 → State 4

The system will enter State 4 if ice can grow at the surface. This will occur when $d\delta/dt > 0$, i.e., the right-hand side of the ice thickness equation (see eq. 2.16c for example) is positive.

State 4 → State 2

The system will enter State 2 from State 4 if the ice thickness (δ) decreases to zero.

State 4 → State 3

The system will enter State 3 from State 4 if the density of the upper layer is greater than the density of the lower layer. This is exactly the same situation as the change from State 2 to State 1, with the condition (2.7) applying to the temperatures and salinities. The new temperature and salinity will be given once again by equations (2.8) and (2.9).

State 1 → State 2

The criteria for determining the change from State 1 to State 2 are found in two steps:

- 1) The density of the uniform layer in State 1 is calculated as a function of time. If it's decreasing, it indicates that convective overturning has stopped and that the system is moving toward establishing a stable stratification with a light upper layer.

2) Next, if the density is decreasing, the critical temperatures and salinities of the lower and upper layers of the two-layer system are calculated for which the system would switch from a one-layer to a two-layer stable system. The temperatures and salinities of these two hypothetical layers are found by using equations (2.8) and (2.9). In these two equations, T and S are known (the temperature and salinity of the convective layer), H and h are constants, and the lower layer temperature T_L and salinity S_L are fixed in the model for all regions except the Arctic. From (2.8) and (2.9), the values of temperature and salinity for the hypothetical upper layer, T_U and S_U , are calculated. Using these values for T_L , T_U , S_L and S_U the densities of the two hypothetical layers are calculated. If the density of the upper layer is less than the density of the lower layer, the system is found to have stabilized, and it can go from State 1 to State 2.

The fact that the system must return to fixed values for the temperature and salinity of the lower layer when switching from a one-layer system to a two-layer system could be seen has a serious limitation in the model. But this could be justified by the fact that this convection only occurs in one region (the Greenland Gyre, which will go from State 4 to State 3 and back to State 4 once every winter; see results in section 3.1) and this convection will only occur in the upper 200 m. Therefore the model is not trying to simulate deep-water formation through convection. As will be explain later, the Gyre consists of two layers: 0 to 40 m and 40 to 200m. The region below 200 m will be the lower layer of the Norwegian Sea, which is always in a two-layer state (see section 3.1). T_L and S_L for the Gyre (for the areas between 40 and 200 m) will be fixed at the same values than T_L and S_L for the Norwegian Sea (for the area below 200 m in that region). So when the Gyre is in a one-layer state (only one layer between 0 and 200 m) and returns to a two-layer state, the lower layer

conditions T_L and S_L (for the Gyre) must return to exactly the same conditions which are found below 200 m. So using fixed values when switching from one layer to two layers in the Gyre region, which is the only case of convection in this simple box model, is like moving the mixed layer depth, at the location of the Gyre, from a depth of 200 m to a depth of 40 m.

State 1 \rightarrow State 3

As in the change from State 2 to State 4, the criterion for the change of state is obtained from the equation for the variation of ice thickness. If $d\delta/dt > 0$, then ice formation takes place, and the system will go to State 3 from State 1.

State 3 \rightarrow State 4

The criteria for change from State 3 to State 4 is similar to that for the change from State 1 to State 2: if the density of the whole convective layer is decreasing, the densities of the upper and lower hypothetical layers are calculated. If $\rho_U < \rho_L$ then the system goes from State 3 to State 4, i.e., from a one-layer to a two-layer system.

State 3 \rightarrow State 1

The system will enter State 1 from State 3 if the ice thickness decreases to zero.

State 3 \rightarrow State 2

The system will enter State 2 from State 3 if the ice thickness decreases to zero and if the condition to go from State 3 to State 4 (stabilization of the system) is true at the same moment.

A few changes of states were not discussed in this list of criteria, namely 2 \rightarrow 3, 1 \rightarrow 4, and 4 \rightarrow 1. These changes happen with a combination of physical changes in the

system; for example formation of ice and convective overturning both occur for the change between State 2 and State 3. These changes are treated sequentially by the model during its numerical integration. On the first time step, one of the two changes occurs and is treated following the set of criteria just shown. During the next time step, the second physical change can occur. To approximate a change like that in two steps works fine if the time steps used in the numerical integration of the equations of the model are relatively small, as they will be in this thesis.

The box model depicted in figure 2.4, with all the rules for state changes just elaborated, is applied to each of the four geographic regions shown in figure 2.1. These four regions are connected together and to the rest of the world oceans through a number of links which represent water or ice transports at the surface only (never below 200 m as will be seen later). This was done to keep the model simple. However, this prevent fresh water anomalies to exit the system through deep water. Fig. 2.5 shows how the model simulates the interactions between the four regions in a simple and crude way. Some regions around these four regions are not simulated to keep the model simple and to concentrate only on a few regions. One of these left out region is the Barents Sea, where water from the Greenland/Norwegian Sea enters, is further cooled down by heat loss to the cold atmosphere, and then partly enters the Arctic Ocean. This process simulated in a simple way by using a specific water current, temperature, and salinity for the water entering the Arctic Ocean. This should simulate the cooling of the water in the Barents Sea without actually simulating it in the model. The numerical values of relevant quantities for these links are given in Table 2.1; these numbers will be used in the model equations which are described in section 2.3.

The values listed in Table 2.1 will be explained below; in this discussion the paper by Aagaard and Carmack (1989) will be referred by "A&C", Carmack (1990) by "C" and Coachman and Aagaard (1974) by "C&A".

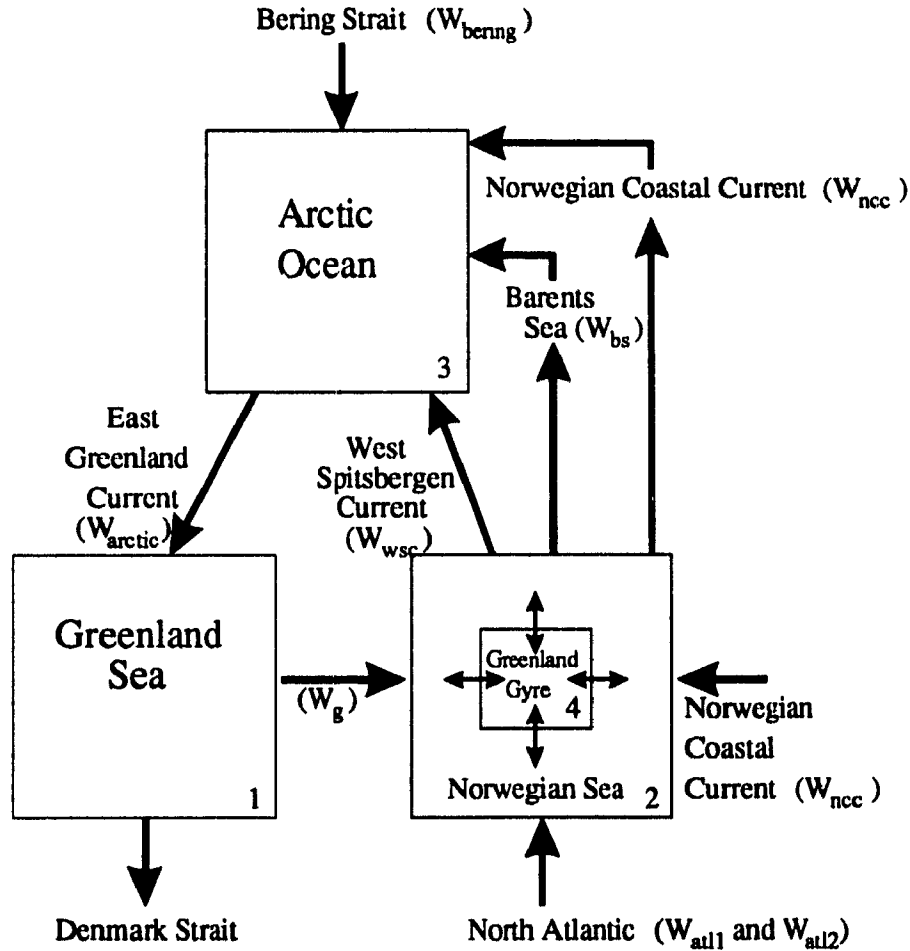


Fig. 2.5. The links between the four regions in the model and the rest of the world oceans. The numerical values of the water transports W are given in Table 2.1. All the arrows indicate water or ice transports, except between the Norwegian Sea and Greenland Gyre where the double arrows indicate diffusion between the two regions.

For the Bering Strait inflow, A&C indicate a long term mean flow of 0.8 Sv (W_{bering}) with a long term mean salinity of 32.5 (S_{bering}). This flow has an approximate temperature (T_{bering}) of $-1.0\text{ }^{\circ}\text{C}$ (Fig. 4.11 in C).

For the East Greenland Current, estimates of its strength (W_{arctic}) vary between 2 and 30 Sv in C, and between 2 and 4.1 Sv in C&A. We chose a value of 5.0 Sv.

Table 2.1 Values of parameters used in the model for the links between the four regions and the rest of the world oceans. W is a water transport (in units of Sv, where $1 \text{ Sv} = 10^6 \text{ m}^3\text{s}^{-1}$). The location in space of these various W are represented schematically in Fig. 2.5.

Name	Symbol	Value	Reference
Bering Strait inflow	W_{bering}	0.8 Sv	Aagaard and Carmack (1989)
	T_{bering}	-1.0 °C	Carmack (1990)
	S_{bering}	32.5	Aagaard and Carmack (1989)
East Greenland Current	W_{arctic}	5.0 Sv	Estimate based on data from Carmack (1990) and Coachman and Aagaard (1974).
West Spitsbergen Current	W_{wsc}	5.0 Sv	Estimate based on data from Carmack (1990) and Coachman and Aagaard (1974).
Barents Sea inflow	W_{bs}	0.5 Sv	Estimates based on data from Coachman and Aagaard (1974) and Midttun (1985)
	T_{bs}	-1.0 °C	
	S_{bs}	34.96	
Norwegian Coastal Current	W_{ncc}	0.7 Sv	Estimates based on data from Aagaard and Carmack (1989) and Carmack (1990)
	T_{ncc}	2.0 °C	
	S_{ncc}	34.4	
North Atlantic Inflow Atlantic Water Modified Atlantic Water	T_{atl}	4.0 °C	Carmack (1990)
	W_{atl1}	3.7 Sv	Aagaard and Carmack (1989)
	S_{atl1}	35.4	Aagaard and Carmack (1989)
	W_{atl2}	2.4 Sv	Aagaard and Carmack (1989)
	S_{atl2}	35.2	Aagaard and Carmack (1989)
Advection from the Greenland Sea to the Norwegian Sea	W_{g}	2.0 Sv	Estimated guess

For the West Spitsbergen Current, estimates of its strength (W_{wsc}) vary between 2 and 8 Sv in C, and between 3 and 4.2 Sv in C&A. The value chosen in this thesis is 5.0 Sv.

For the Barents Sea inflow into the Arctic, C&A Table 1 shows one estimate of a current of 1 Sv, but in the text, they speak only of a northward surficial flow between the Barents Sea and the Arctic. A current of 0.5 Sv for this inflow (W_{bs}) is chosen here. The discussions in C&A don't mention any salinity or temperature measurements of this inflow into the Arctic. Based the conclusions in Midttun (1985), a salinity (S_{bs}) of 34.96 and a temperature (T_{bs}) of -1.0°C are used in the model in this thesis.

For the Norwegian Coastal Current entering the Arctic and Norwegian Sea, its strength (W_{ncc}) and Salinity (S_{ncc}) are taken to be the same as the current that is leaving the Norwegian Sea (see Fig 2.5). For this situation, the values given by A&C are $W_{ncc}=0.7$ Sv and $S_{ncc}=34.4$. The temperature (T_{ncc}) of this current is taken as being less than the temperature entering the Arctic through Fram Strait (Fig. 2.3) and is fixed at 2.0°C . Section 3.2 of this thesis will show that the effects of the Norwegian Coastal Current on the Arctic Ocean region in the model are quite small compared to other processes. Even though the values for this water flux in the Arctic are far from being precise, they are included in the model for reasons of completeness with respect to the currents entering the four regions simulated.

The North Atlantic inflow is defined as having a temperature (T_{atl}) of 4.0°C (based on C where the Atlantic water is defined as being greater than 3°C). This Atlantic water is separated in two parts in A&C: The Atlantic water inflow with a

strength (W_{atl1}) of 3.7 Sv and salinity (W_{atl1}) of 35.4, and a modified Atlantic water with a strength (W_{atl2}) of 2.4 Sv and a salinity (S_{atl2}) of 35.2.

Finally the advection between the Greenland Sea and Norwegian Sea is estimated at 2.0 Sv (see water balance below).

Some of the water currents which have been discussed above were also estimated by taking into account a simple water balance of the water masses entering and leaving the Arctic Ocean, Greenland Sea, and Norwegian Sea regions of the model. This water balance can be described as follow:

Greenland Sea	Inflow	Outflow
•East Greenland Current	5.0 Sv	W_{arctic}
•Advection from the Greenland Sea box to the Norwegian Sea box		2.0 Sv W_g
•Water export through Denmark Strait		3.0 Sv (From C&A)
Total	5.0 Sv	5.0 Sv

Norwegian Sea	Inflow	Outflow
•West Spitsbergen Current		5.0 Sv W_{wsc}
•Advection from the Greenland Sea box to the Norwegian Sea box	2.0 Sv	W_g
•North Atlantic Water	3.7 Sv	W_{atl1}
	2.4 Sv	W_{atl2}
•Export to Barents Sea		2.4 Sv (From A&C)
•Norwegian Coastal Current	0.7 Sv	0.7 Sv W_{ncc}
Total	8.8 Sv	8.1 Sv

Arctic Ocean	Inflow	Outflow
•East Greenland Current		5.0 Sv W_{arctic}
•Water import through Bering Strait	0.8 Sv	W_{bering}
•West Spitsbergen Current	5.0 Sv	W_{wsc}
•Water from the Barents Sea	0.5 Sv	W_{bs}
•Norwegian Coastal Current	0.7 Sv	W_{ncc}
•Water export to the Canadian Arctic Archipelago		1.7 Sv (From A&C)
Total	7.0 Sv	6.7 Sv

While we have not shown a total water balance for all the three regions together, the totals for each region show that no huge imbalances exist in the model. Some of the current were chosen (the West Spitsbergen and East Greenland Currents for example) however, to keep the imbalances in the above totals to a minimum.

The transport of ice out of the Arctic Ocean through Fram Strait (I_{arctic}), the transport entering Greenland Sea (I_{Gs}) and the transport out of the Greenland Sea through Denmark Strait ($I_{denmark}$) are calculated quantities because they will vary with the ice thickness in the Arctic Ocean region. Hence they do not appear in Table 2.1. The quantity of ice leaving the Arctic Ocean region in one year is defined as being equal to $1/12$ of the ice volume in that region. That factor, which will vary with time because $\delta=\delta(t)$ in the Arctic, was chosen because it gives, when converted to Sverdrups, an ice transport through Fram Strait factor similar to that listed in Aagaard and Carmack (1989), namely 0.10 Sv. Thus for our model, with an area of $A_3=9.55 \times 10^{12} \text{ m}^2$ for the Arctic Ocean (Table 2.2), and using an average ice thickness of 4

meters, we obtain an ice export of $(1/12) \times (4) \times (9.55 \times 10^{12}) \text{ m}^3/\text{yr}$ or 0.10 Sv (where $1 \text{ Sv} = 10^6 \text{ m}^3 \text{ s}^{-1}$).

The quantity of ice entering the Greenland Sea (I_{GS}) is defined to be equal to 0.35 of the quantity of ice leaving the Arctic (I_{arctic}). The reduction is due to ice melt. In a box model, the conditions simulated are of a point which should be representative of the region the box covers. In the Greenland Sea region an amount I_{arctic} of ice passes through Fram Strait, but this ice melts while floating southward. If an ice import corresponding to 100% of the value of I_{arctic} was used in the ice thickness equation for the region, this would imply that the ice conditions in the Greenland Sea region we are trying to simulate are the ones close to Fram Strait. By taking only a fraction of I_{arctic} as the ice flux in the ice equations, we are assured that the ice thickness simulated would be for a point farther south from Fram Strait, a point we hope would be more representative of the average conditions over the whole region. Aagaard and Carmack (1989) estimate that 50% of the ice through Fram Strait melts before it reaches 73°N. We increase this percentage to 65% to take into account the fact that the Greenland Sea region used in the model extends southward to 65°N, and that we try to simulate the conditions near a point at 70°N, 15°W. Thus the net amount of ice imported into the Greenland Sea is $0.35 \times I_{\text{arctic}}$. The melted ice ($0.65 \times I_{\text{arctic}}$) is treated in the model as water entering the Greenland Sea region.

The quantity of ice leaving the Greenland Sea region through Denmark Strait (I_{Denmark}) is estimated at 0.20 of the quantity of ice flowing through Fram Strait. This number comes from Aagaard and Carmack (1989).

The parameters employed in the model (e.g., layer thicknesses) are listed in Table 2.2, and the physical constants used are given in Table 2.3.

Table 2.2 Parameters used in the model.

Name	Symbol	Value	Reference
Area			
Greenland Sea	A ₁	0.853x10 ¹² m ²	Aagaard and Carmack (1989)
Norwegian Sea	A ₂	1.707x10 ¹² m ²	Aagaard and Carmack (1989)
Arctic Ocean	A ₃	9.550x10 ¹² m ²	Aagaard and Carmack (1989)
Greenland Gyre	A ₄	1.832x10 ¹¹ m ²	Carmack and Aagaard (1973)
Upper layer depth			Estimates based on data from Björk (1989), Clarke <i>et al.</i> (1990), Holland <i>et al.</i> (1991), and Coachman and Aagaard (1974)
Greenland Sea	h ₁	200 m	
Norwegian Sea	h ₂	200 m	
Arctic Ocean	h ₃	40 m	
Greenland Gyre	h ₄	40 m	
Total Depth			
Greenland Sea	H ₁	2000 m	Estimates based on data from Clarke <i>et al.</i> (1990), Björk (1989), and Coachman and Aagaard (1974)
Norwegian Sea	H ₂	2000 m	
Arctic Ocean	H ₃	200 m	
Greenland Gyre	H ₄	200 m	
Runoff			
Greenland Sea	Runoff ₁	75 km ³ yr ⁻¹	Aagaard and Carmack (1989)
Norwegian Sea	Runoff ₂	345 km ³ yr ⁻¹	Aagaard and Carmack (1989)
Arctic Ocean	Runoff ₃	3300 km ³ yr ⁻¹	Aagaard and Carmack (1989)
Temperature	T _{runoff}	2.0 °C	Carmack (1990)
Precipitation minus Evaporation			
Greenland Sea	PE ₁	263 km ³ yr ⁻¹	Estimates based on data from Aagaard and Carmack (1989)
Norwegian Sea	PE ₂	527 km ³ yr ⁻¹	
Arctic Ocean	PE ₃	900 km ³ yr ⁻¹	
Greenland Gyre	PE ₄	57 km ³ yr ⁻¹	
Lower Layer Temperature			
Greenland Sea	T _{L1}	-0.5 °C	Estimates based on data from Clarke <i>et al.</i> (1990) and in Coachman and Aagaard (1974)
Norwegian Sea	T _{L2}	-0.5 °C	
Greenland Gyre	T _{L2}	-0.5 °C	
Lower Layer Salinity			
Greenland Sea	S _{L1}	34.91	Estimates based on data from Clarke <i>et al.</i> (1990) and in Coachman and Aagaard (1974)
Norwegian Sea	S _{L2}	34.91	
Greenland Gyre	S _{L2}	34.91	

A number of references were considered in choosing the upper layer (h_1) and total (H_1) depths appropriate for the four regions. The upper layer depth used in the model for one region will correspond to the mixed layer depth observed in that region. For the Arctic Ocean, we chose $h_3=40$ m and $H_3=200$ m. In the model of Holland *et al.* (1991) the mixed layer depth is taken as being 30 m. In Björk (1989) the mixed layer in the Arctic is said to be between 25 m and 50 m; so we chose 40 m for h_3 in the model presented here. Under this mixed layer, Björk (1989) defines a transition layer of depth up to 200 m (in the region north of Greenland). This last depth will be our total depth (H_3).

For the Greenland Sea region, Fig. 4 (profile #5 and #6) in Coachman and Aagaard (1974) shows that the conditions of the temperature and salinity change quickly between 150 and 200 m, and are relatively stable deeper than that; thus the choice of a mixed layer in that region of $h_1=200$ m. H_1 was chosen as 2000 m in order to have a box deep enough so that the temperature and salinity are approximately constant.

For the Norwegian Sea region, Fig 4. in Clarke *et al.* (1989) shows mixed layer depths in the 100 to 500 m range. Taking into account this range, the values for the mixed layer and total depth (h_2 and H_2) were chosen to equal 200 m and 2000 m, respectively. These values were also chosen so as to be similar to the values in the Greenland Sea region of the model. Fig. 3.6 and 3.7 below also show that the salinity and temperature are quite constant below 1000 m.

The fourth region, the Greenland Gyre, was created to look at convective and diffusive phenomena in the upper part of the Norwegian Sea region. To do that, in the

region where the gyre is centered, the two layers of this fourth region replace the upper layer of the Norwegian Sea, thus the total depth H_4 will be equal to 200 m. The upper layer of this small region must be less than 200 m, and so we arbitrary specify it to be $h_4=40$ m.

Fig. 3.6 and 3.7 below show the temperature and salinity in the Norwegian Sea (Station 105 to 120). From these two figures we can see that the temperature and salinity do not vary a lot when going deeper than 500 m. The temperature varies between $0.0\text{ }^{\circ}\text{C}$ and $-1.0\text{ }^{\circ}\text{C}$. Thus the lower layer in the Norwegian Sea region has a temperature of $T_{L2} = -0.5\text{ }^{\circ}\text{C}$. The salinity goes from 34.9 to 34.911, with a maximum near 34.912. The lower layer salinity (S_{L2}) is thus taken as being 34.91.

In Coachman and Aagaard (1974), in the section on the water masses of the East Greenland Current (which corresponds to the Greenland Sea region in this model), the water under 150 m (Atlantic intermediate water and deep water) is said to be between 34.87 and 35.0. Fig. 22 in the same reference shows that the temperature below 400 m is between $1\text{ }^{\circ}\text{C}$ and $-1\text{ }^{\circ}\text{C}$, with a salinity under 35.0. Keeping all the ranges of values in mind, the lower layer in the Greenland Sea region of the model is defined to have a temperature $T_{L1} = -0.5\text{ }^{\circ}\text{C}$ and a salinity $S_{L2}=34.91$. These values are the same as those used for the Norwegian Sea region of the model.

As indicated in Table 2.2, the lower layer salinity and temperature in the Greenland Gyre region are taken to be the same than in the lower Norwegian Sea region (T_{L2} and S_{L2}). This is done because the lower layer of the Gyre region is defined as being water from the lower layer of the Norwegian Sea region which is brought up from below 200 m to the region between 40 and 200 m by the cyclonic circulation of the Gyre.

Table 2.3 Physical constants used in the model.

Name	Symbol	Value
Ice Salinity	S_{ice}	5.0
Coefficient of thermal expansion	α	$5.82 \times 10^{-5} \text{ K}^{-1}$
Coefficient of haline contraction	β	8×10^{-4}
Water Density	ρ	$1027.84 \text{ kg m}^{-3}$
Ice Density	ρ_i	900 kg m^{-3}
Thermal Conductivity of Ice	κ_i	$2.0334 \text{ W m}^{-1} \text{ K}^{-1}$
Specific Heat of Sea Water	C_p	$4.18 \times 10^3 \text{ J kg}^{-1} \text{ K}^{-1}$
Latent Heat of ice	L	$2.5 \times 10^5 \text{ J kg}^{-1}$

Table 2.4 Heat and salt exchange coefficients used in the model.

Heat exchange coefficient	Symbol	Value
Sea↔Air	K_{wa}	$25.0 \text{ W m}^{-2} \text{ K}^{-1}$
Ice↔Air	K_{ia}	$10.0 \text{ W m}^{-2} \text{ K}^{-1}$
Ice↔Sea	k	$20.0 \text{ W m}^{-2} \text{ K}^{-1}$
Mixed layer↔Lower Layer		
Greenland Sea	k_{t1}	$7.0 \times 10^{-7} \text{ m s}^{-1}$
Norwegian Sea	k_{t2}	$7.0 \times 10^{-7} \text{ m s}^{-1}$
Arctic Ocean	k_{t3}	$7.0 \times 10^{-7} \text{ m s}^{-1}$
Greenland Gyre	k_{t4}	$3.5 \times 10^{-6} \text{ m s}^{-1}$
Salinity exchange coefficient	Symbol	Value
Mixed layer↔Lower Layer		
Greenland Sea	k_{s1}	$1.0 \times 10^{-7} \text{ m s}^{-1}$
Norwegian Sea	k_{s2}	$1.0 \times 10^{-7} \text{ m s}^{-1}$
Arctic Ocean	k_{s3}	$1.0 \times 10^{-7} \text{ m s}^{-1}$
Greenland Gyre	k_{s4}	$5.25 \times 10^{-7} \text{ m s}^{-1}$

Table 2.4 lists the values for the heat and salt exchange coefficients used in the model. The exchange coefficients for sea-air and ice-air interactions (K_{wa} and K_{ia}) appear in equations (2.1) and (2.2) respectively. The values are taken to be the same for the four regions, and correspond to those used in the simple ice-ocean model for the Greenland Sea developed by Wood and Mysak (1989). The ice-sea exchange coefficient k is also taken to be the same for the four regions. The value used comes from the ratio $q=K_{ia}/k=0.5$ (Wood and Mysak, 1989). The exchange coefficients between the lower layer and upper layer are more difficult to specify. These coefficients parameterize the effects of upwelling, turbulent exchange and double diffusion. The heat exchange coefficient for the first three regions was chosen equal to the one used for the Weddell Sea in Martinson *et al.* (1981).

Røed (1984) used a considerably higher ($6.3 \times 10^{-5} \text{ m s}^{-1}$) value of k_t than used here ($7.0 \times 10^{-7} \text{ m s}^{-1}$) for his model of the Marginal Ice Zone. Wood and Mysak (1989) argued that this was necessary because Røed was studying the behavior of heat exchange processes close to the ice edge. For a gyre-scale model the smaller value applies.

In an ice-free region, the values of k_t and k_s should in principle vary inversely with the mixed layer depth because, as the interface between the two layers comes closer to the surface, it would be nearer the wind-mixing action in the upper ocean. This turbulence mixing across the interface would be increased, which could be parameterized by an increase in the exchange coefficients. This is certainly true for the Norwegian Sea and the Greenland Gyre which have a big difference in mixed layer depth (200 m versus to 40 m). Thus we hypothesize (Darby, personal communication, 1992) that

$$k_{t4} = (h_2/h_4)k_{t2} \quad , \quad (2.10)$$

and similarly for k_{s4} .

The values of k_{t3} and k_{s3} for the Arctic Ocean were chosen equal to the values used for the Greenland and Norwegian Seas, even though the mixed layer of the Arctic is closer to the surface. This was done because the Arctic Ocean is ice-covered for most of the year and therefore the interface will not likely feel the action of the atmospheric winds. The model in this thesis does not include any ice dynamics in the Arctic Ocean and, thus, the possible effect of the ice cover on the mixed layer depth in the Arctic by the action of the keels of ice ridges is not considered.

The salinity exchange coefficient in one region is fixed at 0.15 times the value of the heat exchange coefficient in the same region. This was done in Martinson *et al.* (1981) who inferred this value from laboratory experiments published by Turner (1973).

The sensibility of the model under changes of k_t and k_s in the four regions will be discussed at the end of section 3.1

The heat flux forcing of the four regions requires knowledge of the semi-daily atmospheric surface temperatures in each of the regions (see (2.1) and (2.2)). From monthly mean temperatures, a linear regression is used to obtain these values. For the Arctic region, the temperatures come from data provided by J. Walsh and D. Chapman via Dave Holland (personal communication, 1992). For the other three regions, the monthly mean temperature data are from Shea (1986). For the Arctic Ocean region, the data were taken from a point at 85°N, 120°W; for the Greenland Sea region, from

a point at 70°N, 15°W; for the Norwegian Sea region, from 70°N, 0°; and at 75°N, 0° for the Greenland Gyre.

The only horizontal exchange between the Greenland Gyre and the Norwegian Sea is through diffusion of water between the two upper layers (fig 2.5). The diffusion coefficient will vary according to the volume of the gyre region. For the Greenland Gyre region (region 4), the equations for the variations of upper-layer temperature and salt will include terms of the form

$$A_4 h'_4 \frac{dT_4}{dt} = D_t (T_2 - T_4) \quad \text{and} \quad A_4 h'_4 \frac{dS_4}{dt} = D_s (S_2 - S_4), \quad (2.11)$$

where

$$D_t = \frac{2A_t h'_4}{\epsilon} \quad \text{and} \quad D_s = \frac{2A_s h'_4}{\epsilon}.$$

N.B. Note that for convenience we have dropped the subscript 'u' on T and S to denote 'upper layer'. T_i and S_i will refer to the upper layer temperature and salinity in region 'i', unless convection occurs. In the latter case, T_i and S_i refer to the temperature and salinity of the convecting layer of depth H_i .

Similarly, for the Norwegian Sea region (region 2), the effect of diffusion from the gyre will give rise to terms of the form

$$A_2 h_2 \frac{dT_2}{dt} = D_t (T_4 - T_2) \quad \text{and} \quad A_2 h_2 \frac{dS_2}{dt} = D_s (S_4 - S_2), \quad (2.12)$$

with the same D_t and D_s as in (2.11). The coefficients D_t and D_s are now discussed below.

The factor h'_4 in D_t and D_s is the actual thickness of the upper layer in the box, depending in which state the Greenland Gyre is at the moment (fig 2.4). If the Gyre is in State 2 or 4 (no convective overturning), $h'_4 = h_4$ (see Table 2.2). But if the Gyre is in a state of convective overturning (State 1 or 3), $h'_4 = H_4$.

The factor ϵ in the denominator of D_t and D_s is a coefficient which allows for a smooth transition in temperature and salinity from the Norwegian Sea to the Greenland Gyre. An east-west section of the upper layer of the Norwegian Sea, showing the Greenland Gyre region in the middle, is sketched below (figure 2.6).

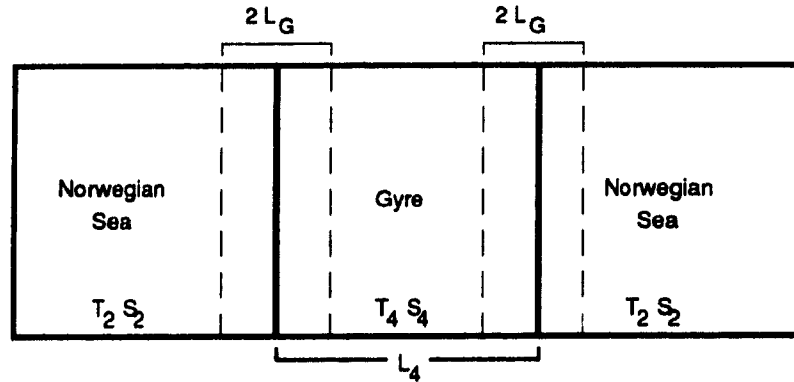


Fig. 2.6. A sketch of an east-west section of the upper layer of the Norwegian Sea and Greenland Gyre.

The transition regions of width $2L_G$ are where the temperature and salinity vary continuously from T_2 and S_2 in the Norwegian Sea to T_4 and S_4 in the Greenland Gyre (M. Darby, personal communication, 1992). L_G is related to L_4 (the width of the gyre) by the equation $L_G = \epsilon L_4$, and in this case we choose $\epsilon = 0.1$.

A_t and A_s are considered as 'mixing' parameters which can be used to tune the model. These parameters control the amount of diffusion between the Greenland Gyre and Norwegian Sea regions, and are not easily measured in practice. Darby and Willmott (1993) used values of A_t and A_s ranging from 250 to 1000 m^2s^{-1} depending on the numerical experiment. In this thesis we shall use the value of 300 m^2s^{-1} for A_t and A_s .

2.3 The governing equations

The governing differential equations, which describe the conservation of energy and salt, and the rate of ice growth, are now given for each region. The equations have as dependent variables the temperature and salinity of the upper (mixed) layer, and ice thickness for the four regions, and the temperature and salinity of the lower layer for the Arctic region. In the other three regions the lower layer temperature and salinity are kept constant. Further, in each of the four regions, four groups of differential equations are given, one for each state the system can be in. For the parameters that describe the current climate, a region will generally occupy one of two or three states over a seasonal cycle. However, the governing equations in each region allow for all four states to occur in the model. This permits us to do anomaly experiments which describe patterns of behaviour not found in the present climate (e.g., a complete meltdown of ice in the Arctic region). In terms of the parameters and constants defined in section 2.2, the equations for each region are as follows. We recall that the values or criteria which determine when a particular region will go from one state into another were also given in section 2.2.

Greenland Sea

State 1

$$A_1 H_1 \frac{dT_1}{dt} = A_1 \frac{Q_{wl}}{\rho C_p} + W_{arctic} (T'_3 - T_1) + (\text{Runoff}_1)(T_{\text{runoff}} - T_1) \quad , \quad (2.13a)$$

$$A_1 H_1 \frac{dS_1}{dt} = (\text{Runoff}_1 + PE_1)(-S_1) + W_{arctic} (S'_3 - S_1) \quad , \quad (2.13b)$$

$$\frac{d\delta_1}{dt} = 0 \quad , \quad (2.13c)$$

State 2

$$A_1 h_1 \frac{dT_1}{dt} = A_1 \frac{Q_{wl}}{\rho C_p} + A_1 k_{il}(T_{L1} - T_1) + W_{arctic}(T'_3 - T_1) + (\text{Runoff}_1)(T_{\text{runoff}} - T_1) , \quad (2.14a)$$

$$A_1 h_1 \frac{dS_1}{dt} = A_1 k_{sl}(S_{L1} - S_1) + (\text{Runoff}_1 + PE_1)(-S_1) + W_{arctic}(S'_3 - S_1) , \quad (2.14b)$$

$$\frac{d\delta_1}{dt} = 0 , \quad (2.14c)$$

State 3

$$A_1 H_1 \frac{dT_1}{dt} = A_1 \frac{k}{\rho C_p}(T_{F1} - T_1) + W_{arctic}(T'_3 - T_1) + (\text{Runoff}_1)(T_{\text{runoff}} - T_1) , \quad (2.15a)$$

$$A_1 H_1 \frac{dS_1}{dt} = (S_1 - S_{ice})A_1 \left(\frac{d\delta_1}{dt} - \frac{1}{A_1}(PE_1 + I_{Gs} - I_{denmark}) \right) + (\text{Runoff}_1)(-S_1) + W_{arctic}(S'_3 - S_1) , \quad (2.15b)$$

$$\frac{d\delta_1}{dt} = \frac{1}{\rho_1 L}[-Q_{il} + k(T_{F1} - T_1)] + \frac{1}{A_1}(PE_1 + I_{Gs} - I_{denmark}) , \quad (2.15c)$$

State 4

$$A_1 h_1 \frac{dT_1}{dt} = A_1 k_{il}(T_{L1} - T_1) + A_1 \frac{k}{\rho C_p}(T_{F1} - T_1) + W_{arctic}(T'_3 - T_1) + (\text{Runoff}_1)(T_{\text{runoff}} - T_1) , \quad (2.16a)$$

$$A_1 h_1 \frac{dS_1}{dt} = (S_1 - S_{ice})A_1 \left(\frac{d\delta_1}{dt} - \frac{1}{A_1}(PE_1 + I_{Gs} - I_{denmark}) \right) + A_1 k_{sl}(S_{L1} - S_1) + (\text{Runoff}_1)(-S_1) + W_{arctic}(S'_3 - S_1) , \quad (2.16b)$$

$$\frac{d\delta_1}{dt} = \frac{1}{\rho_1 L}[-Q_{il} + k(T_{F1} - T_1)] + \frac{1}{A_1}(PE_1 + I_{Gs} - I_{denmark}) . \quad (2.16c)$$

In all the equations, T is the temperature, S is the salinity and δ is the ice thickness. Here the region under study is the Greenland Sea (region 1 in figure 2.1), so the subscript "1" is used for these three variables. For States 1 and 3, the temperature and salinity are those of the overturning layer; for States 2 and 4, they are for the upper layer. T_{F1} is the freezing temperature of sea water in region 1. The freezing temperature T_F in any of the four regions is found using the polynomial relation (Unesco Technical paper in marine science #44, Unesco 1983):

$$T_F = -0.0575 \cdot S + 1.710523 \times 10^{-3} \cdot S^{1.5} - 2.154996 \times 10^{-4} \cdot S^2, \quad (2.17)$$

where the temperature is in degrees Celsius and the salinity in psu.

The equations follow a similar structure for the four states. For the temperature equations, there is a term for the flux of water from the Arctic Ocean and one for the runoff entering the region. For States 1 and 2 (no ice cover), there is a term for the flux of heat from the atmosphere (the term with Q_{w1}), while for the states with ice (States 3 and 4), this term is replaced by a term for the flux of heat through the ice layer (the term with k). In the two states with two layers of water (States 2 and 4), there is an additional term to account for the flux of heat from the lower water layer (the term with k_{l1}).

For the salinity equations there is a term for the flux of water from the Arctic Ocean and one for the runoff entering the region. The Precipitation minus Evaporation term (PE_1) is also treated as a flux term, and is only found in States 1 and 2 because net precipitation is treated as snow in States 3 and 4, and so does not directly affect the salinity in the box. In States 2 and 4, the salinity flux from the lower layer is represented by the term with the coefficient k_{s1} . In States 3 and 4, there is an additional term:

$$(S_l - S_{ice})A_l \left(\frac{d\delta_l}{dt} - \frac{1}{A_l} (PE_l + I_{cis} - I_{denmark}) \right) .$$

This nonlinear term adds to (subtracts from) the salt content of the layer when ice is forming (melting) due to thermodynamic effects.

The ice thickness equations in States 3 and 4 consist of terms for ice advection into the region from the Arctic (I_{Gs}), for ice leaving the region through Denmark Strait ($I_{denmark}$), for net precipitation (PE_l) falling as snow on the ice layer, and terms which cause the ice thickness to change due to the heat flux from the air ($-Q_{il}$) and from the water below (the term proportional to k).

For the flux of water from the Arctic Ocean (region 3), the direct measurements of T_3 and S_3 from this region are not used in the equations here; instead, T'_3 and S'_3 are used. These primed variables take into account the fact that the mixed-layer depth in the Arctic Ocean is much less than the mixed-layer depth in the Greenland Sea region. In their usual states, States 2 and 4 for the Greenland Sea, and State 4 for the Arctic Ocean, the mixed layers are 200 meters for the former region and 40 meters for the latter. In this case, a weighted average of the temperature and salinity at the top and bottom layers for the upper 200 meters of the Arctic Ocean are used for T'_3 and S'_3 in the equations for the Greenland Sea.

Norwegian Sea

State 1

$$A_2 H_2 \frac{dT_2}{dt} = A_2 \frac{Q_{w2}}{\rho C_p} + (\text{Runoff}_2)(T_{\text{runoff}} - T_2) + (W_{\text{atl1}} + W_{\text{atl2}})(T_{\text{atl}} - T_2) + W_g(T_1 - T_2) + W_{\text{ncc}}(T_{\text{ncc}} - T_2) + D_1(T_4 - T_2) \quad , \quad (2.18a)$$

$$A_2 H_2 \frac{dS_2}{dt} = (\text{Runoff}_2 + \text{PE}_2)(-S_2) + W_{\text{atl1}}(S_{\text{atl1}} - S_2) + W_{\text{atl2}}(S_{\text{atl2}} - S_2) + W_g(S_1 - S_2) + W_{\text{ncc}}(S_{\text{ncc}} - S_2) + D_4(S_4 - S_2) \quad , \quad (2.18b)$$

$$\frac{d\delta_2}{dt} = 0 \quad , \quad (2.18c)$$

State 2

$$A_2 h_2 \frac{dT_2}{dt} = A_2 \frac{Q_{w2}}{\rho C_p} + A_2 k_{12}(T_{L2} - T_2) + (\text{Runoff}_2)(T_{\text{runoff}} - T_2) + W_g(T_1 - T_2) + (W_{\text{atl1}} + W_{\text{atl2}})(T_{\text{atl}} - T_2) + W_{\text{ncc}}(T_{\text{ncc}} - T_2) + D_1(T_4 - T_2) \quad , \quad (2.19a)$$

$$A_2 h_2 \frac{dS_2}{dt} = A_2 k_{s2}(S_{L2} - S_2) + (\text{Runoff}_2 + \text{PE}_2)(-S_2) + W_{\text{atl1}}(S_{\text{atl1}} - S_2) + W_{\text{atl2}}(S_{\text{atl2}} - S_2) + W_g(S_1 - S_2) + W_{\text{ncc}}(S_{\text{ncc}} - S_2) + D_4(S_4 - S_2) \quad , \quad (2.19b)$$

$$\frac{d\delta_2}{dt} = 0 \quad , \quad (2.19c)$$

State 3

$$A_2 H_2 \frac{dT_2}{dt} = A_2 \frac{k}{\rho C_p}(T_{f2} - T_2) + (\text{Runoff}_2)(T_{\text{runoff}} - T_2) + W_g(T_1 - T_2) + (W_{\text{atl1}} + W_{\text{atl2}})(T_{\text{atl}} - T_2) + W_{\text{ncc}}(T_{\text{ncc}} - T_2) + D_1(T_4 - T_2) \quad , \quad (2.20a)$$

$$A_2 H_2 \frac{dS_2}{dt} = (S_2 - S_{se}) A_2 \left(\frac{d\delta_2}{dt} - \frac{1}{A_2} (PE_2) \right) + (\text{Runoff}_2)(-S_2) + W_{atl1}(S_{atl1} - S_2) + W_{atl2}(S_{atl2} - S_2) \\ + W_g(S_1 - S_2) + W_{ncc}(S_{ncc} - S_2) + D_s(S_4 - S_2) \quad , \quad (2.20b)$$

$$\frac{d\delta_2}{dt} = \frac{1}{\rho_1 L} [-Q_{i2} + k(T_{i2} - T_2)] + \frac{1}{A_2} (PE_2) \quad , \quad (2.20c)$$

State 4

$$A_2 h_2 \frac{dT_2}{dt} = A_2 k_{i2}(T_{i2} - T_2) + A_2 \frac{k}{\rho C_p}(T_{i2} - T_2) + (\text{Runoff}_2)(T_{\text{runoff}} - T_2) + W_g(T_1 - T_2) \\ + (W_{atl1} + W_{atl2})(T_{atl} - T_2) + W_{ncc}(T_{ncc} - T_2) + D_t(T_4 - T_2) \quad , \quad (2.21a)$$

$$A_2 h_2 \frac{dS_2}{dt} = (S_2 - S_{se}) A_2 \left(\frac{d\delta_2}{dt} - \frac{1}{A_2} (PE_2) \right) + A_2 k_{s2}(S_{L2} - S_2) + (\text{Runoff}_2)(-S_2) \\ + W_g(S_1 - S_2) + W_{atl1}(S_{atl1} - S_2) + W_{atl2}(S_{atl2} - S_2) + W_{ncc}(S_{ncc} - S_2) + D_s(S_4 - S_2) \quad , \quad (2.21b)$$

$$\frac{d\delta_2}{dt} = \frac{1}{\rho_1 L} [-Q_{i2} + k(T_{i2} - T_2)] + \frac{1}{A_2} (PE_2) \quad . \quad (2.21c)$$

The equations for the Norwegian Sea are similar in form to those for the Greenland Sea. The differences, however, include terms representing the inflow of water from the Atlantic Ocean (the terms with W_{atl1} and W_{atl2}), from the Norwegian Coastal Current (W_{ncc}), from the Greenland Sea region (W_g), and from the Greenland Gyre through diffusion (D_t and D_s).

Arctic Ocean

State 1

$$A_3 H_3 \frac{dT_1}{dt} = A_3 \frac{Q_{w1}}{\rho C_p} + (\text{Runoff}_1)(T_{\text{runoff}} - T_1) + W_{\text{bering}}(T_{\text{bering}} - T_1) + W_{\text{ncc}}(T_{\text{ncc}} - T_1) + W_{\text{wac}}(T_2 - T_1) + W_{\text{bs}}(T_{\text{bs}} - T_1) \quad , \quad (2.22a)$$

$$A_3 H_3 \frac{dS_1}{dt} = (\text{Runoff}_1 + \text{PE}_1)(-S_1) + W_{\text{wac}}(S_2 - S_1) + W_{\text{bering}}(S_{\text{bering}} - S_1) + W_{\text{ncc}}(S_{\text{ncc}} - S_1) + W_{\text{bs}}(S_{\text{bs}} - S_1) \quad , \quad (2.22b)$$

$$\frac{d\delta_3}{dt} = 0 \quad , \quad (2.22c)$$

$$\frac{dT_{L3}}{dt} = 0 \quad , \quad (2.22d)$$

$$\frac{dS_{L3}}{dt} = 0 \quad , \quad (2.22e)$$

State 2

$$A_3 h_3 \frac{dT_3}{dt} = A_3 \frac{Q_{w3}}{\rho C_p} + A_3 k_{13}(T_{L3} - T_3) + (\text{Runoff}_3)(T_{\text{runoff}} - T_3) + W_{\text{bering}}(T_{\text{bering}} - T_3) + W_{\text{ncc}}(T_{\text{ncc}} - T_3) \quad , \quad (2.23a)$$

$$A_3 h_3 \frac{dS_3}{dt} = A_3 k_{s3}(S_{L3} - S_3) + (\text{Runoff}_3 + \text{PE}_3)(-S_3) + W_{\text{bering}}(S_{\text{bering}} - S_3) + W_{\text{ncc}}(S_{\text{ncc}} - S_3) \quad , \quad (2.23b)$$

$$\frac{d\delta_3}{dt} = 0 \quad , \quad (2.23c)$$

$$A_3 (H_3 - h_3) \frac{dT_{L3}}{dt} = A_3 k_{13}(T_3 - T_{L3}) + W_{\text{wac}}(T_2 - T_{L3}) + W_{\text{bs}}(T_{\text{bs}} - T_{L3}) \quad , \quad (2.23d)$$

$$A_3 (H_3 - h_3) \frac{dS_{L3}}{dt} = A_3 k_{s3}(S_3 - S_{L3}) + W_{\text{wac}}(S_2 - S_{L3}) + W_{\text{bs}}(S_{\text{bs}} - S_{L3}) \quad , \quad (2.23e)$$

State 3

$$A_1 H_1 \frac{dT_1}{dt} = A_1 \frac{k}{\rho C_p} (T_{f1} - T_1) + (\text{Runoff}_3)(T_{\text{runoff}} - T_3) + W_{\text{bering}}(T_{\text{bering}} - T_3) \quad , \quad (2.24a)$$

$$+ W_{\text{ncc}}(T_{\text{ncc}} - T_1) + W_{\text{wsc}}(T_2 - T_3) + W_{\text{bs}}(T_{\text{bs}} - T_3)$$

$$A_1 H_1 \frac{dS_1}{dt} = (S_1 - S_{\text{ncc}})A_1 \left(\frac{d\delta_1}{dt} - \frac{1}{A_1}(\text{PE}_3 - I_{\text{arctic}}) \right) + (\text{Runoff}_3)(-S_3) + W_{\text{wsc}}(S_2 - S_3) \quad , \quad (2.24b)$$

$$+ W_{\text{bering}}(S_{\text{bering}} - S_1) + W_{\text{ncc}}(S_{\text{ncc}} - S_3) + W_{\text{bs}}(S_{\text{bs}} - S_3)$$

$$\frac{d\delta_1}{dt} = \frac{1}{\rho_1 L} [-Q_{11} + k(T_{f1} - T_1)] + \frac{1}{A_1}(\text{PE}_3 - I_{\text{arctic}}) \quad , \quad (2.24c)$$

$$\frac{dT_{L3}}{dt} = () \quad , \quad (2.24d)$$

$$\frac{dS_{L3}}{dt} = () \quad , \quad (2.24e)$$

State 4

$$A_3 h_1 \frac{dT_1}{dt} = A_3 \frac{k}{\rho C_p} (T_{f1} - T_1) + A_3 k_{13}(T_{L3} - T_3) + (\text{Runoff}_3)(T_{\text{runoff}} - T_3) \quad , \quad (2.25a)$$

$$+ W_{\text{bering}}(T_{\text{bering}} - T_1) + W_{\text{ncc}}(T_{\text{ncc}} - T_3)$$

$$A_3 h_1 \frac{dS_1}{dt} = (S_1 - S_{\text{ncc}})A_3 \left(\frac{d\delta_1}{dt} - \frac{1}{A_3}(\text{PE}_3 - I_{\text{arctic}}) \right) + A_3 k_{13}(S_{L3} - S_3) + (\text{Runoff}_3)(-S_3) \quad , \quad (2.25b)$$

$$+ W_{\text{bering}}(S_{\text{bering}} - S_1) + W_{\text{ncc}}(S_{\text{ncc}} - S_3)$$

$$\frac{d\delta_1}{dt} = \frac{1}{\rho_1 L} [-Q_{11} + k(T_{f1} - T_1)] + \frac{1}{A_3}(\text{PE}_3 - I_{\text{arctic}}) \quad , \quad (2.25c)$$

$$A_1(H_1 - h_1) \frac{dT_{L3}}{dt} = A_1 k_{11}(T_3 - T_{L3}) + W_{\text{wsc}}(T_2 - T_{L3}) + W_{\text{bs}}(T_{\text{bs}} - T_{L3}) \quad , \quad (2.25d)$$

$$A_1(H_1 - h_1) \frac{dS_{L3}}{dt} = A_1 k_{13}(S_3 - S_{L3}) + W_{\text{wsc}}(S_2 - S_{L3}) + W_{\text{bs}}(S_{\text{bs}} - S_{L3}) \quad . \quad (2.25e)$$

Two new variables appear in the equations of the Arctic Ocean region, T_{L3} and S_{L3} , the temperature and salinity of the lower layer. These variables are necessary because as the West Spitsbergen Current flows north through Fram Strait, it cools and therefore sinks down and affects only the lower layer of the model Arctic Ocean. This inflow is taken into account through the terms with W_{WSC} . The Barents Sea inflow (W_{BS}) is also specified as entering the Arctic Ocean through the lower layer of the region. The other water inflows into the Arctic Ocean are from the Bering Strait (the term with W_{bering}) and from the Norwegian Coastal Current (W_{ncc}). Note that we have neglected any outflow from the western Arctic into the Canadian Arctic Archipelago.

Greenland Gyre

State 1

$$A_4 H_4 \frac{dT_4}{dt} = A_4 \frac{Q_{w4}}{\rho C_p} + D_i (T_2 - T_4) + A_4 k_{i2} (T_{L2} - T_4) \quad , \quad (2.26a)$$

$$A_4 H_4 \frac{dS_4}{dt} = D_s (S_2 - S_4) + A_4 k_{s2} (S_{L2} - S_4) + PE_4 (-S_4) \quad , \quad (2.26b)$$

$$\frac{d\delta_4}{dt} = 0 \quad , \quad (2.26c)$$

State 2

$$A_4 h_4 \frac{dT_4}{dt} = A_4 \frac{Q_{w4}}{\rho C_p} + D_i (T_2 - T_4) + A_4 k_{i4} (T_{L2} - T_4) \quad , \quad (2.27a)$$

$$A_4 h_4 \frac{dS_4}{dt} = D_s (S_2 - S_4) + A_4 k_{s4} (S_{L2} - S_4) + PE_4 (-S_4) \quad , \quad (2.27b)$$

$$\frac{d\delta_4}{dt} = 0 \quad , \quad (2.27c)$$

State 3

$$A_4 H_4 \frac{dT_4}{dt} = A_4 C_4 \left(\frac{k}{\rho C_p} (T_{F4} - T_4) \right) + A_4 (1 - C_4) \frac{Q_{w4}}{\rho C_p} + D_1 (T_2 - T_4) + A_4 k_{12} (T_{L2} - T_4) \quad , \quad (2.28a)$$

$$A_4 H_4 \frac{dS_4}{dt} = C_4 (S_4 - S_{ice}) A_4 \left(\frac{d\delta_4}{dt} - \frac{1}{A_4} (PE_4) \right) + D_1 (S_2 - S_4) + A_4 k_{12} (S_{L2} - S_4) + (1 - C_4) PE_4 (-S_4) \quad , \quad (2.28b)$$

$$\frac{d\delta_4}{dt} = \frac{1}{\rho_i L} [-Q_{i4} + k(T_{F4} - T_4)] + \frac{1}{A_4} (PE_4) \quad , \quad (2.28c)$$

State 4

$$A_4 h_4 \frac{dT_4}{dt} = A_4 C_4 \left(\frac{k}{\rho C_p} (T_{F4} - T_4) \right) + A_4 (1 - C_4) \frac{Q_{w4}}{\rho C_p} + D_1 (T_2 - T_4) + A_4 k_{14} (T_{L2} - T_4) \quad , \quad (2.29a)$$

$$A_4 h_4 \frac{dS_4}{dt} = C_4 (S_4 - S_{ice}) A_4 \left(\frac{d\delta_4}{dt} - \frac{1}{A_4} (PE_4) \right) + D_1 (S_2 - S_4) + A_4 k_{14} (S_{L2} - S_4) + (1 - C_4) PE_4 (-S_4) \quad , \quad (2.29b)$$

$$\frac{d\delta_4}{dt} = \frac{1}{\rho_i L} [-Q_{i4} + k(T_{F4} - T_4)] + \frac{1}{A_4} (PE_4) \quad . \quad (2.29c)$$

The equations for the Greenland Gyre were developed using the same principles as for the other regions. But there are a few differences. The gyre is the only region without any runoff (because of its location in the middle of another water basin) and without any advection from the other regions. Its only link with the four other basins is through diffusion with the Norwegian Sea. Another difference is the inclusion of some open water in the region even when the gyre is in States 3 or 4. This feature makes the system more realistic. An examination of sea-ice cover in the gyre region (Mysak and Wang 1991) shows that around 75°N, 0° (where the gyre is centered), the ice cover reaches a maximum of between 1/10 and 5/10 in winter. Thus to consider a region with complete ice cover at the instant ice is formed in the gyre is not very realistic. To simulate the region of open water when ice is formed, the quantity C_4 is

introduced: the concentration, in tenths, of sea ice in a unit area in the gyre region. This quantity is taken to be 0.3 in the Greenland Gyre. During ice-cover periods, the quantities C_4 and $(1-C_4)$ thus appear in the various heat flux and freshwater flux terms.

The presence of two different sets of exchange coefficients should also be noted in the equations: k_{t2} , k_{s2} and k_{t4} , k_{s4} . This occurs because the gyre is a relatively small region embedded in the Norwegian region, a bigger and deeper region. When the gyre is in a two-layer state (States 2 or 4), its lower layer (lying between 40 and 200 meters) uses fixed parameters, and the top layer (of thickness of 40 meters) exchanges temperature and salinity with that lower layer using the coefficients k_{t4} and k_{s4} . This lower layer can be seen as a dome of deep water occupying the depth range between 40 and 200 meters in the gyre region. This deep water is brought up in this region because of the upward movement of the water due to the cyclonic circulation of the gyre. When the gyre is in a one-layer state (States 1 or 3), the top 200 meters is now a layer exchanging temperature and salinity with a still deeper layer, the layer starting at a depth of 200 meters. This layer is exactly the same lower layer used for the Norwegian Sea region, and the exchange coefficients used are thus the same, i.e., k_{t2} and k_{s2} .

3. First Experiment: The control run

3.1 Results in the four regions.

The differential equations presented in the previous section were integrated numerically using a Runge-Kutta numerical scheme of the fourth order, adapted from a fortran subroutine given in Press *et al.* (1989). The computer program for this integration was coded using the fortran computer language on a workstation (IBM RISC 6000). Using all the physical parameters prescribed in the previous section, the system was run for a period of 130 years using a time step of 12 hours. The climatological air temperatures used are given in Table 3.1 (from the references given on page 29) and the initial conditions in Table 3.2. Figures 3.1 to 3.4 show the time evolution of all the different variables of the system in the four regions for the last five years of the 130-year integration. The 130-year period was chosen to allow the model enough time to reach an equilibrium state. From various experiments with different initial conditions, it was found that the equilibrium state is not sensitive to the initial state. The initial conditions in Table 3.2 represent realistic values (as shown later in this section). The sensitivity of the model to some of the parameters is discussed at the end of section 3.1.

In the Greenland Sea (figure 3.1), the temperature of the upper layer of water falls slowly from a late summer maximum of 0.17 °C to a late spring minimum of -0.63 °C during the year. The salinity varies between 34.243 and 34.320 and the region has up to 0.46 meters of ice during the winter. Note that during the ice growth season (late fall, early winter), the salinity rapidly increases. The ice melts completely during the summer.

Table 3.1 Monthly mean air temperatures used in the model (in degrees Celsius).

	Greenland Sea	Norwegian Sea	Arctic Ocean	Greenland Gyre
January	-12.50	-2.50	-31.560	-10.00
February	-8.25	-1.50	-34.600	-7.50
March	-8.25	-1.25	-26.220	-7.50
April	-7.50	-1.25	-23.080	-7.50
May	-2.50	3.00	-10.390	2.50
June	2.00	5.00	-0.990	2.50
July	4.00	7.50	-0.850	5.00
August	4.00	7.50	-1.393	5.00
September	1.25	7.00	-9.469	1.75
October	-2.50	5.00	-22.960	-5.00
November	-7.50	1.00	-29.220	-5.00
December	-12.50	0.00	-33.760	-7.50

Table 3.2 Initial conditions used in the control run.

Greenland Sea	Norwegian Sea	Arctic Ocean	Greenland Gyre
$T_1 = -1.0\text{ }^{\circ}\text{C}$ $S_1 = 34.0$ $\delta_1 = 0.5\text{ m}$	$T_2 = 2.0\text{ }^{\circ}\text{C}$ $S_2 = 35.0$ $\delta_2 = 0.0\text{ m}$	$T_3 = -1.5\text{ }^{\circ}\text{C}$ $S_3 = 33.0$ $\delta_3 = 4.0\text{ m}$ $T_{L3} = 0.0\text{ }^{\circ}\text{C}$ $S_{L3} = 34.5$	$T_4 = -1.0\text{ }^{\circ}\text{C}$ $S_4 = 34.9$ $\delta_4 = 0.1\text{ m}$

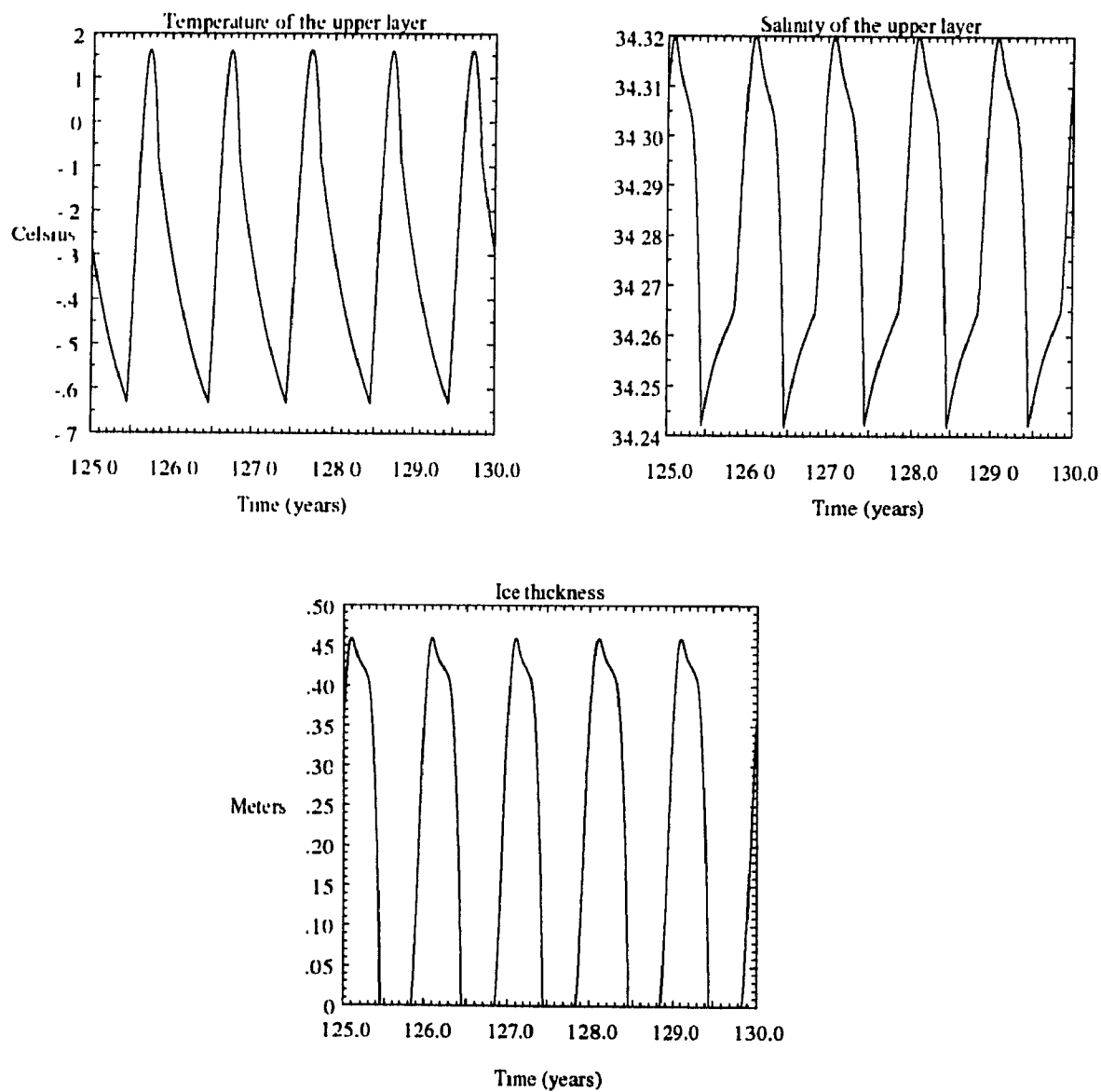


Fig. 3.1. Results from the control run for the Greenland Sea region.

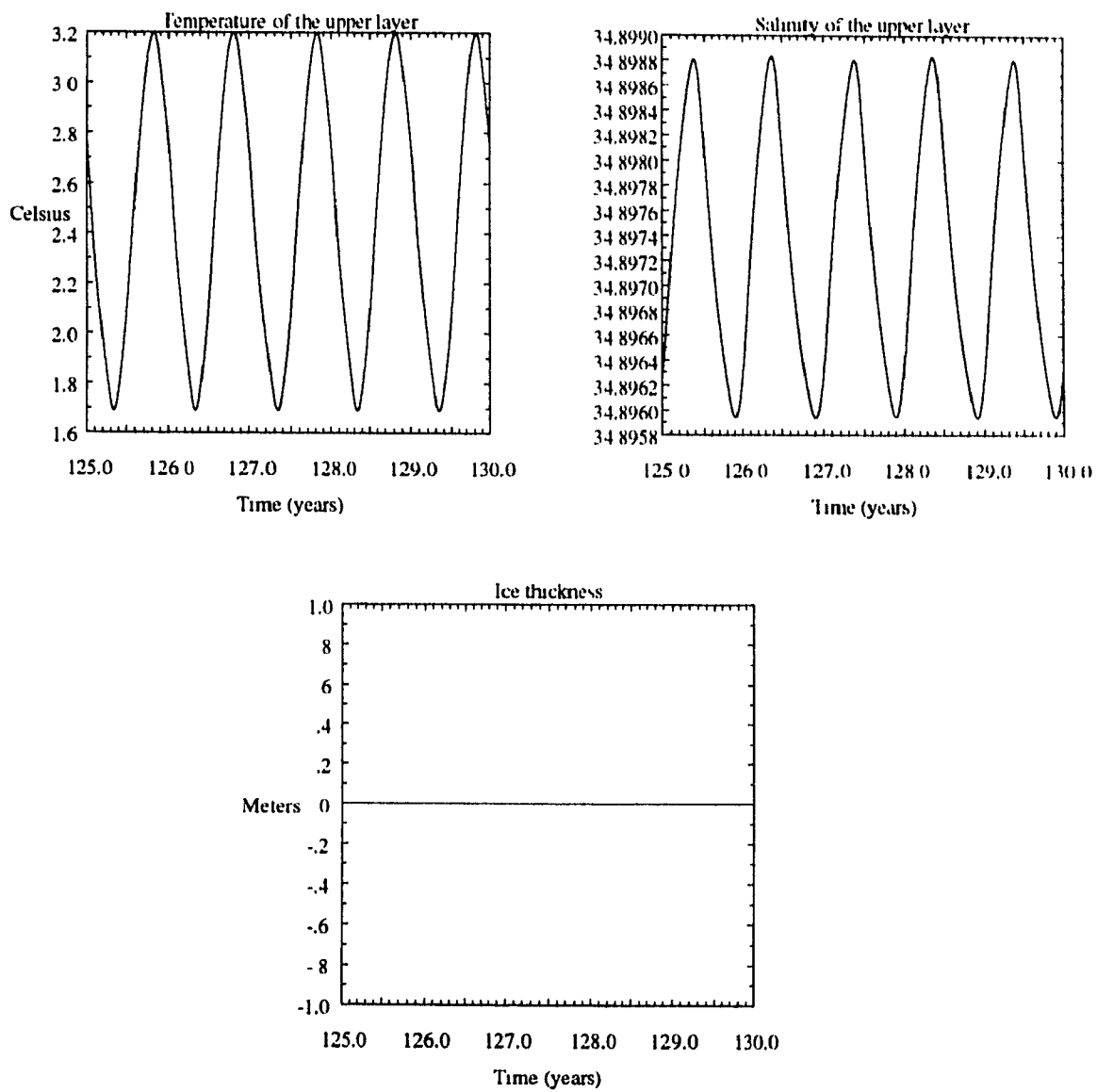


Fig. 3.2. Results from the control run for the Norwegian Sea region.

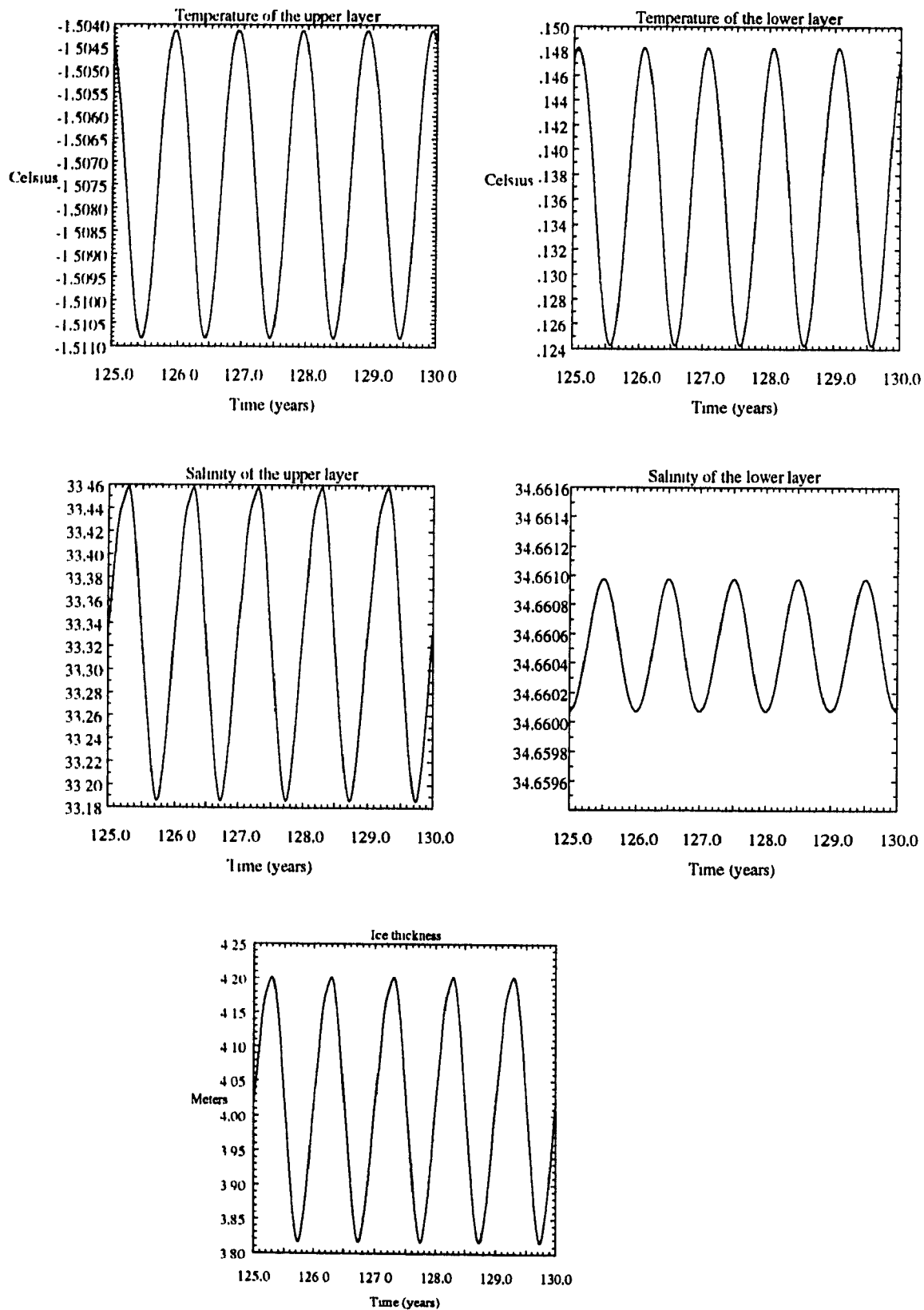


Fig. 3.3. Results from the control for the Arctic Ocean region.

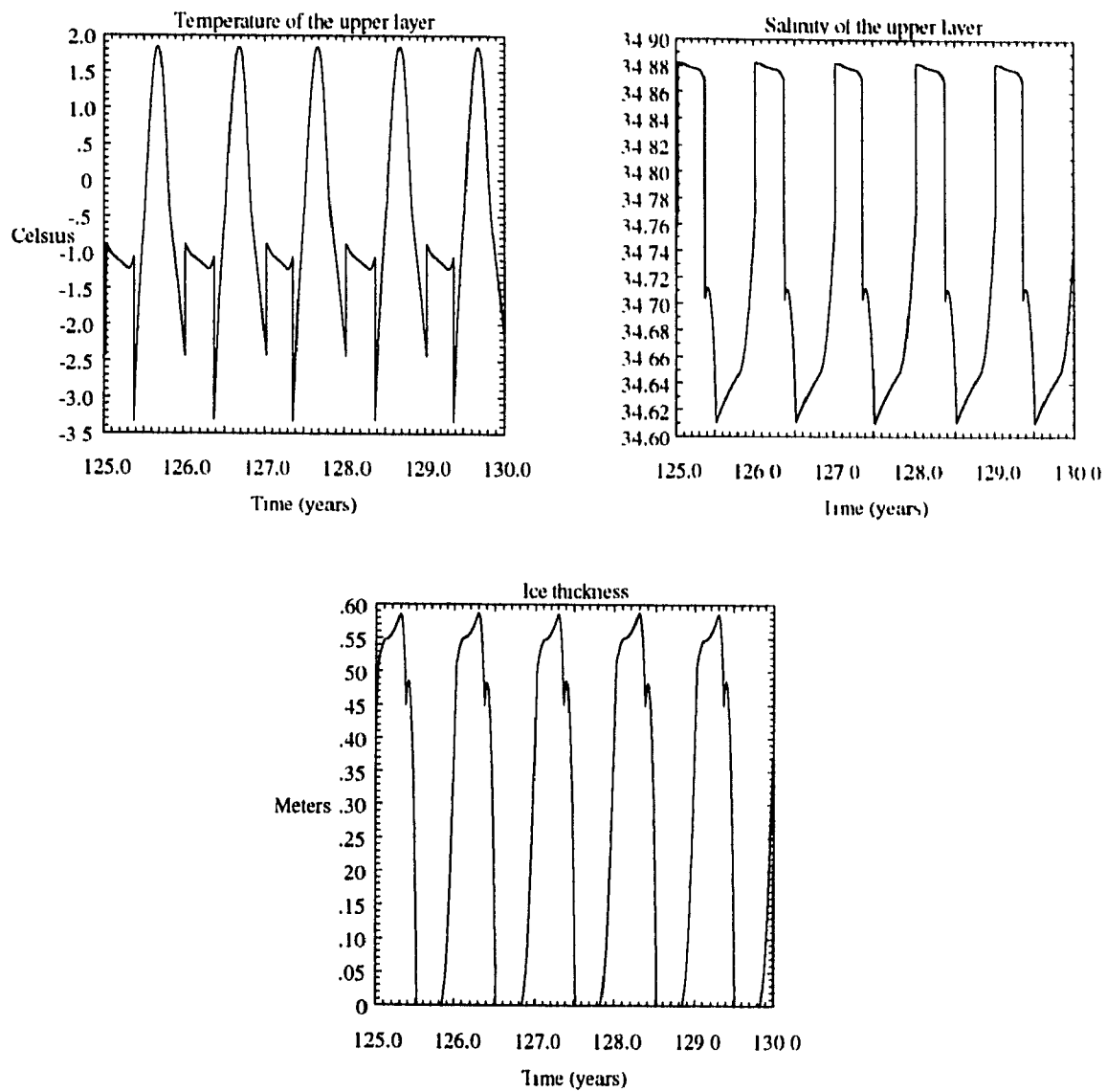


Fig. 3.4. Results from the control run for the Greenland Gyre region.

In the Norwegian Sea (figure 3.2), the upper layer is warmer and saltier than in the Greenland Sea. The temperature oscillates between 1.7°C and 3.2°C but the salinity is quite stable, varying only between 34.8960 and 34.8988. This is because the ice never appears during the course of a year in this region.

In the Arctic Ocean (figure 3.3), the system has a cold and fresh upper layer lying over a relatively warm and salty lower layer. The upper layer is on average at -1.507°C and has an average salinity of 33.34; the lower layer is on average at 0.135°C , with a average salinity of 34.6605. The ice thickness in the Arctic Ocean region oscillates during the year with an amplitude of about 0.38 m and a mean of about 4.03 m.

Finally, for the Greenland Gyre (Figure 3.4), the temperature cycle over a year exhibits a larger amplitude than in the other regions, with temperatures ranging from -3.4°C (for a very brief period at the end of the winter) to 1.8°C , but above -1.2°C for most of the year. The large amplitude is due to a shallower mixed layer in that region (40 meters as opposed to 200 meters in the Greenland and Norwegian Seas) which is very sensitive to atmospheric temperatures. At the end of the winter, the region experiences, for a brief period, very low temperatures at the surface. Since the lower layer temperature and salinity are fixed, when the system switches from one layer to two layers, the region must return to these fixed lower layer conditions. The rapid decrease in the temperature of the water occurs because a conservation of temperature and salinity through the whole box is used while switching from one layer to two. This conservation assures that the average temperature and salinity over the two layers are equal to the temperature and salinity of the single layer to start with. At the end of the winter the upper layer is below -0.5°C (the fixed lower temperature). When the system switches from one to two layers, with the lower layer going to a

fixed value of -0.5°C , the model must compensate for the warmer condition at the lower layer, and thus the region experiences an artificial low temperature at the surface (to conserve the temperature in the whole column of water). Hence the temperature drops to -3.4°C for a short period. This artificial cooling should not have any significant effects on the other results in the model because it occurs only in the shallow upper layer of the gyre region, lasts only for a part of the spring period, and the effect of the temperature of the gyre on the temperature of the upper layer in the Norwegian Sea is small (see Table 3.5). Nevertheless, this non-physical behaviour should be eliminated from the model in the future. This could be done by allowing the temperature and salinity of the lower layer in the Greenland/Norwegian Sea and Greenland Gyre to vary through time.

Figure 3.5 shows the different states each region achieves during a year. The Greenland Sea goes from State 2 (no ice with two layers) to State 4 (ice with two layers) during winter, and then back in State 2 in the spring. The Norwegian Sea stays all the time in State 2 while the Arctic is always in State 4. The Greenland Gyre region has a more complex behaviour. During the summer, the region is in State 2. When the air temperature gets cold enough, ice forms and the system enters State 4. With the formation of this ice, salt is rejected into the upper layer of the water column. This flux of salt, linked to colder atmospheric temperatures increases the density of the upper layer until it reaches the density of the lower layer. When this happens the two layers are mixed together in one thick layer, with still an ice cover on it (State 3). State 3 will continue until spring when, due to warmer atmospheric temperatures and hence ice melt, the system goes to State 4 (two-layer system with ice). The system stabilizes itself because of the freshwater created during this period of ice melt. The region stays in State 4 until the ice completely melts, which makes the region go to State 2 (two-layer state with no ice).

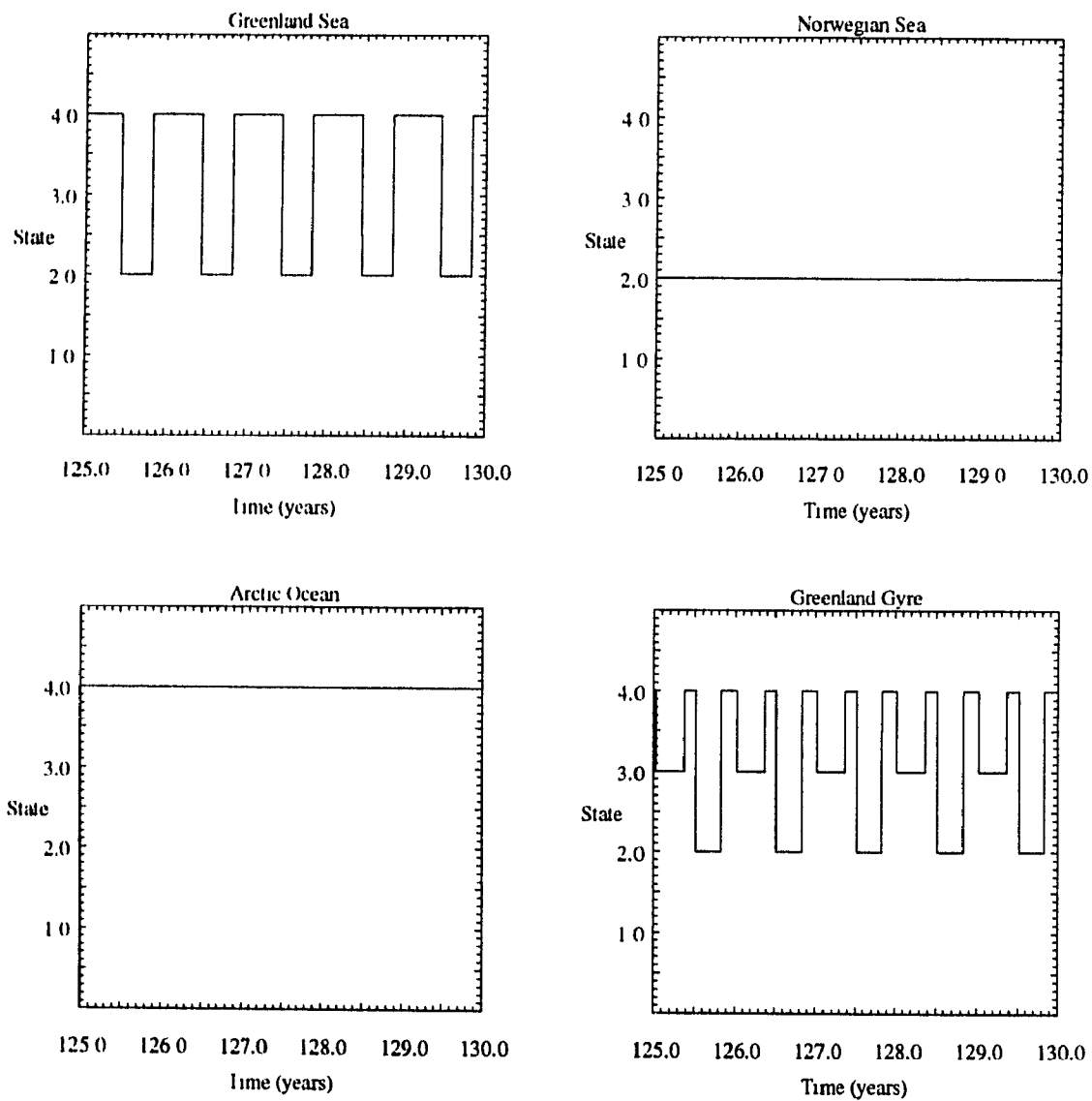


Fig. 3.5. States for the four regions in the control run.

The results plotted in figures 3.1 to 3.4 generally agree with observations. We first compare our results with ice thickness observations. Bourke and Garrett (1987) show seasonal ice thickness values observed in the regions modelled in this thesis. The ice thickness in the central part of the Arctic Ocean region is generally observed to be in the 3 to 5 m range during the whole year. A considerable part of the Norwegian Sea is ice free during the whole year. The Greenland Sea region is nearly completely ice free during the summer, and has an ice thickness between 0 and 2 m during the winter. For the Greenland Gyre region, the observations show no ice during the summer. In winter the region sits close to the ice edge, and therefore sometimes has partial ice cover.

Upon comparing the above observations with the calculated ice thicknesses we conclude that the model simulates relatively well the ice cover thickness in the Arctic Ocean and Norwegian Sea regions (see Fig. 3.2 and 3.3), but does less well for the Greenland Sea (Fig. 3.1) and the Greenland Gyre (Fig. 3.4). The model ice is not thick enough during winter in the Greenland Sea, and in the Greenland Gyre, the ice cover is too persistent. The former discrepancy may indicate a lack of sensitivity of the model to ice advection from the Arctic Ocean.

From Coachman and Aagaard (1974) we note that observations of the surface layer in the Arctic Ocean show temperatures of the order of -1 to -2 °C. Between 100 and 200 meters the water temperatures become warmer (getting closer to 0 °C). These two estimates agree with the results from the model (Fig. 3.3). Figure 3.6 shows the results from temperature observations published in Clarke *et al.* (1990) for the February-June 1982 period. The figure shows a southeast-northwest section of the Greenland Sea and Norwegian Sea region, with the station numbers at the top of the

figure. The Norwegian Sea in this model is represented by the stations between 105 and 120. The Greenland Gyre in this model is situated near the stations 57 and 59. For the Norwegian Sea, the observations show upper-layer temperatures in the 1 to 5 °C range. A temperature profile for the Greenland Sea in Coachman and Aagaard (1974) shows temperatures in the upper 200 m (their Fig 4., profile #5) ranging from 1 °C to -1.5 °C. The model simulates well this difference between the two regions (see Figs. 3.1 and 3.2). For the Greenland Gyre, the temperature observed at the surface in Fig. 3.6 is -1.2 °C, which is colder than the surrounding temperatures. This colder temperature for the Greenland Gyre region has been simulated in the model during winter time (Fig. 3.4).

From Coachman and Aagaard (1974) we note that the salinity in the upper waters of the Eurasian Basin (part of the region in the Arctic Ocean between the North Pole and Fram Strait) is observed to lie in the 33 to 34 range. At greater depths, the salinity increases up to 34.5. This is simulated by the model, although the lower layer is a little too saline (Fig. 3.3). The sea surface salinity field in the Norwegian Sea can be seen in Fig. 3.7 and in figure 2.2 for the Greenland, Norwegian Sea and Greenland Gyre as defined in this model. For the Greenland Gyre, the surface salinity is close to 34.9. The Norwegian Sea region shows salinity usually higher (in the 35.0 to 35.2 range for most of the region). For the Greenland Sea, the decrease in the salinity field west of the 0° line between 75°N and 80°N (Fig. 2.2) seems to indicate values of salinity lower than 34.4 for the area near the east coast of Greenland. This also can be seen in figure 5 of Coachman and Aagaard (1974) who show salinities for that region in the 31 to 34 range. This east-west variation in the salinity field is simulated fairly well by the model, although the modelled-predicted salinity for the Greenland Sea is somewhat higher than the average of the observed values, and the salinity predicted for the Norwegian Sea is less than the average of the observed values.

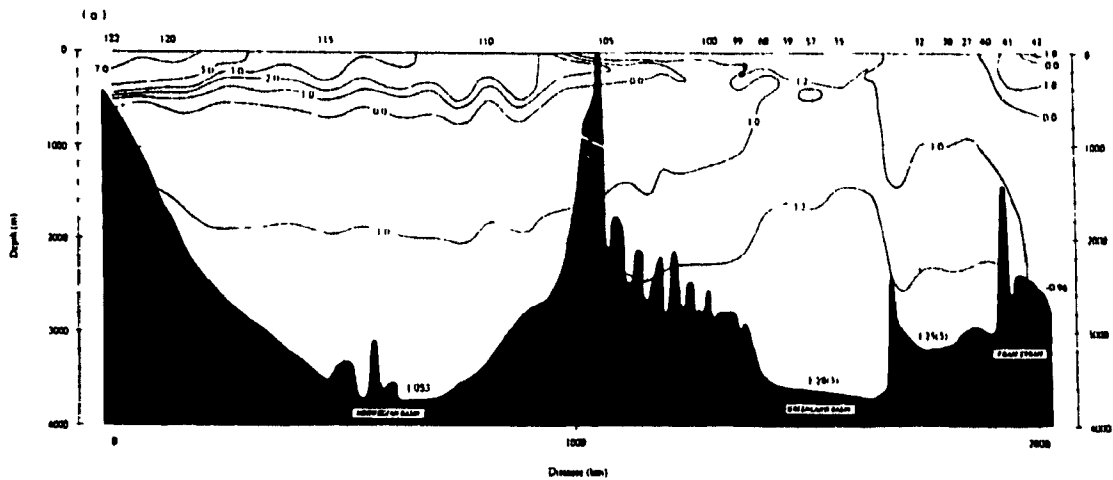


Fig 3.6. Potential temperature in the Norwegian and Greenland basins (from Clarke *et al* , 1990).

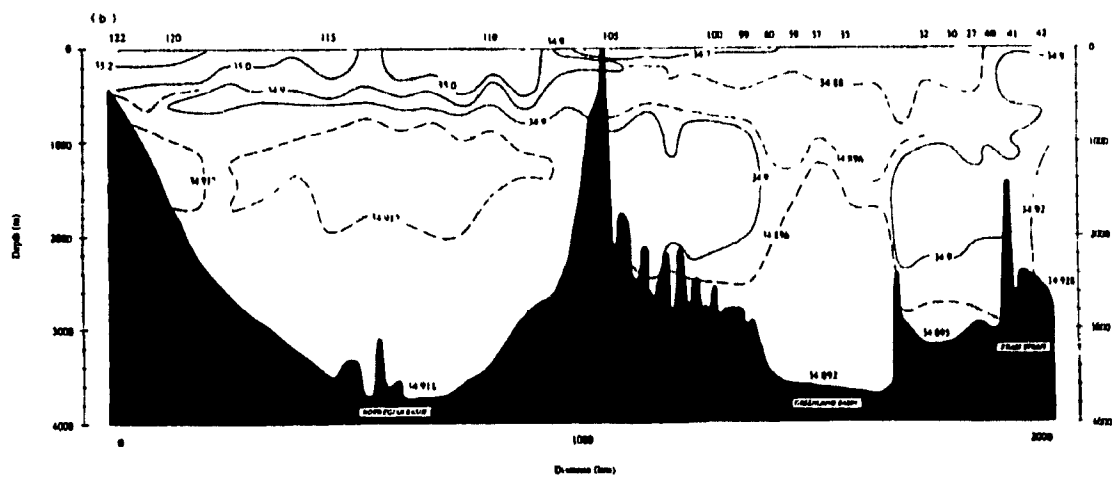


Fig 3.7. Salinity in the Norwegian and Greenland basins (from Clarke *et al* , 1990)

This model, as in any model, is sensitive to changes in some of its parameters. For example, an increase in the lower temperature in the Norwegian Sea and Greenland Gyre from -0.5°C to 0.0°C will make the convection at the surface of the gyre occur until the end of the winter, which means a period of convection in winter $1\frac{1}{2}$ month longer than before.

As written at the end of section 2.2, the parameters A_t and A_s are used to tune the model. A variation of these parameters will change the sensitivity of the Gyre region to the conditions in the Norwegian Sea. If these parameters are changed inside the range of values used in Darby and Willmott (1993), the upper layer convection in the Gyre can be stopped completely because the Gyre is moving toward a more stable condition as found in the Norwegian Sea.

The sensitivity of the model to the exchange coefficients k_t and k_s is relatively small. The coefficients k_t and k_s can be increase or decrease by a factor 100 before small changes start to occur in the states of the four regions. Naturally the basic properties in the four regions (water temperature, salinity, and ice thickness) will vary as k_t and k_s are changed, but these variations are not enough to actually change the state a region is in normally. This result could signify that different k_t and k_s could be used in the model to actually get better results (to tune the results toward some observations) without changing the overall picture of the four regions (i.e., the states of the four regions).

3.2 Scale Analysis of the different terms in the governing equations.

Another way to analyse the results of the control run is to determine the magnitudes of the different terms of the differential equation for each state for each region in the model. From this analysis we can determine, on a regional basis, which processes are most important in the simulation. For each differential equation in the model, the different terms were plotted as a function of time, and the resulting graphs are shown in the appendix. These graphs are in units of $10^{-10} \text{ }^{\circ}\text{C s}^{-1}$ for the variations in temperature, in units of 10^{-10} s^{-1} for the variations in salinity, and in units of $10^{-10} \text{ m s}^{-1}$ for the variations in ice thickness. In Tables 3.3 to 3.9 these graphs are summarized in terms of the average, maximum and minimum for each term. These tables and graphs give a good indication of the relative magnitude of each term in one type of differential equation (e.g., temperature, salinity or ice thickness).

For the Greenland Sea in State 2 (no ice cover, two-layer system, see table 3.3), the atmospheric heat flux is the most important process for causing the variations in temperature; the water coming in from the Arctic Ocean is the second most important term, but is an order of magnitude smaller. For the salinity equation, the principal terms are the water advection from the Arctic and the Precipitation minus Evaporation. It is interesting to note the relatively low impact of the runoff on the variations of temperature and salinity. This will be generally true for all the equations in each region; i.e., runoff will be at least an order of magnitude smaller than the most important term. The small effect of runoff is due to the fact that in a box model runoffs from localized sources are smeared out over a relatively large region.

For the same region, but now in State 4 (ice-cover, two-layer system, see table 3.4), the upward heat flux through the ice-water interface is the most important term in the temperature equation, while in the salinity equation the variation in the ice thickness is the most important term. This variation in salinity is caused by salt rejection when the ice is forming, and by freshwater input when the same ice is melting. For both equations the advection of water from the Arctic Ocean is the second most important term. For the ice thickness, the heat fluxes are of primary importance, and the ice advection terms are of secondary importance.

In conclusion, in the Greenland Sea the most important effects are: the atmospheric forcing, the ice-water heat flux, and the advection of water from the Arctic Ocean via the East Greenland Current.

Table 3.3 Numerical estimate of the terms for the Greenland Sea (State 2).

Temperature Terms (from Fig. A-1)	Average	Maximum	Minimum
Atmospheric flux	498.76	1257.60	-1403.25
Flux from the lower layer	-13.88	4.52	-23.11
Arctic Ocean water	-28.70	127.49	-106.73
Runoff	0.29	0.37	0.26
Salinity Terms (from Fig. A-2)	Average	Maximum	Minimum
Flux from the lower layer	3.43	3.50	3.38
Runoff	-4.77	-4.77	-4.77
Precipitation minus Evaporation	-16.75	-16.74	-16.75
Arctic Ocean water	36.40	47.83	31.17

Table 3.4 Numerical estimate of the terms for the Greenland Sea (State 4).

Temperature Terms (from Fig. A-3)	Average	Maximum	Minimum
Flux from the lower layer	-3.35	4.56	-14.68
Flux across the ice-water interface	-344.02	-290.53	-419.11
Arctic Ocean water	64.17	127.91	-33.02
Runoff	0.33	0.37	0.29
Salinity Terms (from Fig. A-4)	Average	Maximum	Minimum
Variations in the ice thickness	-41.30	87.40	-378.91
Runoff	-4.78	-4.77	-4.78
Flux from the lower layer	3.20	3.50	3.09
Arctic Ocean water	31.48	47.71	24.31
Ice Thickness Terms (from Fig. A-5)	Average	Maximum	Minimum
Atmospheric flux	1031.76	2054.28	-1481.95
Flux across the ice-water interface	-1313.79	-1109.53	-1600.57
Precipitation minus Evaporation	97.79	97.79	97.79
Ice imported from Fram Strait	422.97	434.76	399.70
Ice exported through Denmark Strait	-241.70	-228.40	-248.44

The Norwegian Sea is always in State 2 (no ice, two-layer system, see table 3.5). In this region, as in the case of the Greenland Sea region, the atmospheric flux has the largest effect on the temperature variations, with the advection of relatively warm water from the northern North Atlantic being of secondary importance. In the salinity equations, the saline water from the northern North Atlantic is the most important forcing term in the system.

Table 3.5 Numerical estimate of the terms for the Norwegian Sea (State 2).

Temperature Terms (from Fig. A-6)	Average	Maximum	Minimum
Atmospheric flux	5.01	1517.42	-1473.79
Flux from the lower layer	-102.73	-76.52	-129.17
Runoff	-0.14	0.10	-0.38
Advection West-East	-159.99	-132.28	-192.18
North Atlantic Water	278.31	412.41	143.00
Norwegian Coastal Current	31.94	47.33	16.41
Diffusion from the Gyre	-51.98	-7.09	-124.33
Salinity Terms (from Fig. A-7)	Average	Maximum	Minimum
Flux from the lower layer	-0.07	-0.08	0.06
Runoff	-11.17	-11.17	-11.18
Precipitation minus Evaporation	-17.06	-17.06	-17.06
North Atlantic Water	75.76	76.00	75.49
Advection West-East	-36.08	-33.80	-38.47
Norwegian Coastal Current	-10.20	-10.17	-10.23
Diffusion from the Gyre	-1.31	-0.51	-2.02

In the Arctic Ocean, the system is always in State 4 (ice cover, two-layer system, see table 3.6). The temperature in the upper layer varies mainly because of heat fluxes from above or below: a cooling due to the upward heat flux through the ice-water interface or a warming due to the heat flux from the lower layer of water. For the salinity of the upper layer, the biggest effect is due to the variations of ice thickness which occurs because of salt rejection or ice melt. The runoff is the second most important term; it is only in the Arctic that this effect has any noticeable consequences. The effects of runoff are certainly important locally, but in a region like the Arctic Ocean its effects are smoothed out over the whole basin. For the variations in the ice thickness, the two most important effects are from atmospheric heat flux, and the heat flux across the ice-water interface.

The Greenland Gyre can be found in three states over the course of a seasonal cycle: State 2 (no ice, two-layer system), State 3 (ice cover, one-layer system), and State 4 (ice, two-layer system). In State 2 (see Table 3.7) the most important process affecting the temperature of the upper layer of water is the atmospheric forcing due to the air temperatures. But the heat flux from the lower layer of water and the diffusion of heat from the Norwegian Sea are also not negligible. In the right hand side of the salinity equation, the two dominant terms are the Precipitation minus Evaporation and the diffusion from the Norwegian Sea.

For State 3 (see table 3.8) the temperature changes are mainly due to the large atmospheric heat flux through the leads (which occurs because of the big temperature differences between the air and the water in winter) and the diffusion of heat from the Norwegian Sea. Salinity changes are caused by three processes with the same order of

Table 3.6 Numerical estimate of the terms for the Arctic Ocean (State 4).

Temperature Terms (from Fig. A-8)	Average	Maximum	Minimum
Flux from the lower layer	286.96	288.65	285.20
Flux across the ice-water interface	-371.46	-362.63	-379.19
Runoff	9.60	9.61	9.59
Bering Strait water	10.63	10.70	10.56
Norwegian Coastal Current	64.27	64.33	64.21
Salinity Terms (from Fig. A-9)	Average	Maximum	Minimum
Variations in the ice thickness	53.91	308.29	-258.54
Runoff	-91.23	-90.84	-91.59
Flux from the lower layer	34.92	38.62	31.49
Bering Strait water	-17.32	-14.36	-20.06
Norwegian Coastal Current	19.66	22.25	17.26
Ice Thickness Terms (from Fig. A-10)	Average	Maximum	Minimum
Atmospheric flux	359.81	721.11	-82.10
Flux across the ice-water interface	-283.72	-276.97	-289.62
Precipitation minus Evaporation	29.86	29.86	29.86
Ice exported through Fram Strait	-106.05	-100.79	-110.95

Table 3.7 Numerical estimate of the terms for the Greenland Gyre (State 2).

Temperature Terms (from Fig. A-11)	Average	Maximum	Minimum
Atmospheric flux	728.41	6951.04	-7907.50
Flux from the lower layer	-1350.44	-98.03	-2040.19
Diffusion from the Norwegian Sea	578.11	1173.44	330.21
Salinity Terms (from Fig. A-12)	Average	Maximum	Minimum
Flux from the lower layer	36.47	39.22	45.12
Diffusion from the Norwegian Sea	86.93	94.16	80.81
Precipitation minus Evaporation	-84.66	-84.61	-84.71

Table 3.8 Numerical estimate of the terms for the Greenland Gyre (State 3).

Temperature Terms (from Fig. A-13)	Average	Maximum	Minimum
Flux across the ice-water interface	-56.45	-47.70	-71.76
Atmospheric flux through the leads	-1155.32	662.33	-1847.69
Flux from the lower layer	21.19	25.56	13.54
Diffusion from the Norwegian Sea	1029.50	1158.48	911.88
Salinity Terms (from Fig. A-14)	Average	Maximum	Minimum
Variations in the ice thickness	-6.85	6.42	-61.24
Flux from the lower layer	0.17	0.22	0.15
Diffusion from the Norwegian Sea	6.45	9.86	4.72
P-E through the leads	-11.94	-11.93	-11.94
Ice Thickness Terms (from Fig. A-15)	Average	Maximum	Minimum
Atmospheric flux	565.71	1022.26	-613.47
Flux across the ice-water interface	-718.66	-607.28	-913.54
Precipitation minus Evaporation	97.79	97.79	97.79

magnitude: variation in ice thickness, the net precipitation through the leads in the ice, and the diffusion from the Norwegian Sea. The ice thickness is controlled by heat fluxes from the air and from the water below.

For State 4 (see table 3.9) the most important terms in the temperature equations are the atmospheric flux term through the leads and the diffusion from the Norwegian Sea; the heat flux from the lower layer is third in order of importance. For the salinity, the variation in ice thickness is the most important term, followed by the diffusion from the Norwegian Sea and Precipitation minus Evaporation through the leads. For the ice thickness, the atmospheric flux and the flux across the ice-water interface are the most important.

The system in the Greenland Gyre region will change each winter, from an ice covered two-layer to a one-layer state, and then back to a two-layer state as follows: State 4 to State 3, and then back to State 4. The analysis of the figures in these tables shows that these changes of states in winter are mainly due to the ice variations which add or remove salt from the water. At high latitudes salt has more effect on density changes than the temperature because the coefficient β is approximately ten times bigger than the coefficient α in the density equation (2.5), and temperature changes are small. The effect of temperature changes is still important in the variation of density, but any variation in the salt content of the layer of water (as occurs when the ice forms or melts) has more impact. Since the variation in ice thickness has an important effect on the salinity and hence density of the water in both States 3 and 4, convective overturning in the region in winter is driven mainly by the ice changes in the region. Also, any change in the salinity of the upper layer of the gyre (e.g., a freshening) can have a major impact on these changes of states, as we will see in section 4.2.

Table 3.9 Numerical estimate of the terms for the Greenland Gyre (State 4).

Temperature Terms (from Fig. A-16)	Average	Maximum	Minimum
Flux across the ice-water interface	-140.69	493.10	-539.68
Atmospheric flux through the leads	-1167.57	5890.01	-7148.27
Flux from the lower layer	874.27	2459.37	-127.20
Diffusion from the Norwegian Sea	1316.26	1666.64	823.60
Salinity Terms (from Fig. A-17)	Average	Maximum	Minimum
Variations in the ice thickness	-9.69	322.19	-876.19
Flux from the lower layer	28.54	39.00	18.34
Diffusion from the Norwegian Sea	67.16	93.63	41.47
P-E through the leads	-59.37	-59.23	-59.50
Ice Thickness Terms (from Fig. A-18)	Average	Maximum	Minimum
Atmospheric flux	314.60	1376.82	-2571.15
Flux across the water-ice interface	-358.20	1255.44	-1374.03
Precipitation minus Evaporation	97.79	97.79	97.79

4. Anomaly Experiments

In this section the model will be used for a series of anomaly experiments. The first will study the model response to an increase in the air temperature of each region which is a simple representation of global warming. The second experiment will try to simulate the evolution in the model of a phenomenon like the Great Salinity Anomaly by introducing a negative salinity anomaly in the upper layer of the Norwegian Sea for a short period of time. The third experiment will examine the model response to an increase in the ice transport through Fram Strait.

4.1 Effect of warmer temperatures in each region.

The first experiment is designed to determine the response of the different regions to an increase in air temperature. Such an experiment would simulate the possible high-latitudes effects of a global warming of the earth's lower troposphere. In this anomaly experiment, the model was run with exactly the same parameters as in the control run except for the air temperature in the four regions (Table 3.1), which are increased in each region by 3 °C for the whole year. The results of this experiment for the four regions are shown in figures 4.1 to 4.5.

In this anomaly experiment the largest changes occur in the temperature of the upper layer of water in each region. An increase in the air temperature has the smallest effect on the water temperature in the Arctic Ocean (compare figures 3.3 and 4.3) because the complete ice cover year-round acts as a very good insulator between the water and the air. The increase from the control run for the upper layer is 0.109 °C. The Norwegian Sea region has a large response (a 1.6 °C increase;

compare figures 3.2 and 4.2) because of the absence of ice cover throughout the whole seasonal cycle in that region.

Salinity is found to have decreased in the four regions in this experiment. The decrease is on average 0.092 in the Greenland Sea (compare figures 3.1 and 4.1), 0.020 in the Norwegian Sea (see figures 3.2 and 4.2), 0.35 for the upper layer of water in the Arctic Ocean (see figures 3.3 and 4.3), and 0.04 for the Greenland Gyre (see figures 3.4 and 4.4). This is due to the changes in ice thickness caused by the increase in air temperature (discussed in next paragraph). As can be seen in the governing equations in section 2.3, the salinity equations for States 3 and 4 have a non-linear term which is proportional to the ice thickness variations. Thus a decrease in ice formation in one region causes a decrease in salt rejection, and hence a decrease in the maximum salt content of the upper layer of water, which then gets advected as a negative salinity anomaly around the four regions.

Ice thickness changes occur in two of the regions which have ice sometime during the year. In the Greenland Sea, the maximum ice thickness goes from 0.46 m in the control run (Fig. 3.1) to 0.15 m (Fig. 4.1), while in the Arctic Ocean it decreases from 4.20 m (Fig. 3.3) to 3.10 m (Fig. 4.3).

In the Greenland Gyre the situation is a little different. An increase in the air temperature of 3 °C does not significantly affect the ice thickness in that region (decrease of 0.10 m; compare figures 3.4 and 4.4). This is due to a lack of convective overturning during winter in the gyre. In the control run, the gyre had a period of overturning when the region was in State 3 (see figure 3.5). But in this temperature anomaly experiment, the convective overturning completely ceases. This is caused by

the increase in air temperature which decreases the rate of ice formation in the gyre region at the beginning of the winter. This change in the rate of ice formation lowers the salt content of this region by reducing salt rejection at the beginning of the winter. With less salt rejection, the upper layer does not reach the critical water density which enables it to mix with the water below (which has a warmer temperature and a higher salinity). Thus the upper-layer water density is just low enough (because of the lower salinity) to maintain a stable two-layer configuration during the whole year. This lack of convective overturning also keeps the temperature of the upper layer of water colder during winter by not bringing up the warmer water from below. In figure 4.4, the water temperature in winter is at -1.7°C while in the control run (figure 3.4), the water temperature is around -1.0°C . This colder water temperature tends to increase the ice formation during the latter part of the winter season in the gyre. The end result of all these processes is an ice layer just a little thinner than in the control run despite an increase in the air temperatures of 3°C in the region.

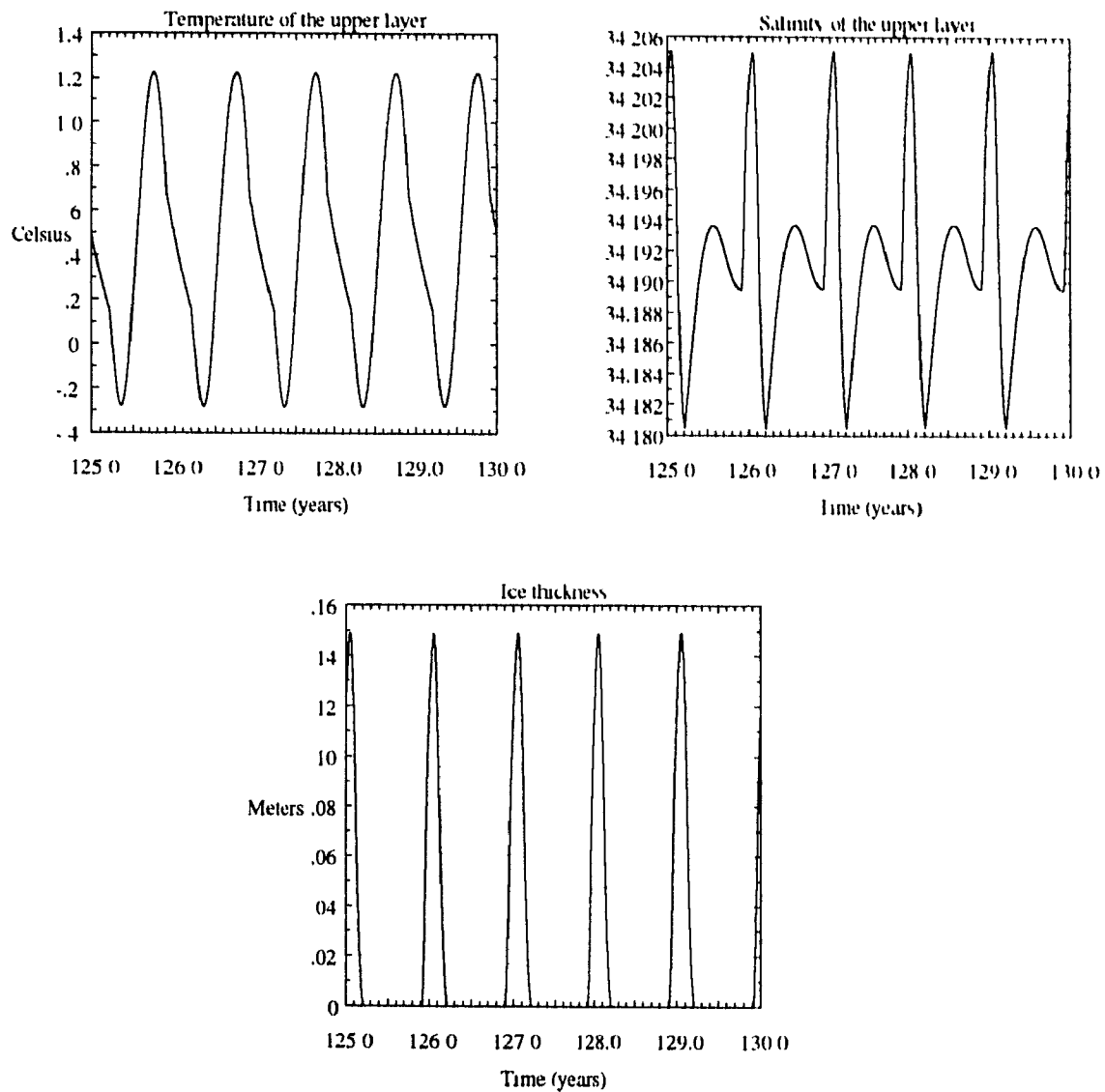


Fig. 4.1. Greenland Sea results for the temperature increase experiment.

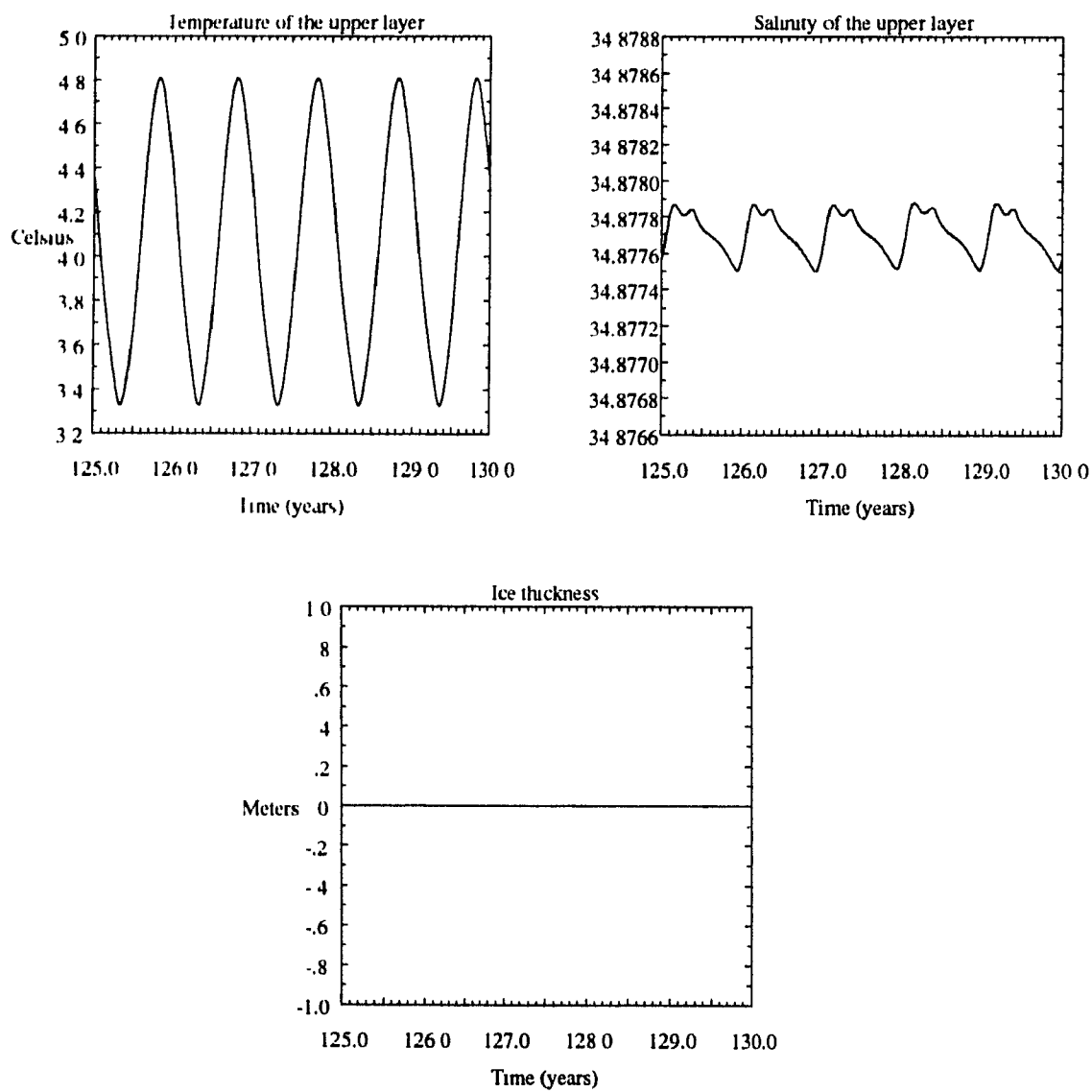


Fig. 4.2. Norwegian Sea results for the temperature increase experiment.

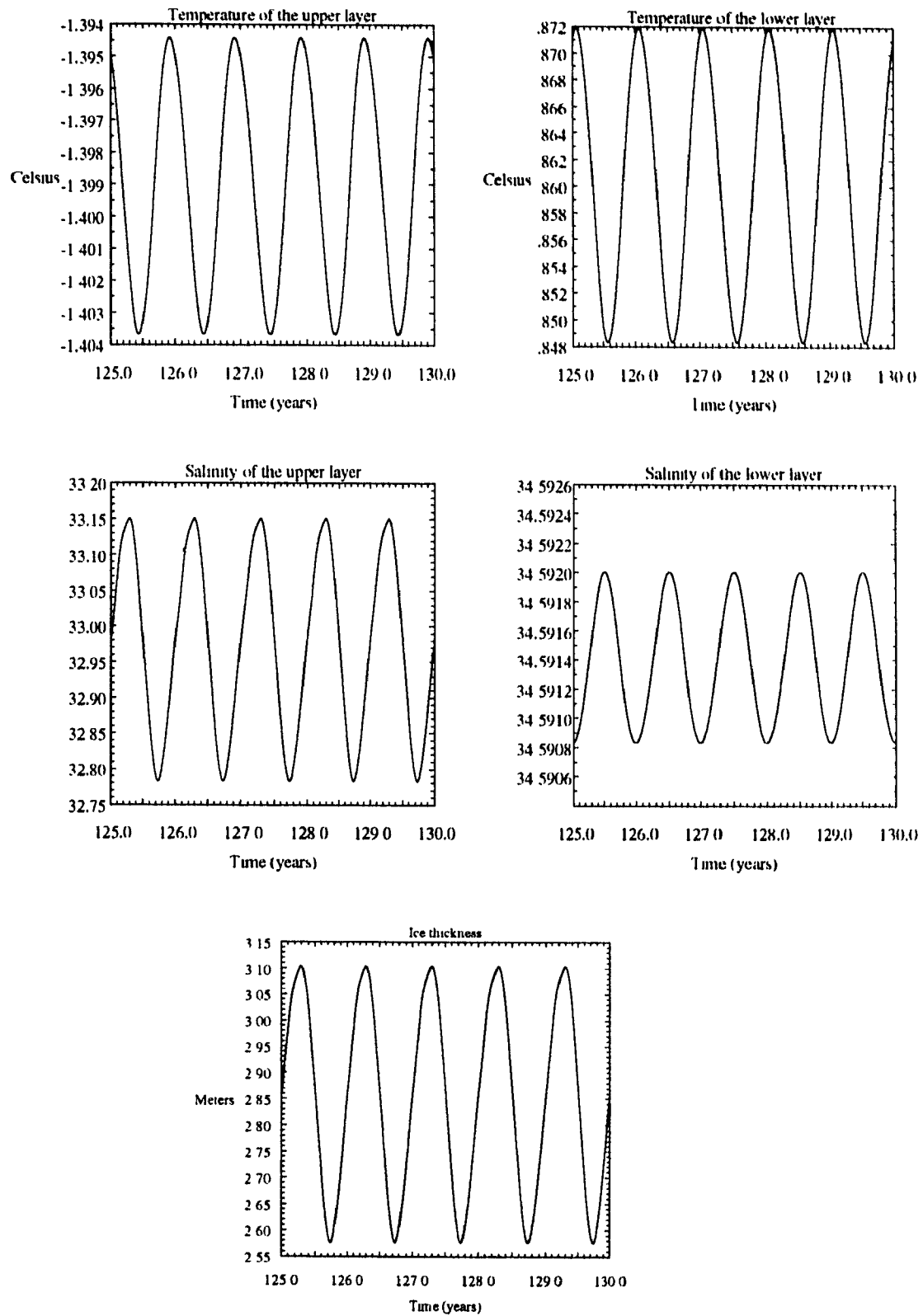


Fig. 4.3. Arctic Ocean results for the temperature increase experiment.

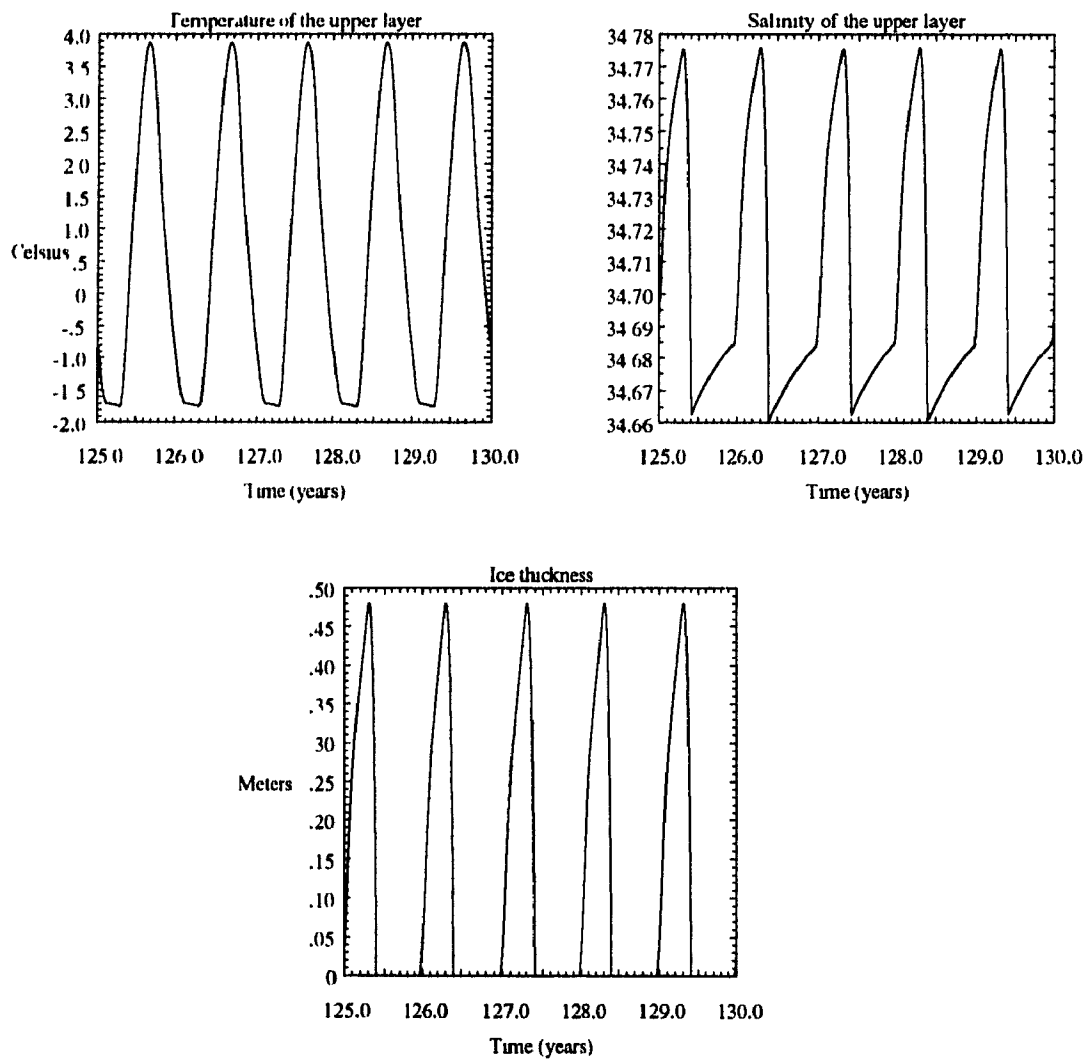


Fig. 4.4. Greenland Gyre results for the temperature increase experiment.

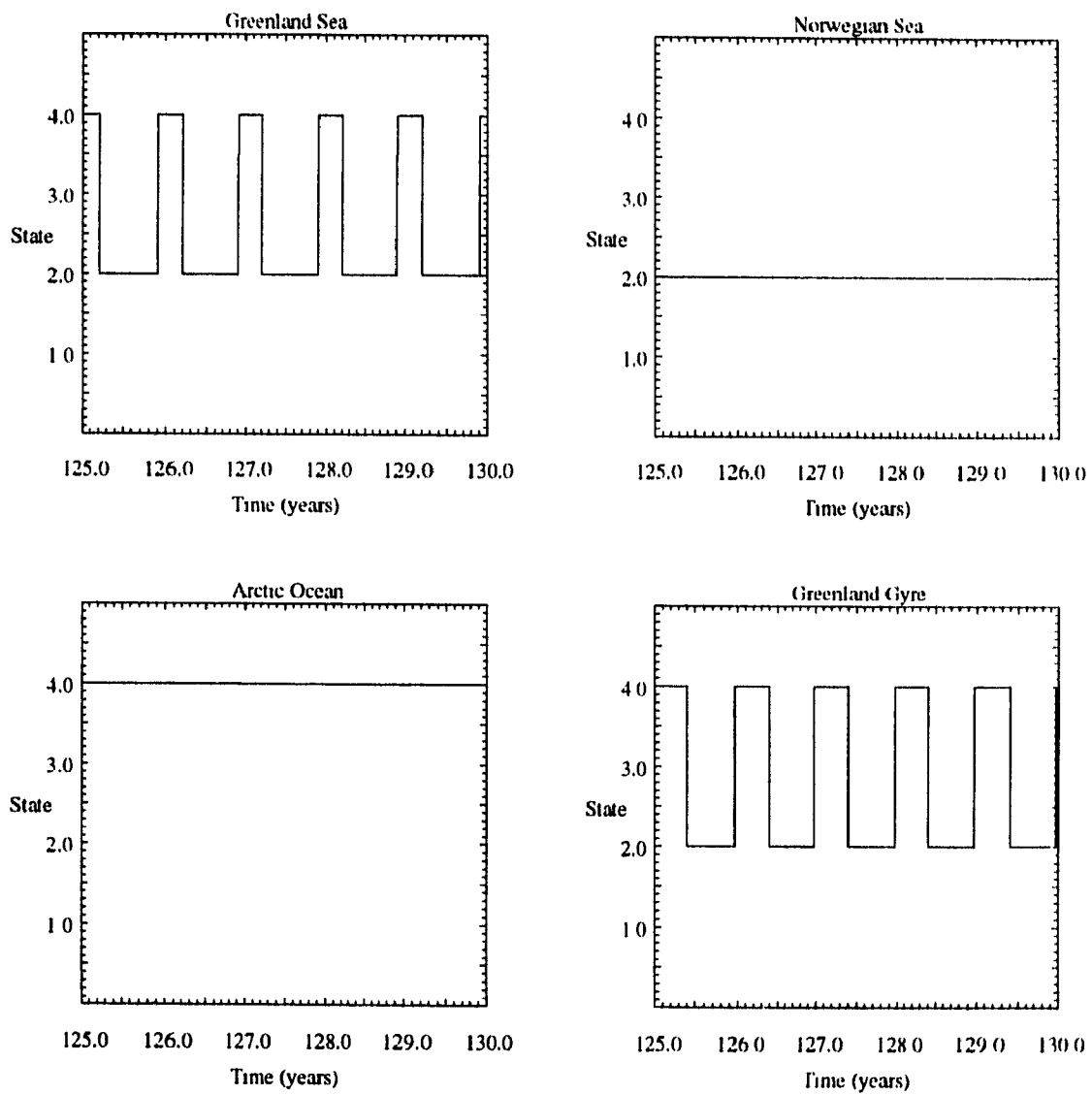


Fig. 4.5. States of the system in the temperature increase experiment.

4.2 Great Salinity Anomaly Experiment.

In figure 5 of Dickson et al. (1988), a large freshening in the upper waters of the region north of Iceland is shown. This region corresponds to an area situated on the western side of the "Norwegian Sea box" in our model. This negative salinity anomaly, which is part of what is now known as the "Great Salinity Anomaly" or GSA, shows salinity decreases of the order of 0.3 psu during the 1967 to 1971 period with a peak of 0.6 psu in the year 1968. During the same period, the area east of Greenland shows ice extents which are larger than the 1953-88 climatology (Mysak and Wang, 1991). In an attempt to simulate some aspects of the GSA, a flux of low salinity water was added to the Norwegian Sea region using a term of the same form as the other water fluxes in the salinity equation 2.19b, i.e., $W(S_0 - S_2)$, where W and S_0 are chosen to model a salinity anomaly. In this term, the quantity W increases linearly from zero for a year, stabilizes at a constant value W_0 for a period of two years, and then decreases linearly back to zero in the final year. The salinity S_0 and the strength of the flux W are prescribed values such that the Norwegian Sea upper layer salinity decreases by a fixed amount after about two years.

As a first experiment, a negative salinity anomaly of maximum value 0.25 psu is simulated, as seen in figure 4.6. To achieve this, we use $W_0=1.2$ Sv and $S_0=20$ psu. The anomaly is inserted in the year 107, and then disappears four years later in a manner described above. The effects of this salinity anomaly on the Greenland Gyre are shown in figure 4.7.

The duration of convective overturning in the Greenland Gyre in winter is greatly affected by this salinity anomaly. Instead of a well defined period when the system goes from State 4 (two-layer system with ice) to State 3 (one-layer system with

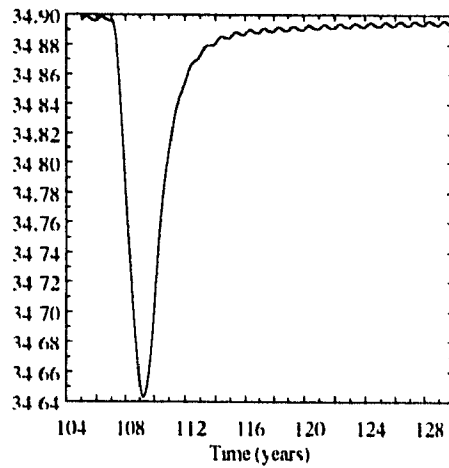


Fig. 4.6. Salinity of the upper layer in the Norwegian Sea for the 0.25 psu salinity anomaly experiment.

ice) and back to State 4 during winter, as in the control run, the system oscillates rapidly back and forth between State 3 and State 4 (the black area in the graph of the state of the gyre in figure 4.7). This means the system is essentially between the conditions for the two states, and cannot "make up its mind" between the two, i.e., the system is unstable. That is the conditions affecting the density of the upper layer of water are not strong enough to move the system completely from one state to the other. With less convective overturning during winter, less warm water is brought up from below, and thus more ice is produced in the gyre, as seen in figure 4.7.

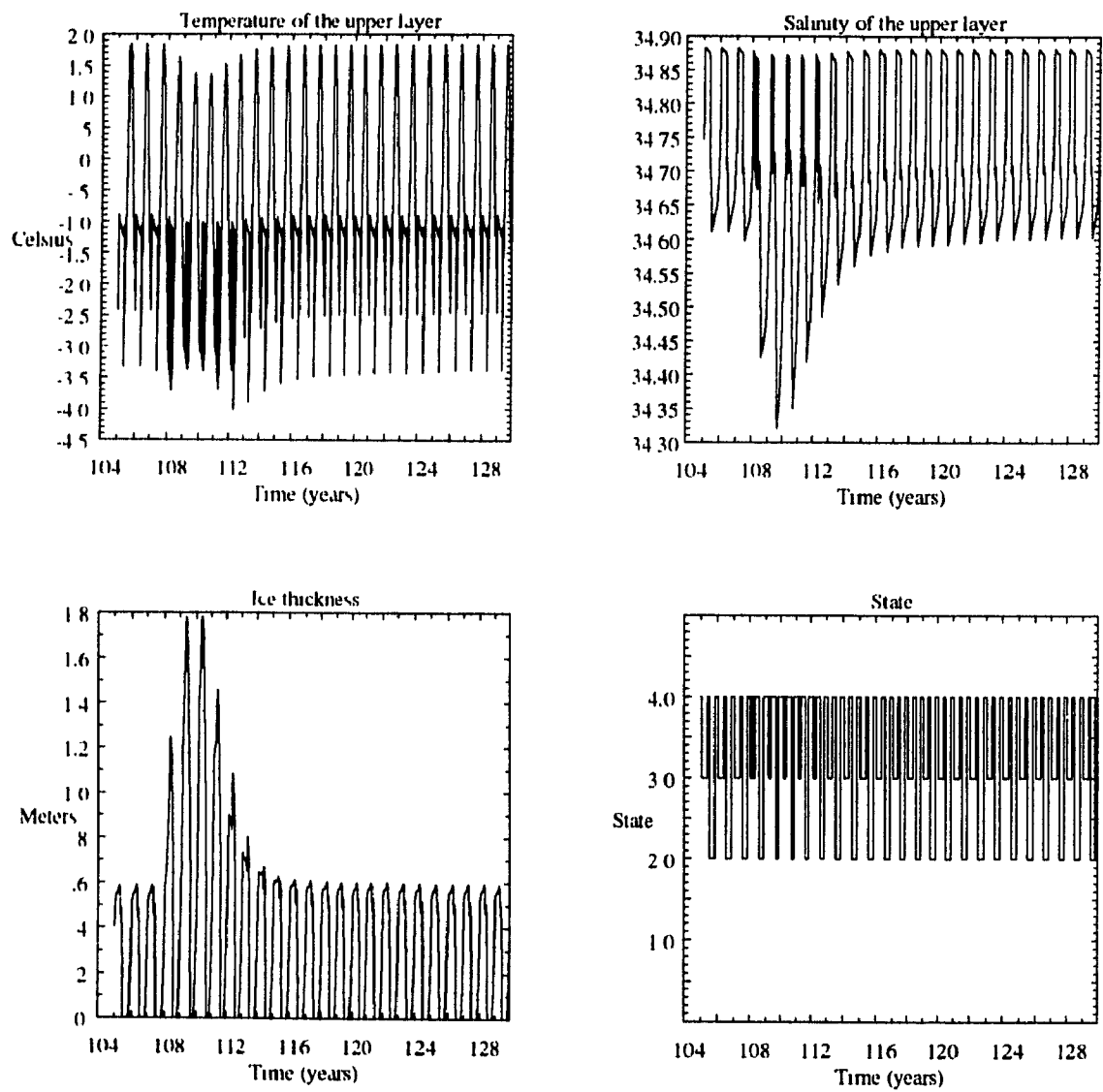


Fig. 4.7. Results for the Greenland Gyre for the 0.25 psu salinity anomaly experiment.

If the negative salinity anomaly is increased to 0.6 psu (using $W_0=2.8$ Sv and $S_0=20$ psu) in the Norwegian Sea (figure 4.8), the system will have a different behaviour, as seen in figure 4.9.

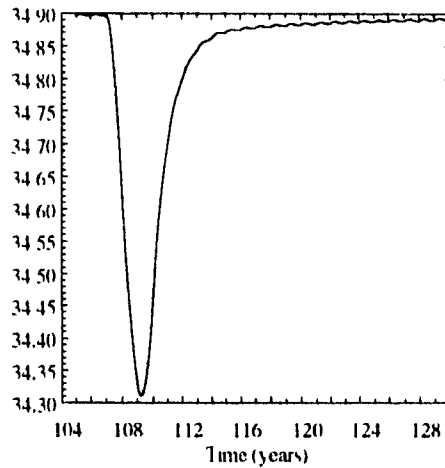


Fig. 4.8. Salinity of the upper layer in the Norwegian Sea for the 0.6 psu salinity anomaly experiment.

For a negative salinity anomaly of 0.6 psu, the convective overturning in winter in the gyre region is disturbed for the same period as in the previous anomaly experiment. But now convective overturning is completely shut down for two winters. Because of the lack of convective overturning, a large increase in the ice thickness for the region occurs. This is in agreement with observations which show that the Great Salinity Anomaly is accompanied by an increase in ice thickness in the same region some time later. For this reason, Mysak and Power (1992) have renamed events like the GSA to "Great Ice and Salinity Anomalies", or GISAs for short.

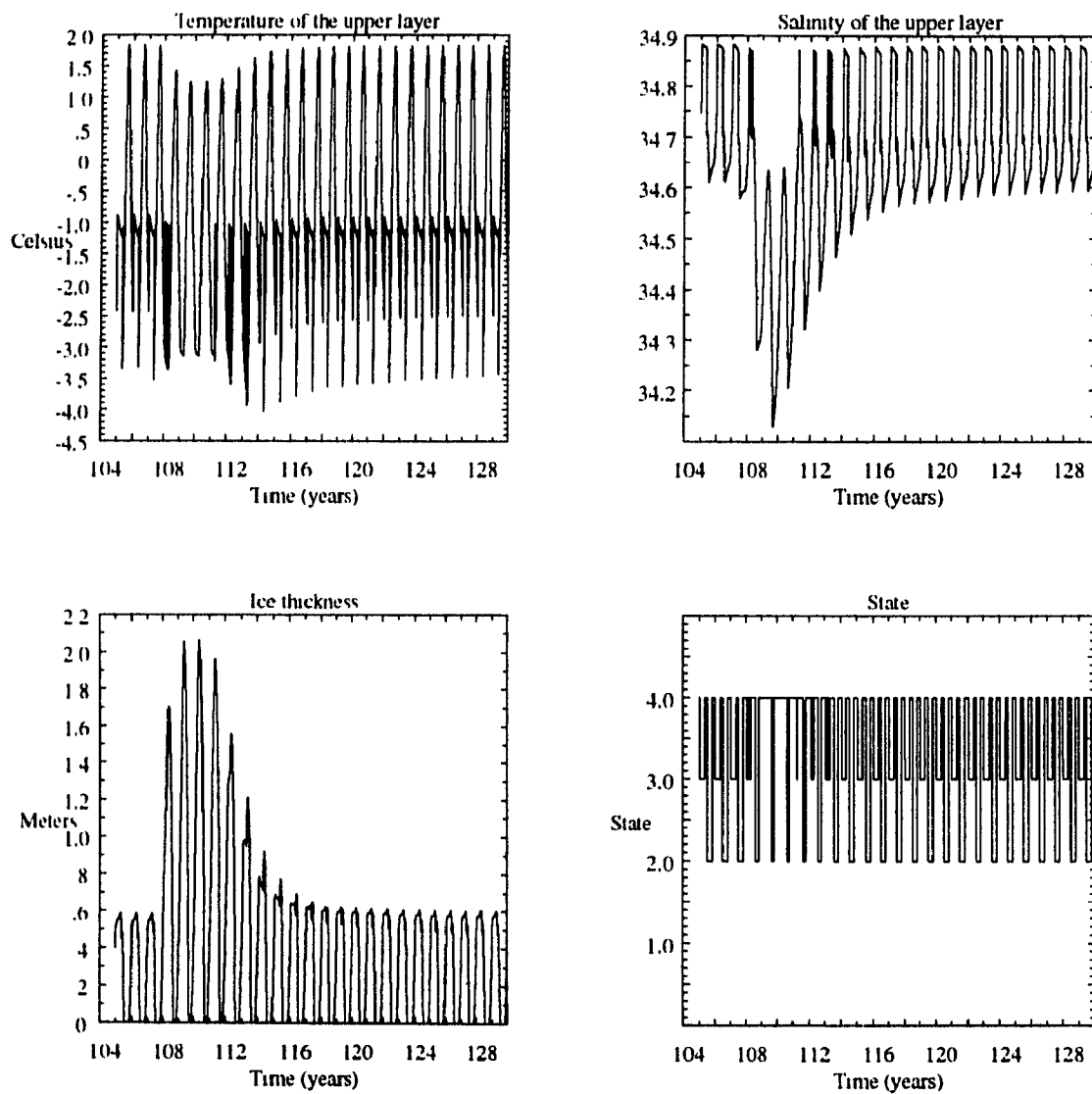


Fig. 4.9. Results for the Greenland Gyre for the 0.6 psu salinity anomaly experiment.

4.3 Effect of more ice advection through Fram Strait.

One of the mechanisms proposed to explain the Great Salinity Anomaly is an increase in the northerly winds north of the Greenland Sea region that would increase the amount of advected ice out of the Arctic and into the Greenland Sea region (Dickson *et al.*, 1988, Serreze *et al.*, 1992). To simulate this process, the ice transport out of the Arctic (the term I_{arctic} which is described in section 2.2) was varied in the same manner as was done for the low-salinity water flux in the previous section (linear increase for one year starting in year 107, constant flux for two years, and a linear decrease for one year). The maximum ice flux during this four-year period is twice the normal amount used in the control run.

This increase in the ice flux leaving the Arctic has several effects on this region. The mean ice thickness decreases by about 0.40 meters (Fig. 4.10). After the prescribed ice flux out of the Arctic returns to its normal value, the Arctic region, to return to its equilibrium state for the ice thickness, is required to produce more ice which results in an increase in the salt rejection in the area. This creates a positive salinity anomaly of 0.20 psu a few years after the ice flux anomaly was introduced.

In the Greenland Sea (Fig. 4.11), the system experiences a small ice thickness increase due to the increased ice advection from the north. The melting of this positive anomaly in the spring decreases the salinity. The water coming later from the Arctic is more saline, which in turn increases the salinity of the Greenland Sea region by 0.12 psu in the years following the decrease in salinity. This sequence of salinity anomalies (a negative anomaly followed by a positive one) then propagates to the

Norwegian Sea and the Greenland Gyre (Figures 4.12 and 4.13), with the anomalies getting smaller as they travel from one region to the other.

In the gyre, the effects of the initial anomaly are damped considerably. But the effects will be nevertheless felt in the system, mainly as a decrease in the period of convection in winter. However, this effect is very small and cannot be seen in Fig 4.14.

In conclusion, a factor of two increase for a few years of the ice flux out of the Arctic Ocean has significant effects on that region, but has weaker effects in the other regions. This could indicate an underestimate by the model of the effects of advection of temperature, salinity, or ice from one region to another. This shows the limitations of a box model which uses very large areas.

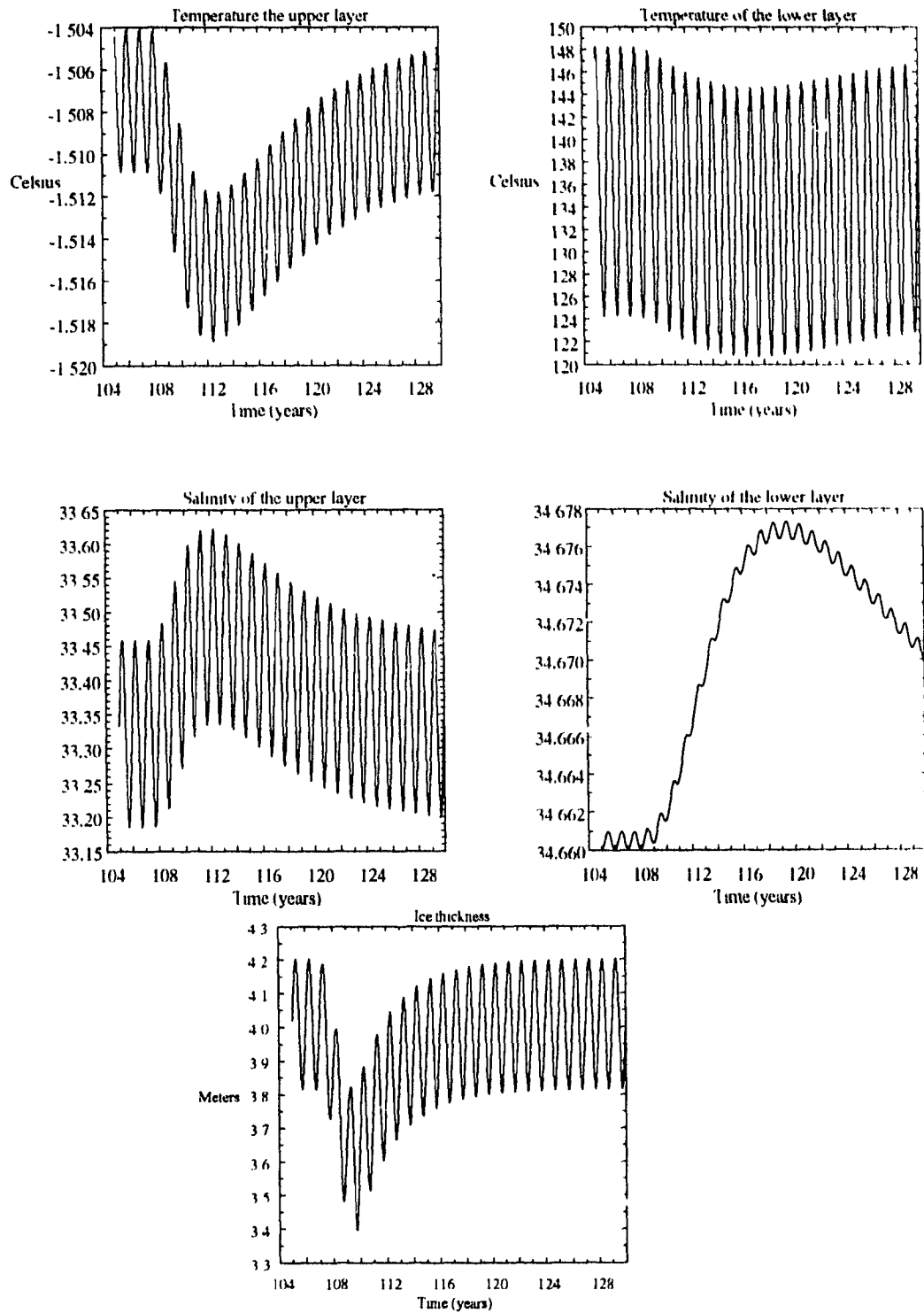


Fig. 4.10. Results for the Arctic Ocean in the ice advection experiment.

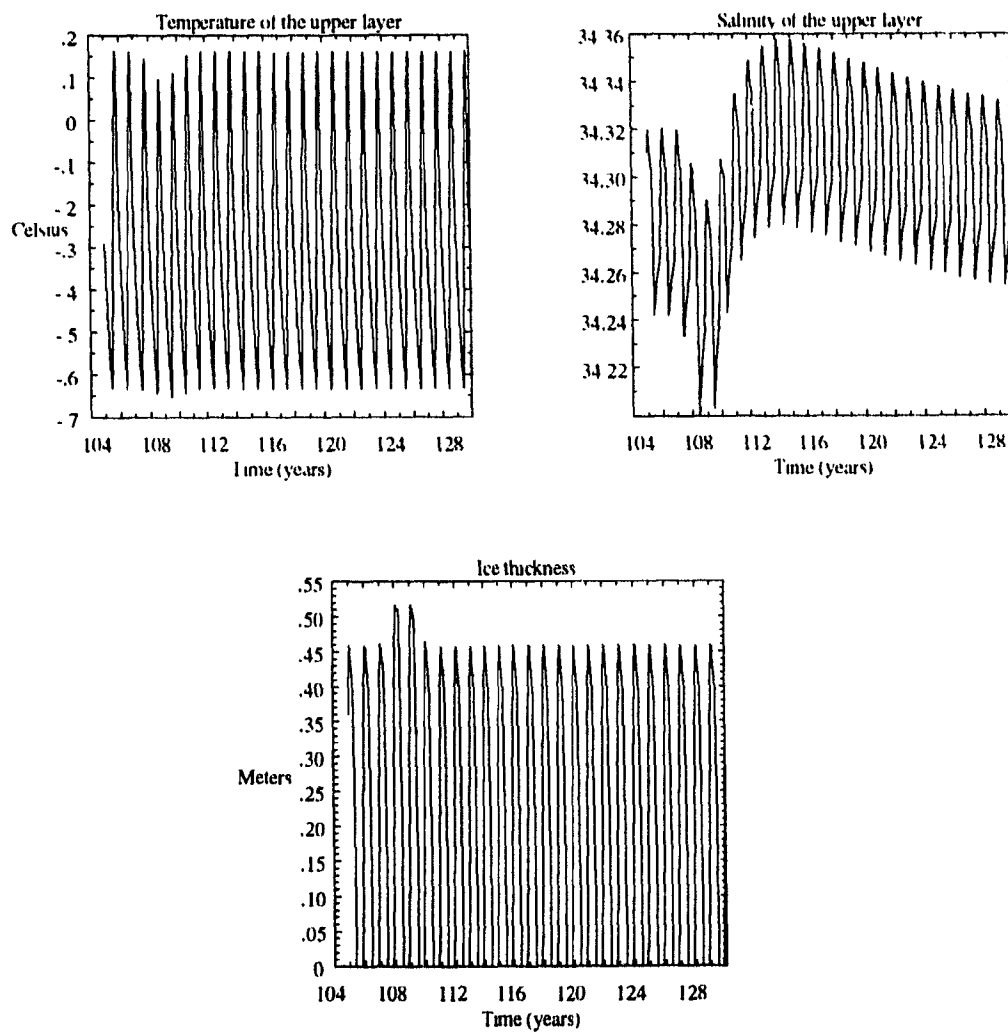


Fig. 4.11. Results for the Greenland Sea in the ice advection experiment.

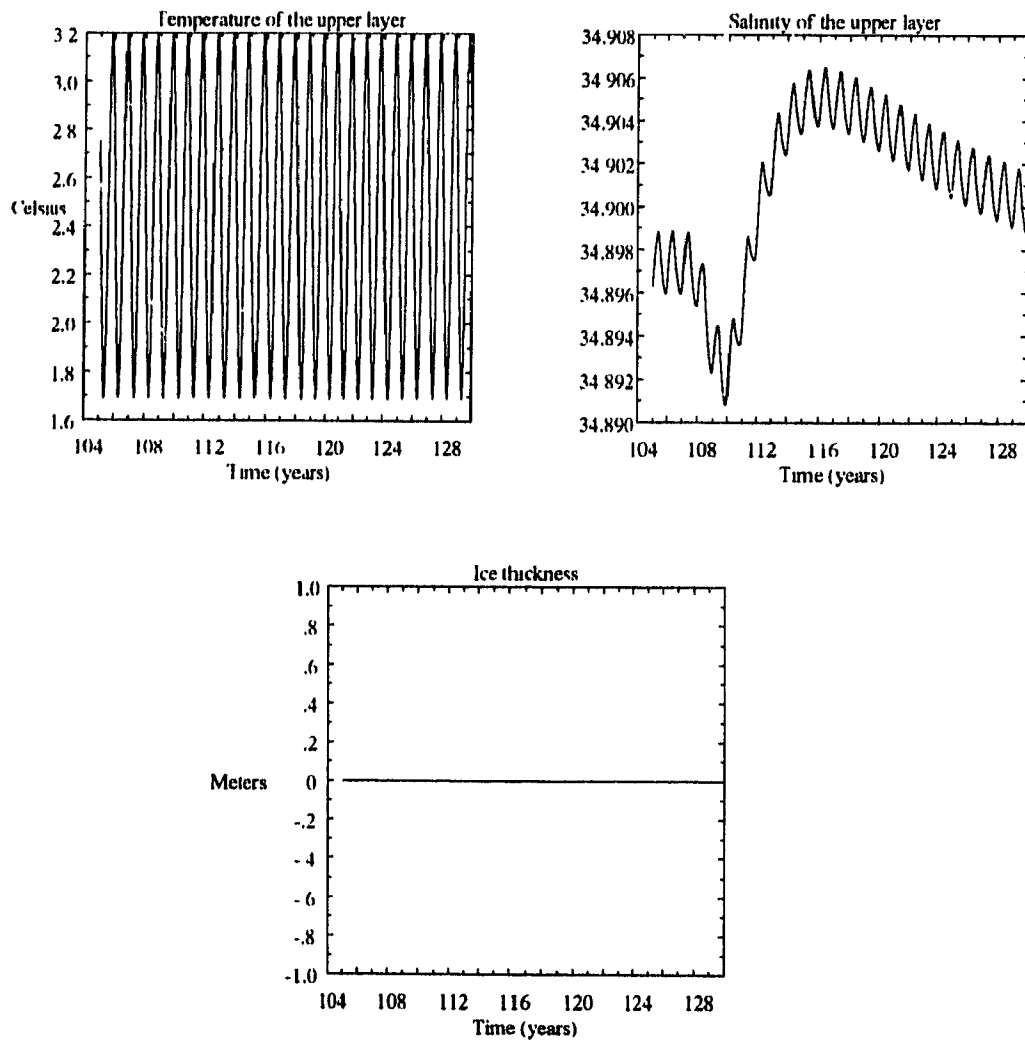


Fig. 4.12. Results for the Norwegian Sea in the ice advection experiment.

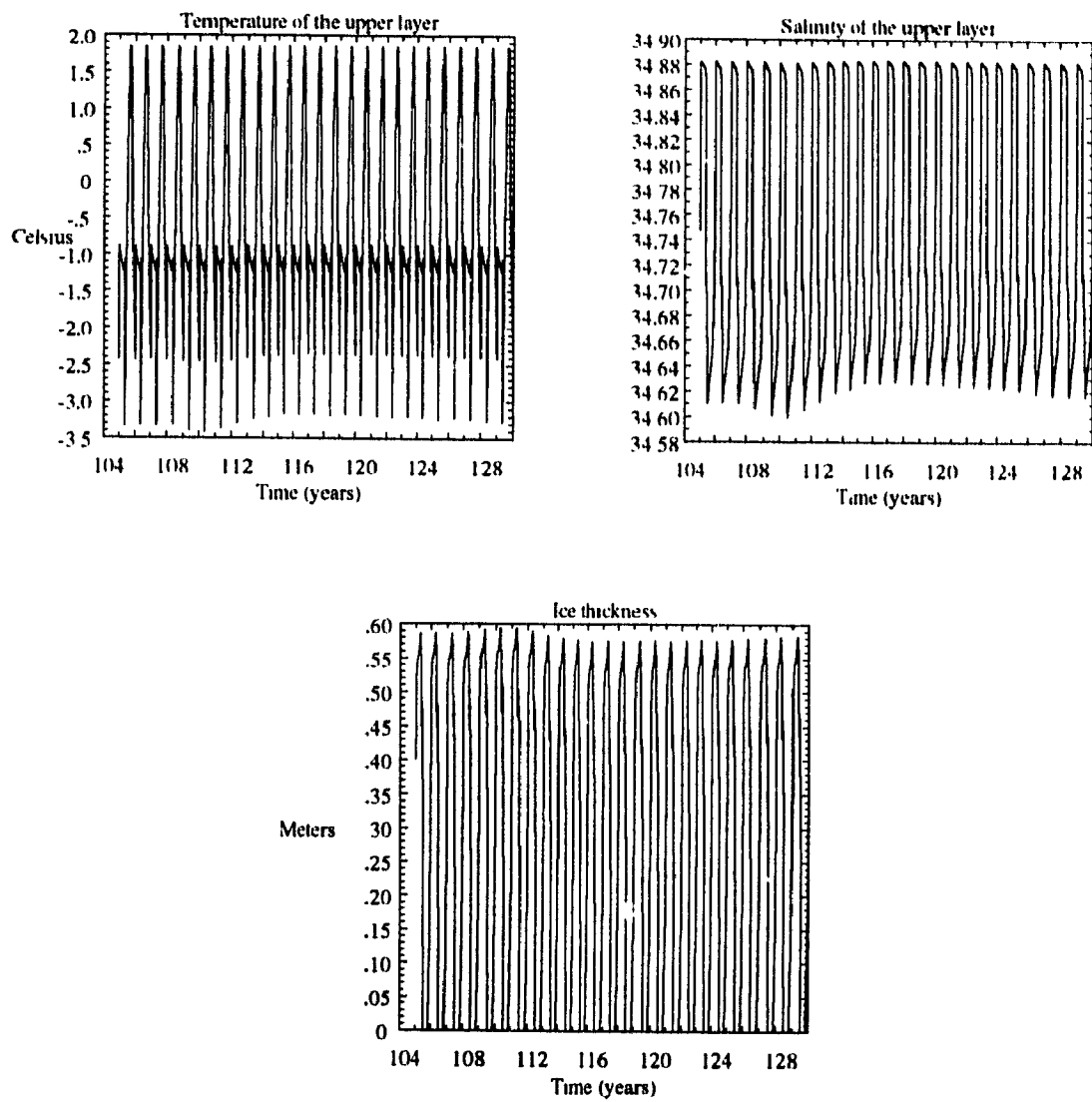


Fig. 4.13. Results for the Greenland Gyre in the ice advection experiment.

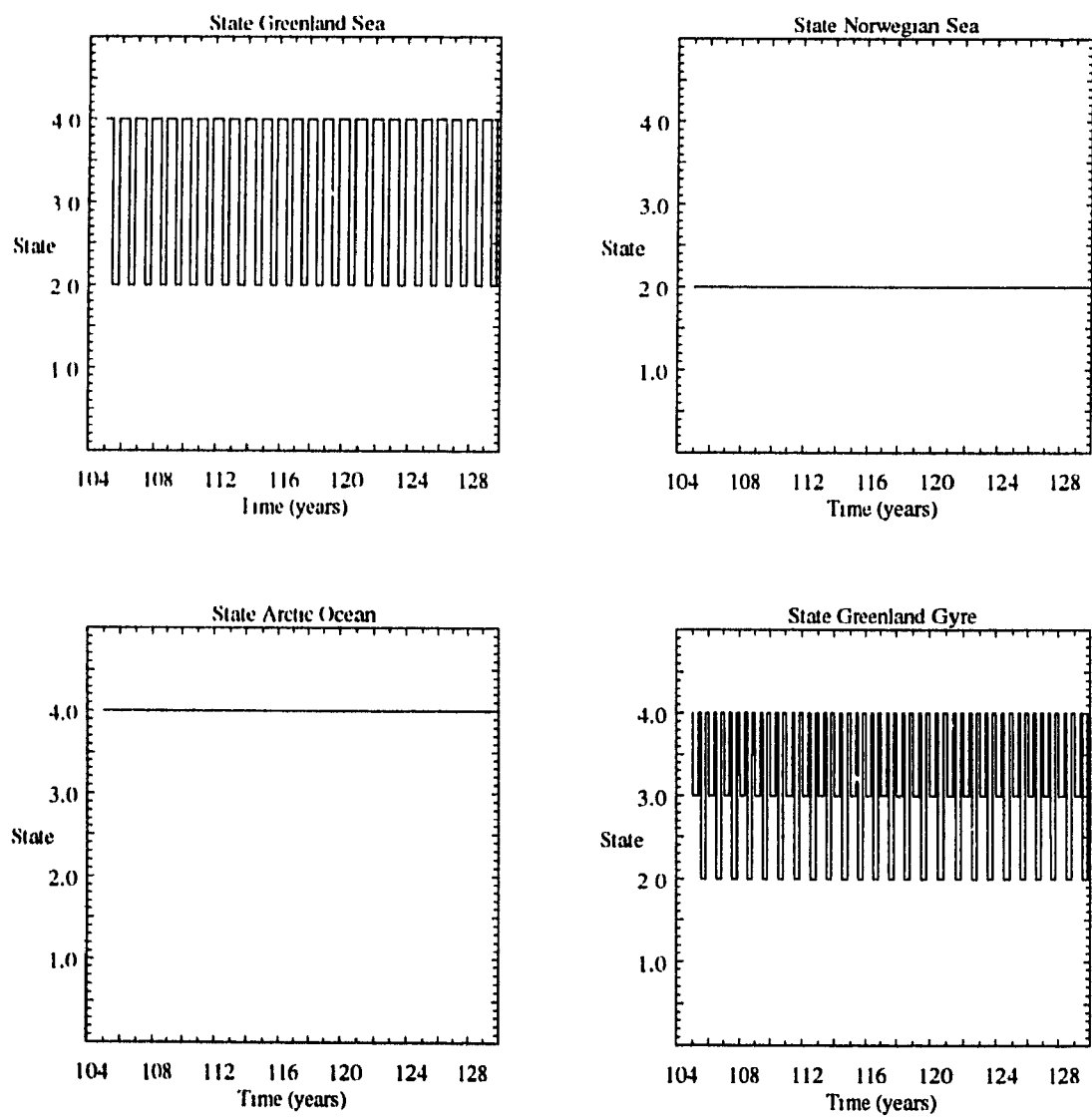


Fig. 4.14. States of the system for the ice advection experiment.

5. Summary and Conclusions

In section 2 a multi-box model of four Arctic regions (defined as the Greenland Sea, the Norwegian Sea, the Arctic Ocean, and the Greenland Gyre) was presented. This model is based on a single-box model of the Weddell Sea polynya developed by Martinson *et al.* (1981). The model consists of a simple thermodynamic ice model covering either a one or two layers of water, depending on a series of criteria. The system is forced by mean monthly atmospheric temperatures in the four regions, as well as inflows from various current systems.

The regions are connected together through a series of links representing different advection and diffusion processes at the surface. The model predicts the ice thickness, the temperature and salinity of the upper layer in the four regions, and also the temperature and salinity of the lower layer in the Arctic region. In addition, the model predicts the convective state of each region, i.e., whether or not the region is in an active overturning mode.

In section 3, the results from a model run using parameters describing the current climate (the 'control run') were shown to be generally consistent with the observations. Although the model does not exactly reproduce reality, the general features of the four regions under study were reproduced. The Greenland Sea is relatively cold and fresh because of the water inflow from the Arctic Ocean, while the Norwegian Sea is relatively warm and saline due to the water inflow from the northern North Atlantic. The Greenland Sea has an ice cover for the winter part of the year, while the Norwegian Sea is completely ice free for the whole year. The Arctic Ocean is colder and fresher than the Norwegian Sea and has an ice cover during the whole year. The Greenland Gyre has a partial ice

cover that is similar in thickness and duration to the one in the Greenland Sea. The gyre region is also characterized by a period of shallow convective overturning in the upper 200 m of water in winter. This overturning is controlled by salt rejection during ice formation, freshwater production during ice melt, and by the atmospheric temperature.

For the control run the relative size of each term in the governing equations of the model was also found. From the analysis of these terms, the most important processes in these regions were found and discussed (Table 3.3 to 3.9). In the Greenland Sea region, the most important effects on the ice thickness, and the temperature and salinity of the upper layer are: the atmospheric forcing, the ice-water heat flux, and the advection of water from the Arctic Ocean via the East Greenland Current. For the Norwegian Sea region, the atmospheric flux has the largest effect on the temperature variations, and the saline water from the northern North Atlantic is the most important forcing term on the salinity equation. In the Arctic Ocean region, the fluxes from the ice-water interface and from the lower layer of water are the most important effects on the temperature and ice thickness equations. The variation in ice thickness has the biggest effect of the salinity equation. In the Greenland Gyre, the atmospheric flux and the diffusion from the Norwegian Sea are generally the two most important effects on the variations of temperature, salinity and ice thickness in the region.

In section 4 three anomaly experiments were performed with the model. In section 4.1 the atmospheric temperatures were increased by 3 °C in the four regions. This was done to simulate, in a simple way, a possible global warming of the atmosphere. In the Arctic Ocean and Greenland Sea, a decrease in the ice thickness was observed. In the Greenland Gyre region, the ice thickness stayed approximately the same. This was due to the suppression of the convective overturning in that region. The stabilization of the

system inhibits the upwelling of the warmer water in the lower layer; thus the upper layer decreases in temperature. Because of this colder water temperature, the region forms nearly as much ice as before, even in the presence of higher air temperatures.

In section 4.2 the salinity in the Norwegian Sea was decreased to simulate in the model the effect of the Great Salinity Anomaly. The rate of (shallow) convective overturning of the gyre region is decreased by this decrease in the salinity; hence the anomaly stabilizes the system. For a negative anomaly of 0.25 psu, convective overturning takes place for only a short time during winter. For a negative salinity anomaly of 0.6 psu, the system is found to have no overturning for two complete winters, and the overturning is greatly reduced during the few winters before and after these two completely stable winters.

In section 4.3, the ice advection through Fram Strait was doubled over a two-year period to simulate in the model the effect of anomalous winds advecting more ice out of the Arctic. With this increase in advection, the ice thickness in the Arctic is decreased by 0.40 m. After the ice anomaly leaving the region has stopped, the region experiences an increase in ice formation in the subsequent years, which then increases the salt rejection in the region. These salinity changes will be advected into the Greenland Sea and Norwegian Sea in the following years.

Based on these experiments, we conclude that the model can generally reproduce the general features of the four regions under study. Using a few simple physical considerations (e.g., smaller mixed layer depth because of the cyclonic motion of the water around the gyre region), it has been shown that the region where the Greenland Gyre is situated can very easily become a zone of convection, at least in the upper 200 m of the

ocean. This could be a contributing region to deep water formation that is suspected to occur in the Greenland Gyre, but this model cannot be used to prove or refute that hypothesis. A phenomenon like the Great Salinity Anomaly of the late 1960s can also be simulated in the model, and the occurrence of the zone of convection in the gyre could be partly suppressed by the GSA.

The model will need more improvement to increase its ability to reproduce the observed conditions in the four regions. This will have to be done before it could be used as an useful and precise tool in the study of decadal scale variability and of advection of anomalies between the different regions. There are a number of ways in which the model could be improved. One would like to have a better representation of the Arctic Ocean. This could be done by separating the Arctic Ocean region used in the model into two or three different areas. This could give a better representation of the local features in this big region. These local features tend to be averaged out in a model using an ocean scale representation of the Arctic with only one system of equations for the whole ocean. Also, by using a few subregions for the Arctic, we could get a better simulation of the advection of ice and salinity from one region to another.

Another way to improve the model is to introduce a variable mixed-layer depth in each region. This feature would make the system a lot more complex, but the simulation of a phenomenon like the zone of convection in the gyre region would be a lot more realistic and more interesting to analyze from a physical point of view.

Appendix

In this appendix all the terms for each differential equation in the model (section 2.3) are shown for the last four years of the 130-year integration for the control run. A general discussion of these different terms can be found in section 3.2. For the temperature terms, the units are $10^{-10} \text{ }^{\circ}\text{C s}^{-1}$, for the salinity, 10^{-10} s^{-1} , and for the ice thickness, $10^{-10} \text{ m s}^{-1}$.

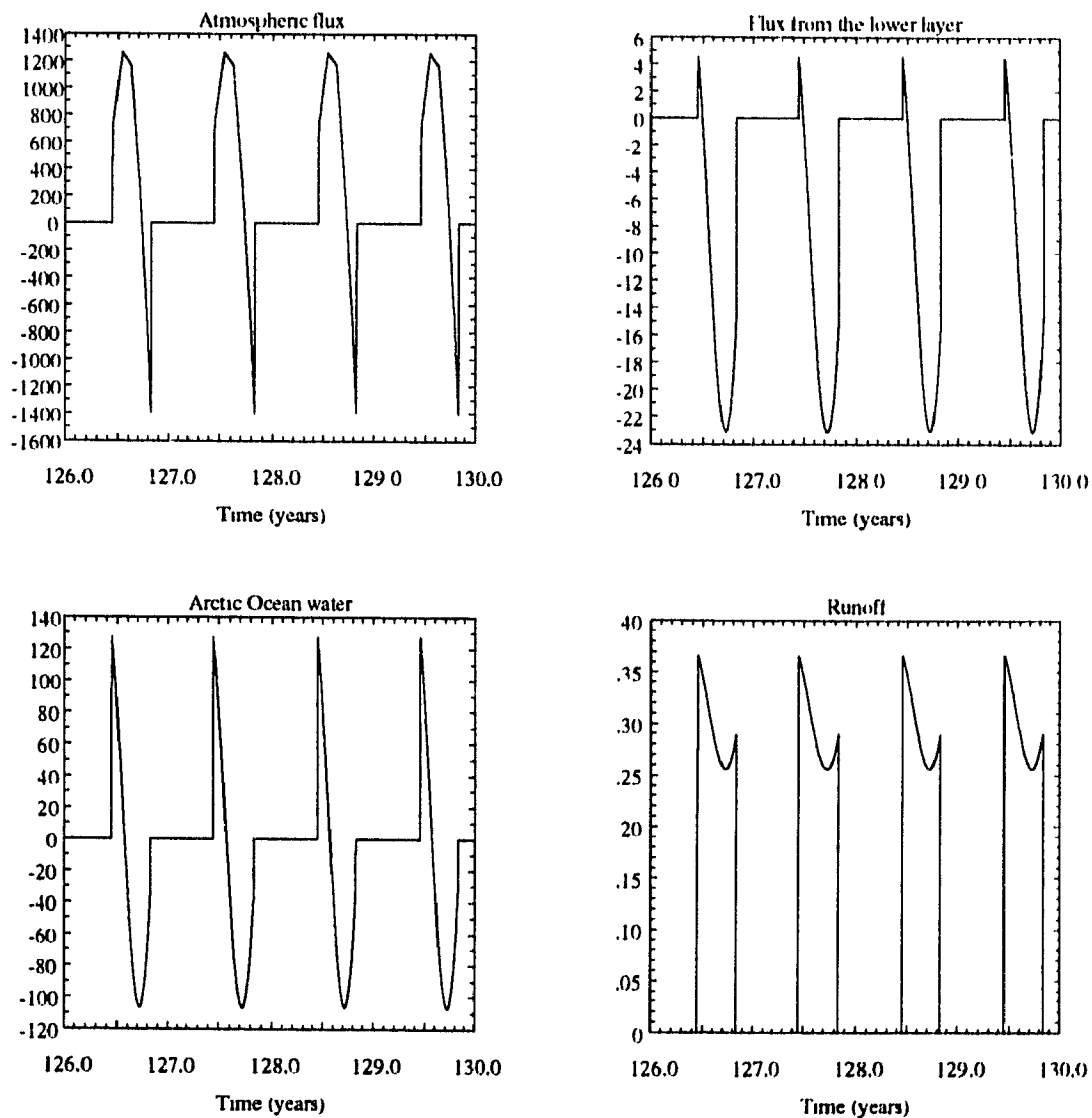


Fig. A-1. Numerical estimate of the temperature terms in the Greenland Sea (State 2).

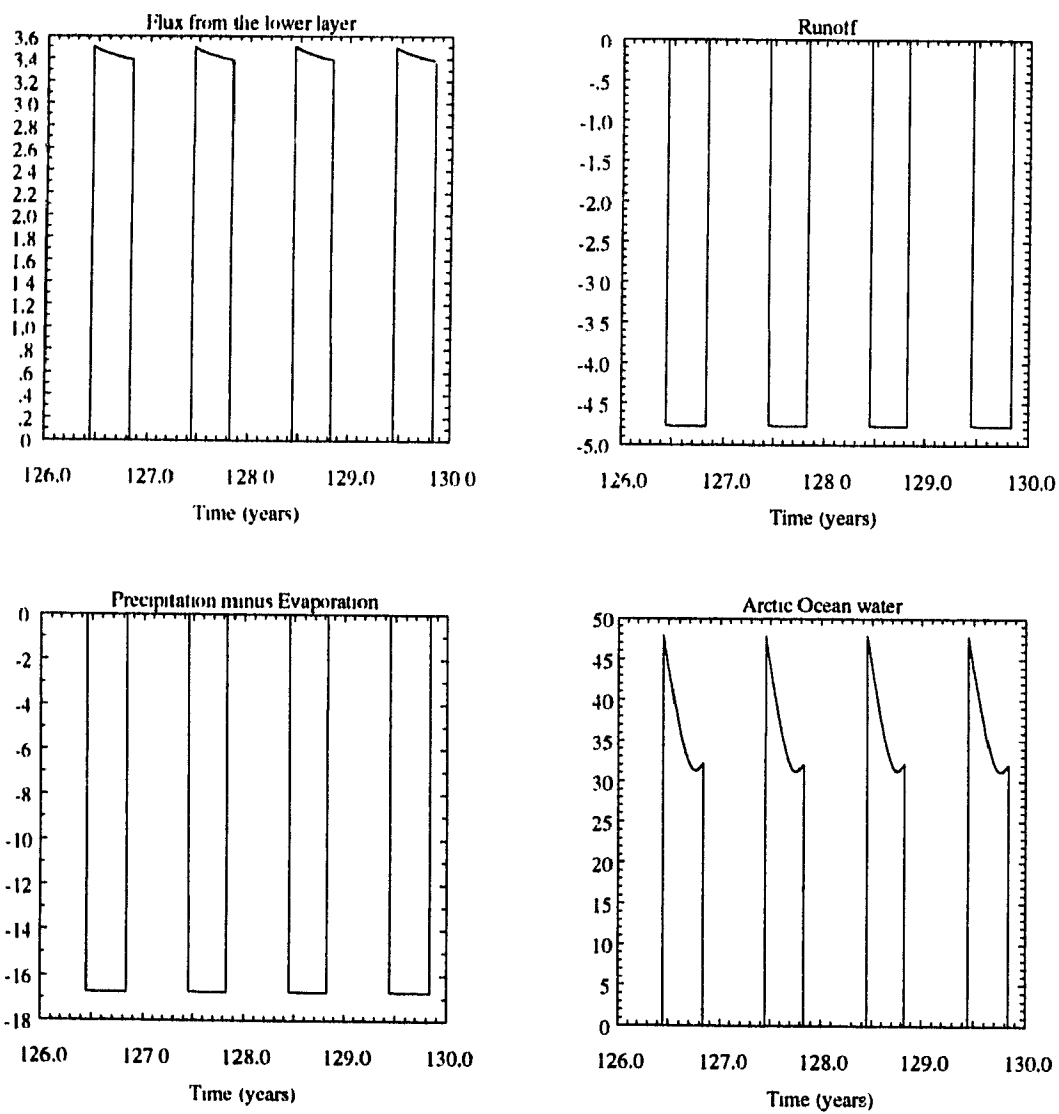


Fig. A-2. Numerical estimate of the salinity terms in the Greenland Sea (State 2).

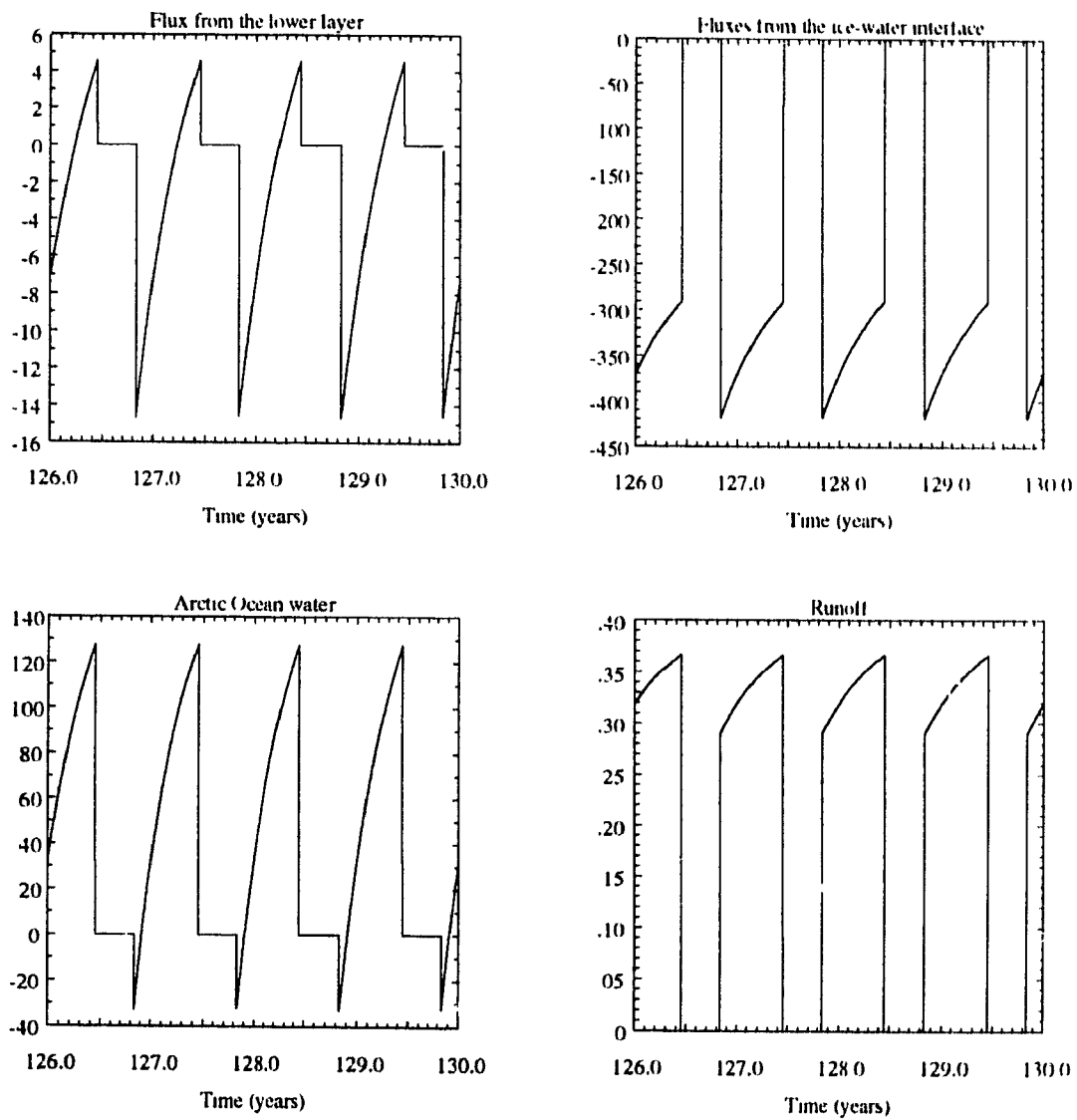


Fig. A-3. Numerical estimate of the temperature terms in the Greenland Sea (State 4).

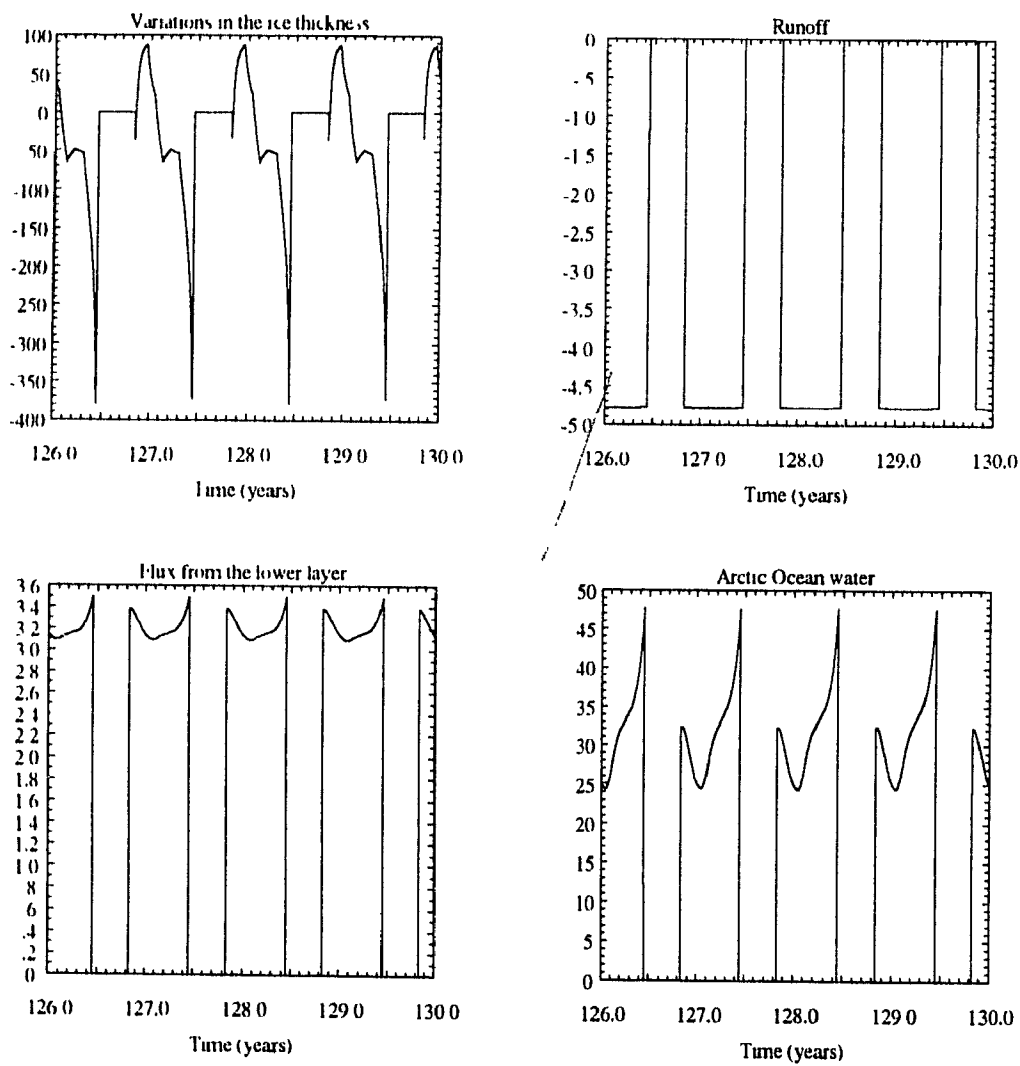


Fig. A-4. Numerical estimate of the salinity terms in the Greenland Sea (State 4).

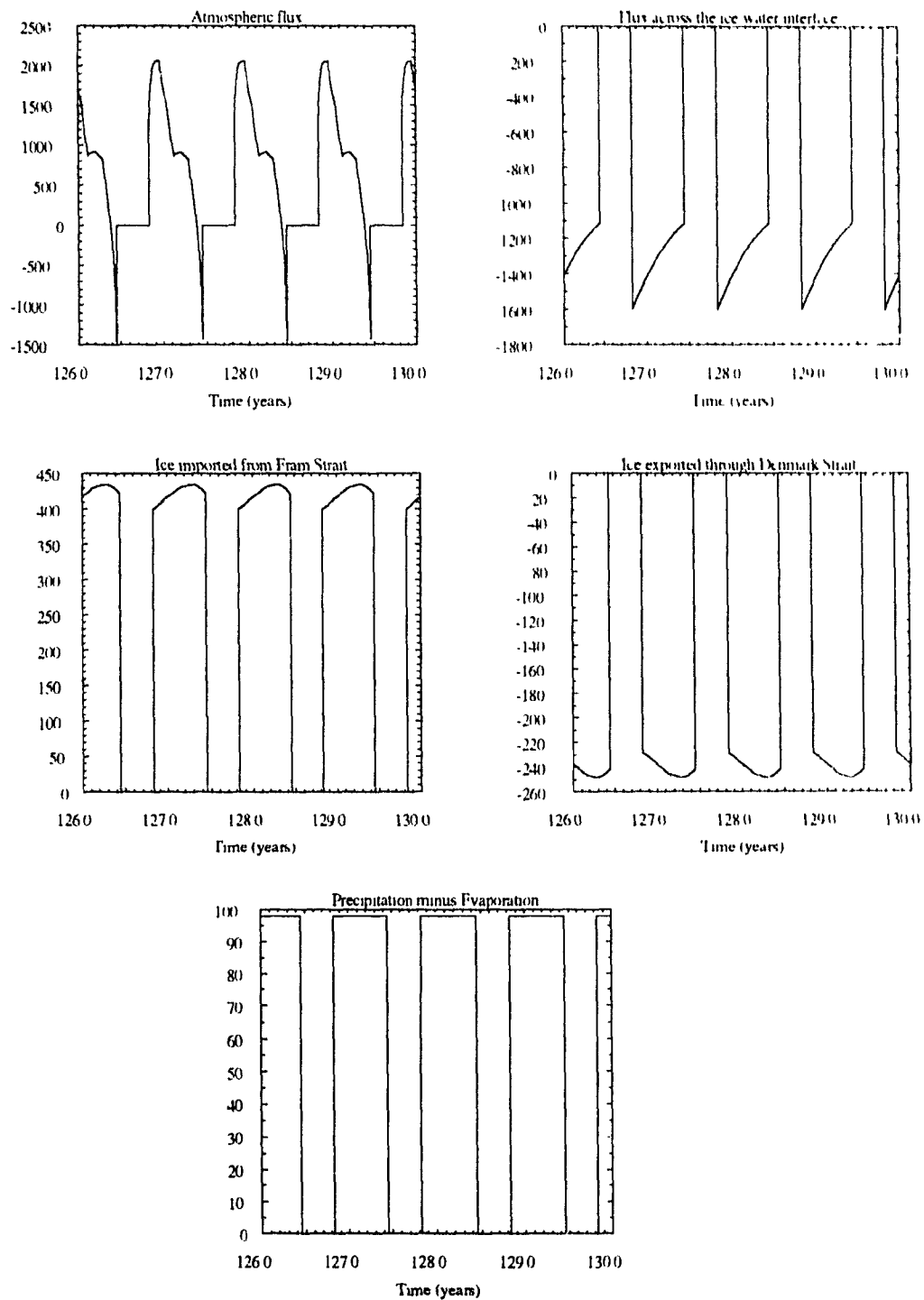


Fig. A-5. Numerical estimate of the ice thickness terms in the Greenland Sea (State 4).

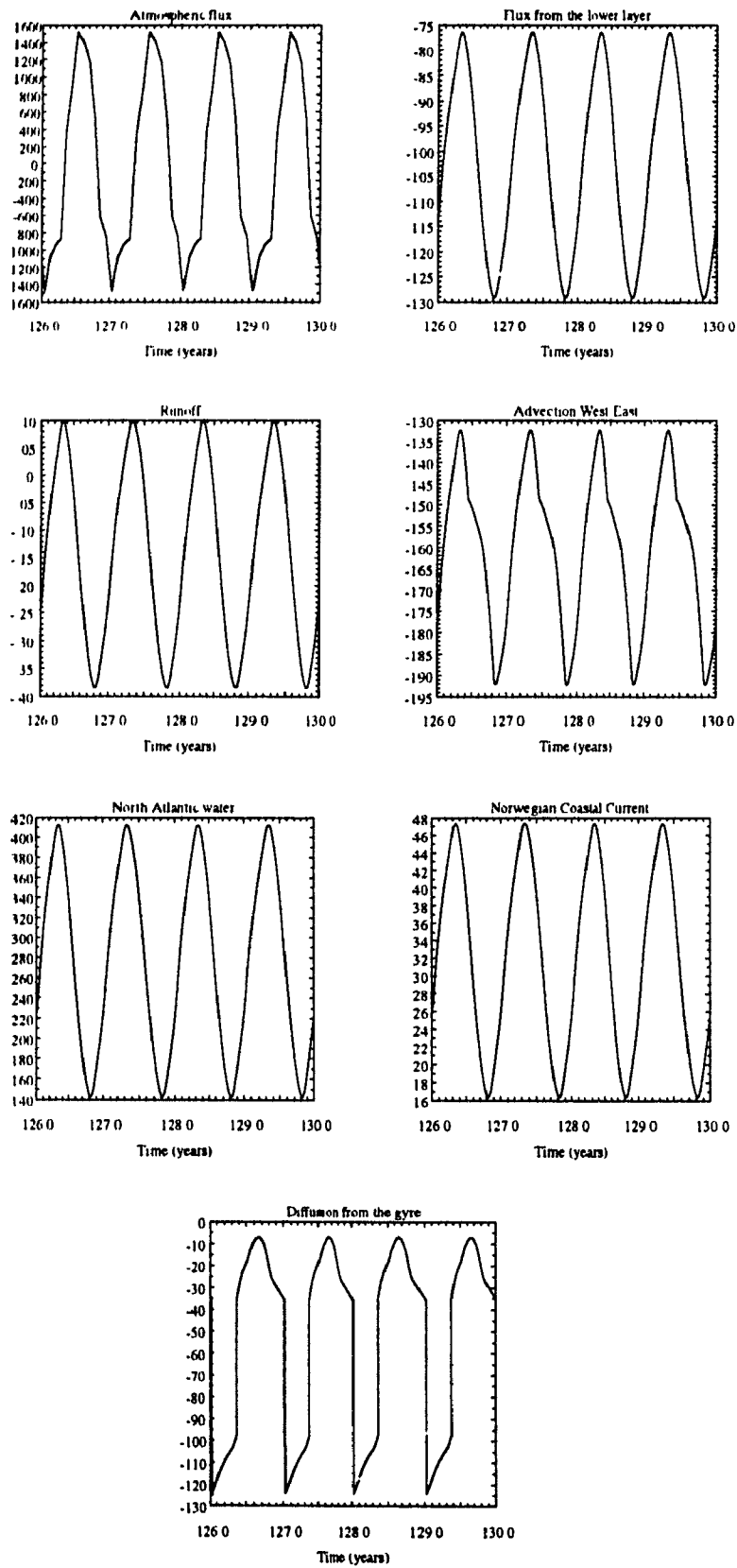


Fig. A-6. Numerical estimate of the temperature terms in the Norwegian Sea (State 2).

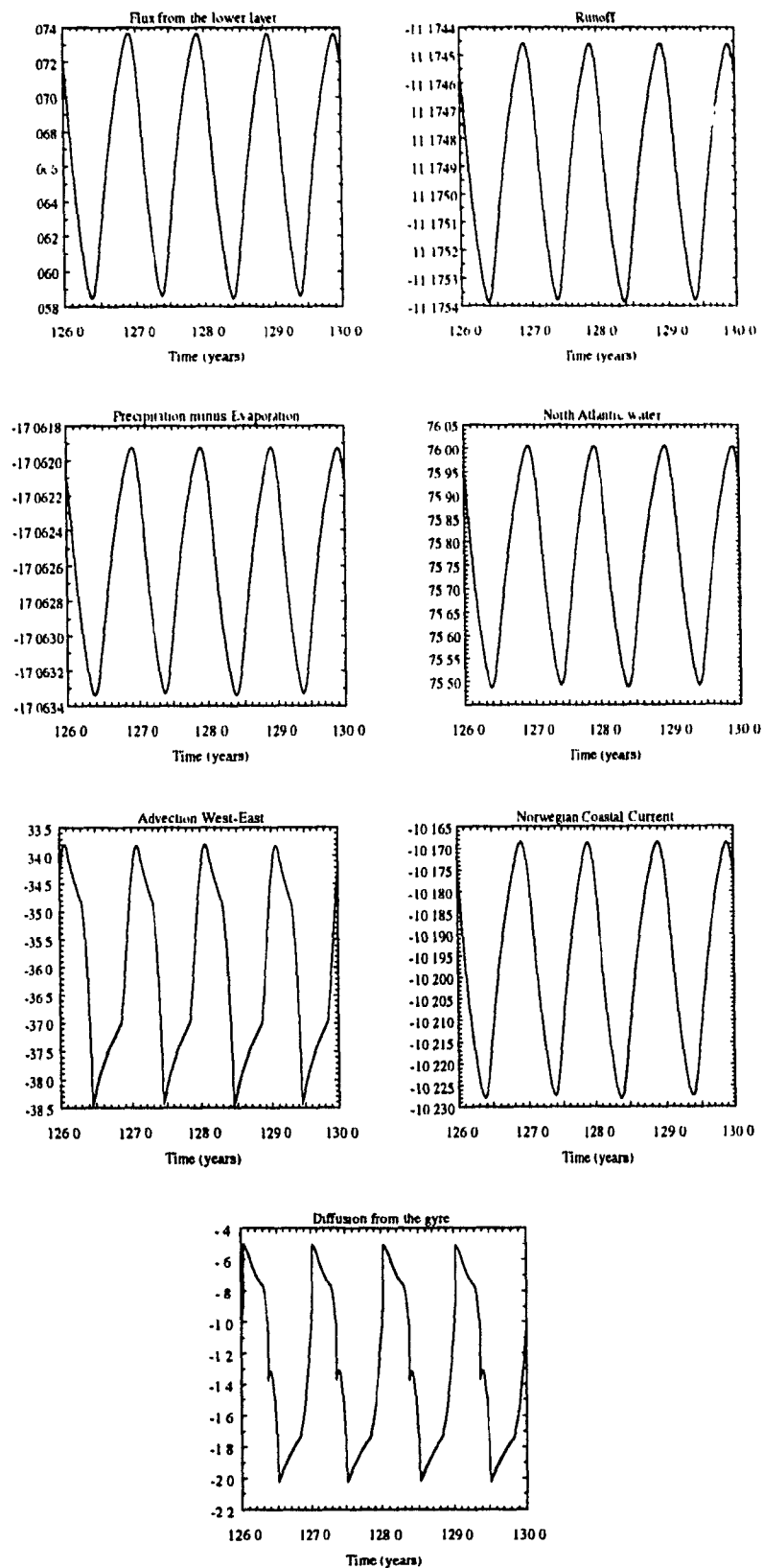


Fig. A-7. Numerical estimate of the salinity terms in the Norwegian Sea (State 2).

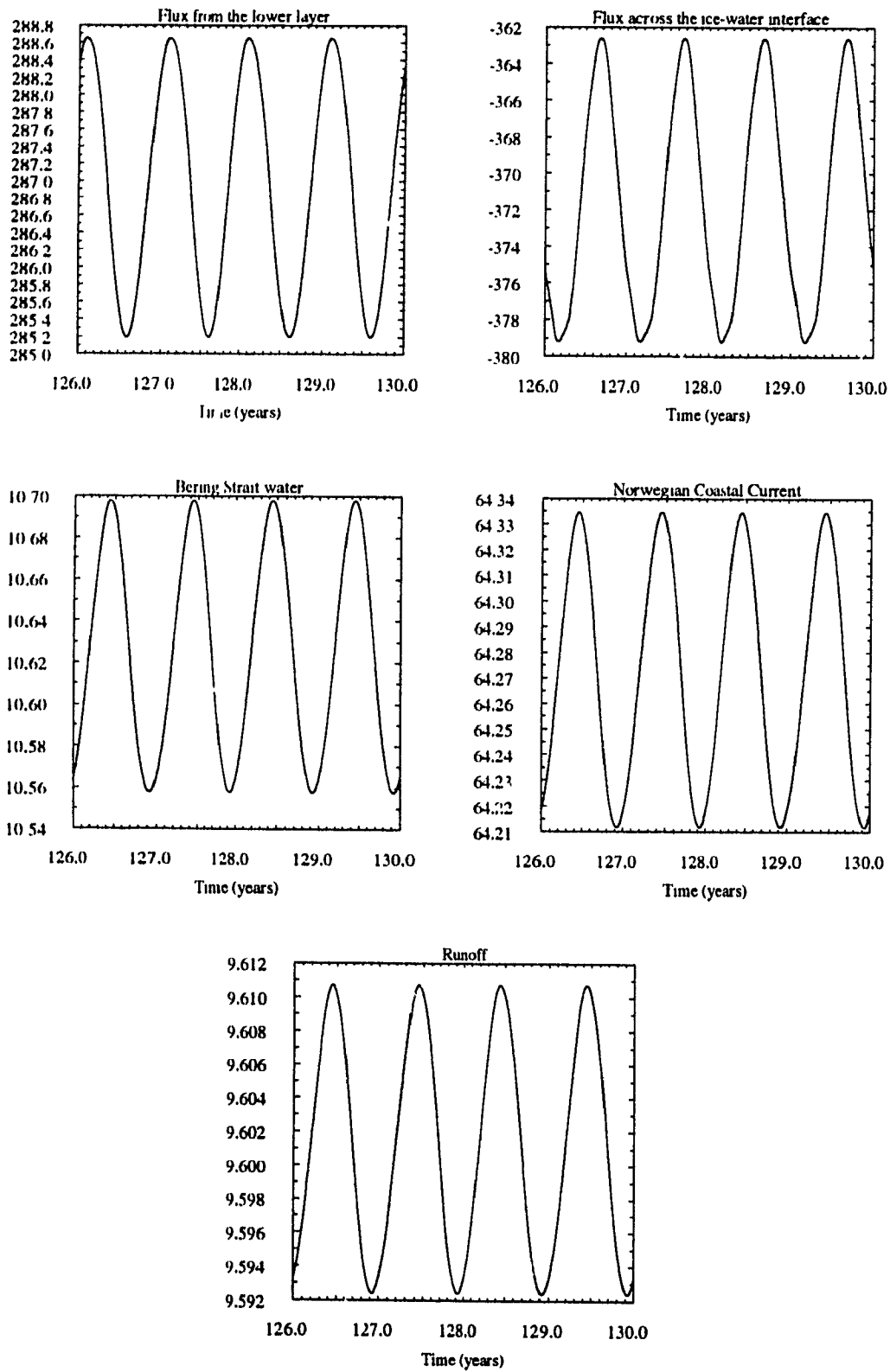


Fig. A-8. Numerical estimate of the temperature terms in the Arctic Ocean (State 4).

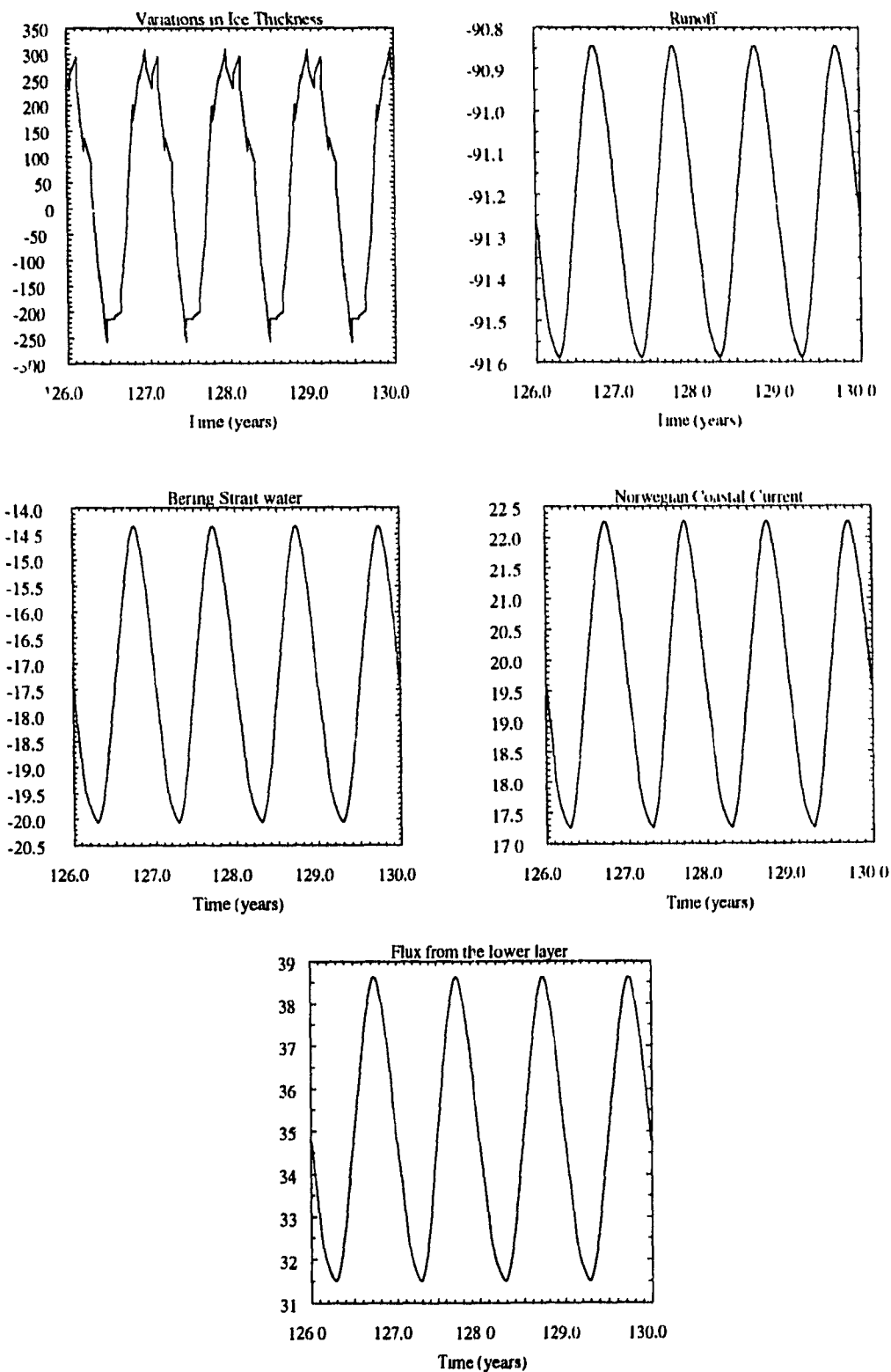


Fig. A-9. Numerical estimate of the salinity terms in the Arctic Ocean (State 4).

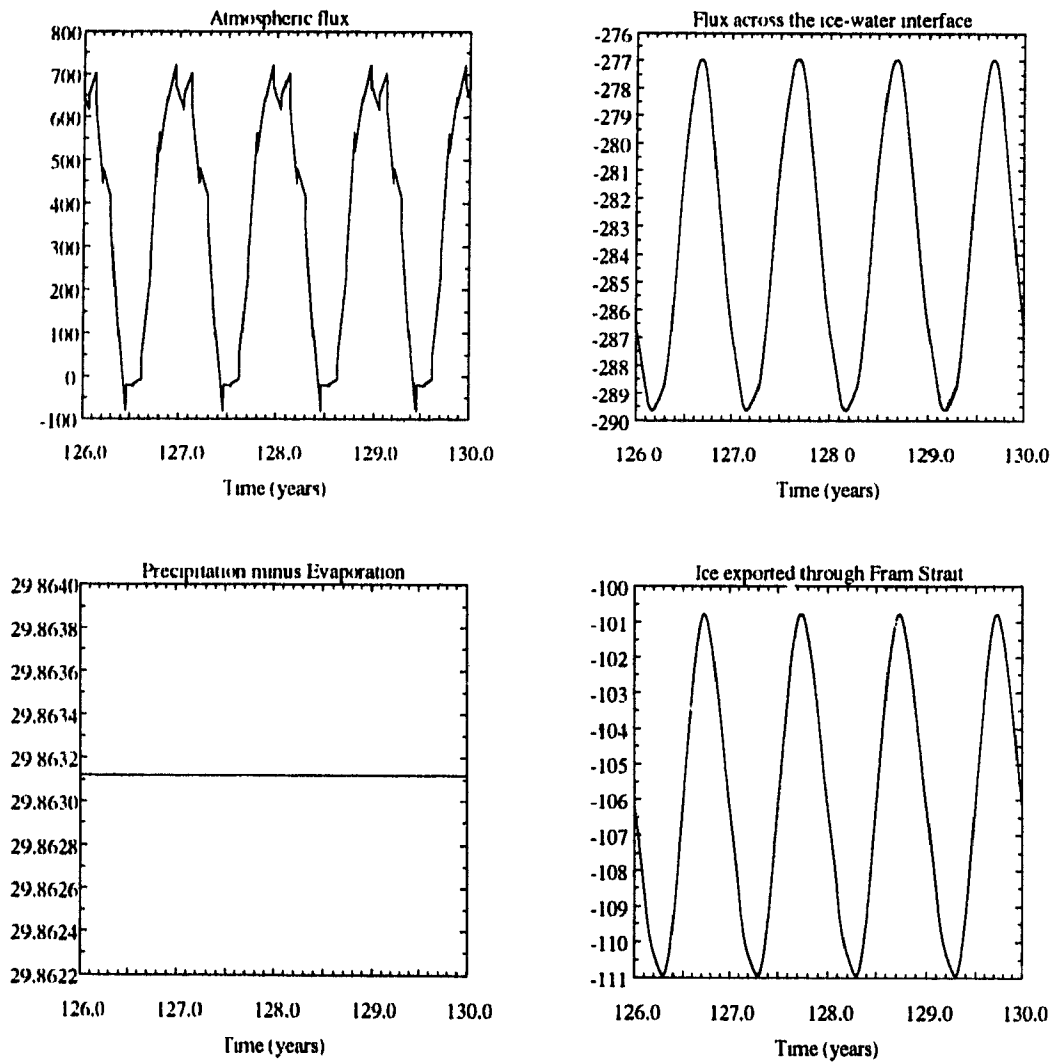


Fig. A-10. Numerical estimate of the ice thickness terms in the Arctic Ocean (State 4).

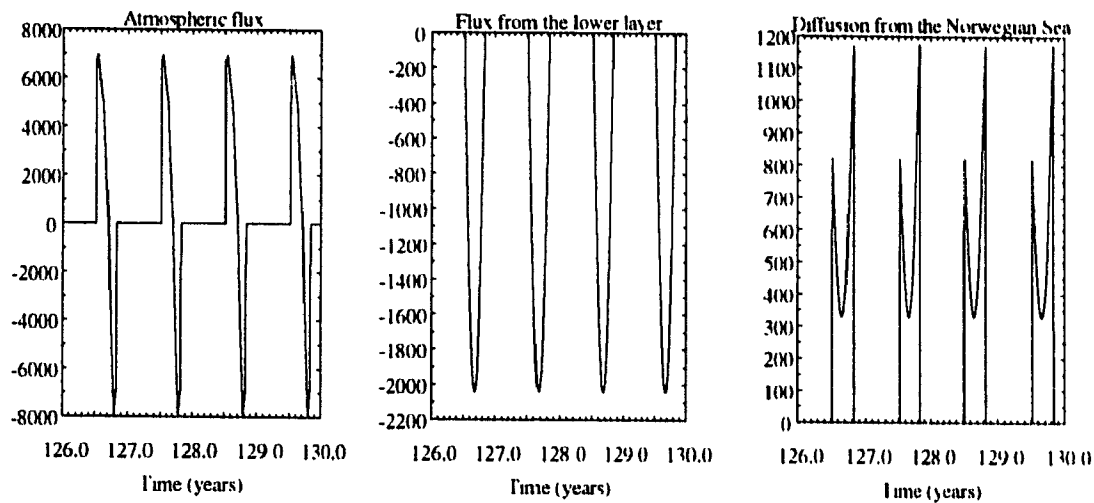


Fig. A-11. Numerical estimate of the temperature terms in the Greenland Gyre (State 2).

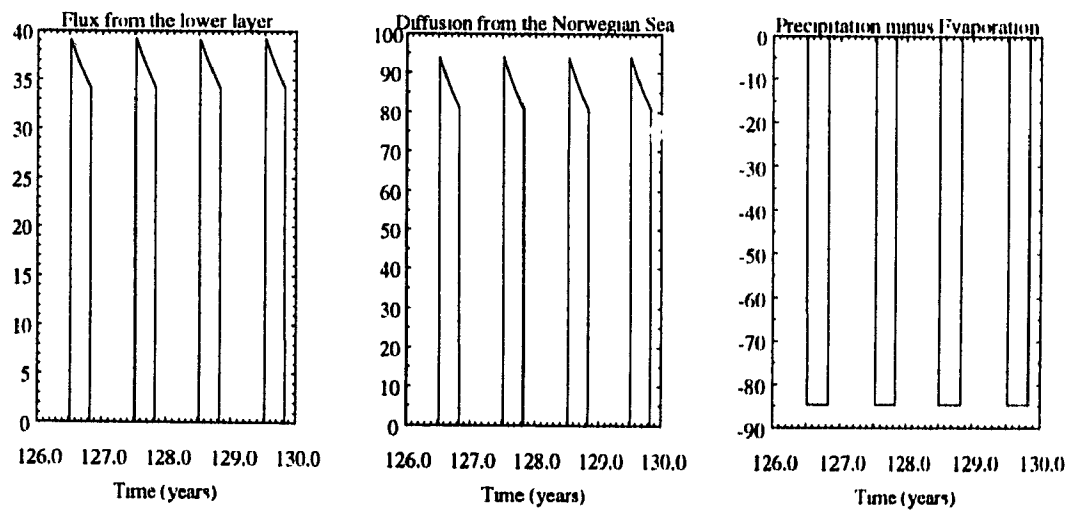


Fig. A-12. Numerical estimate of the salinity terms in the Greenland Gyre (State 2).

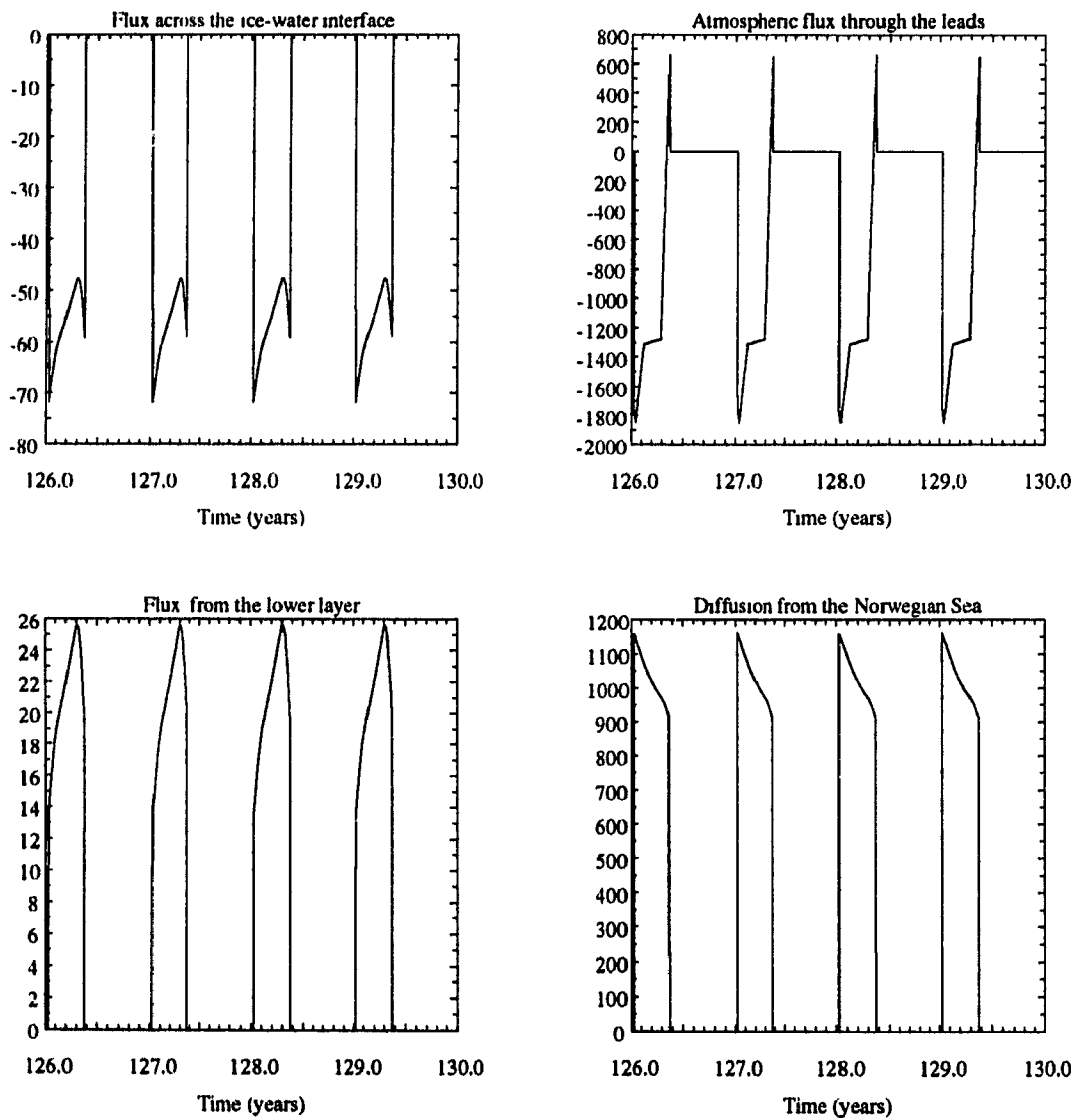


Fig. A-13. Numerical estimate of the temperature terms in the Greenland Gyre (State 3).

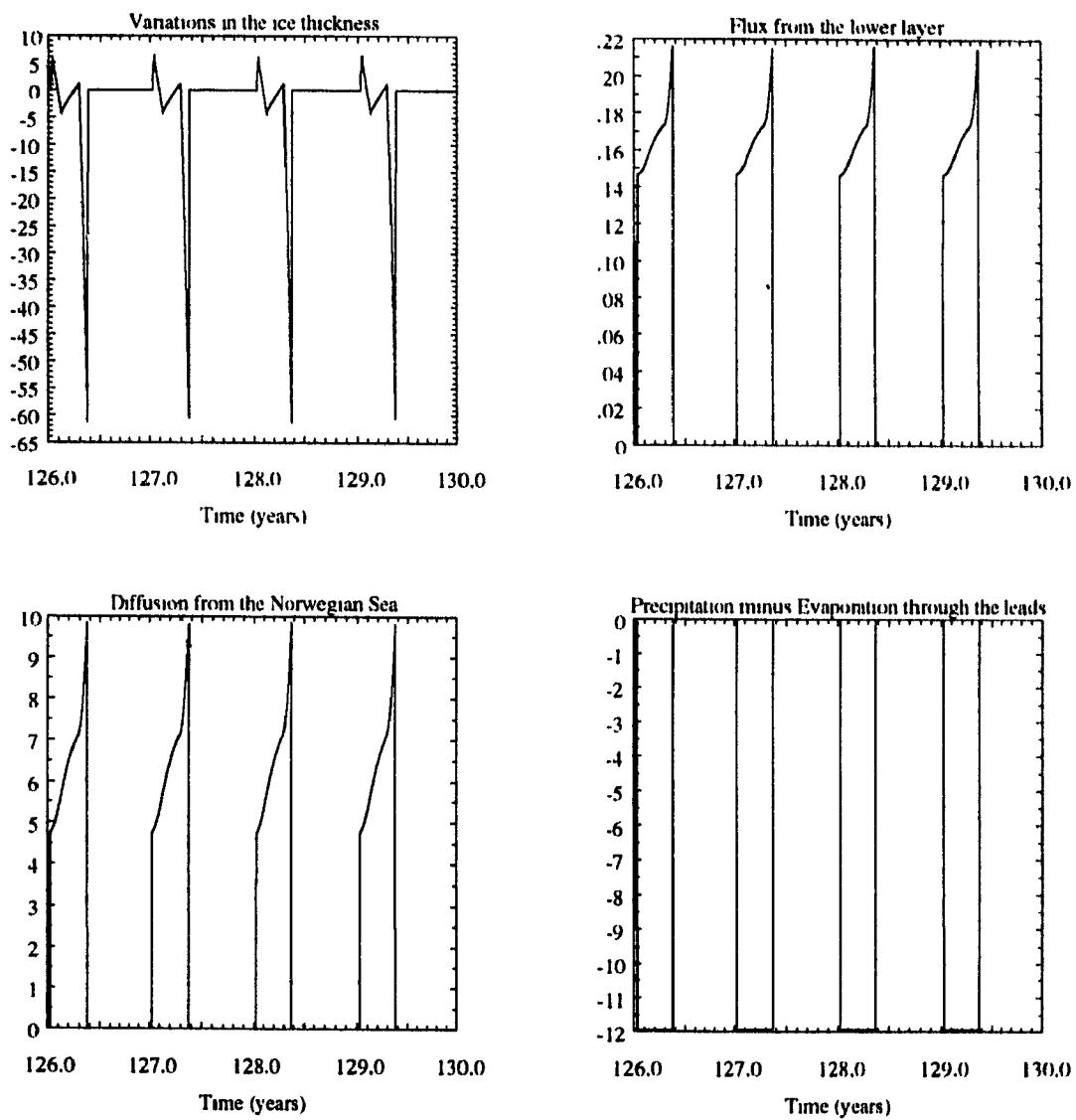


Fig. A-14. Numerical estimate of the salinity terms in the Greenland Gyre (State 3).

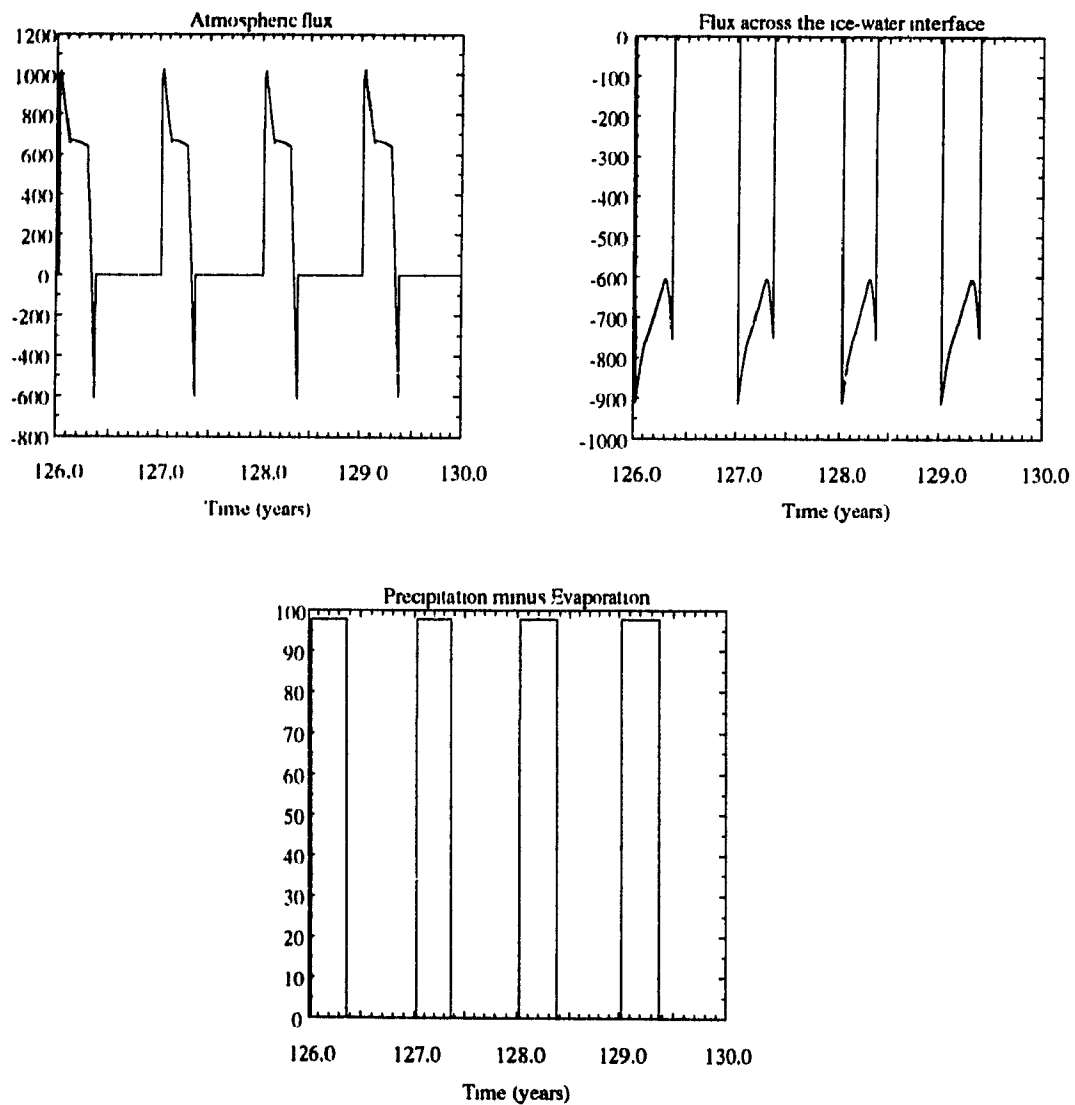


Fig. A-15. Numerical estimate of the ice thickness terms in the Greenland Gyre (State 3).

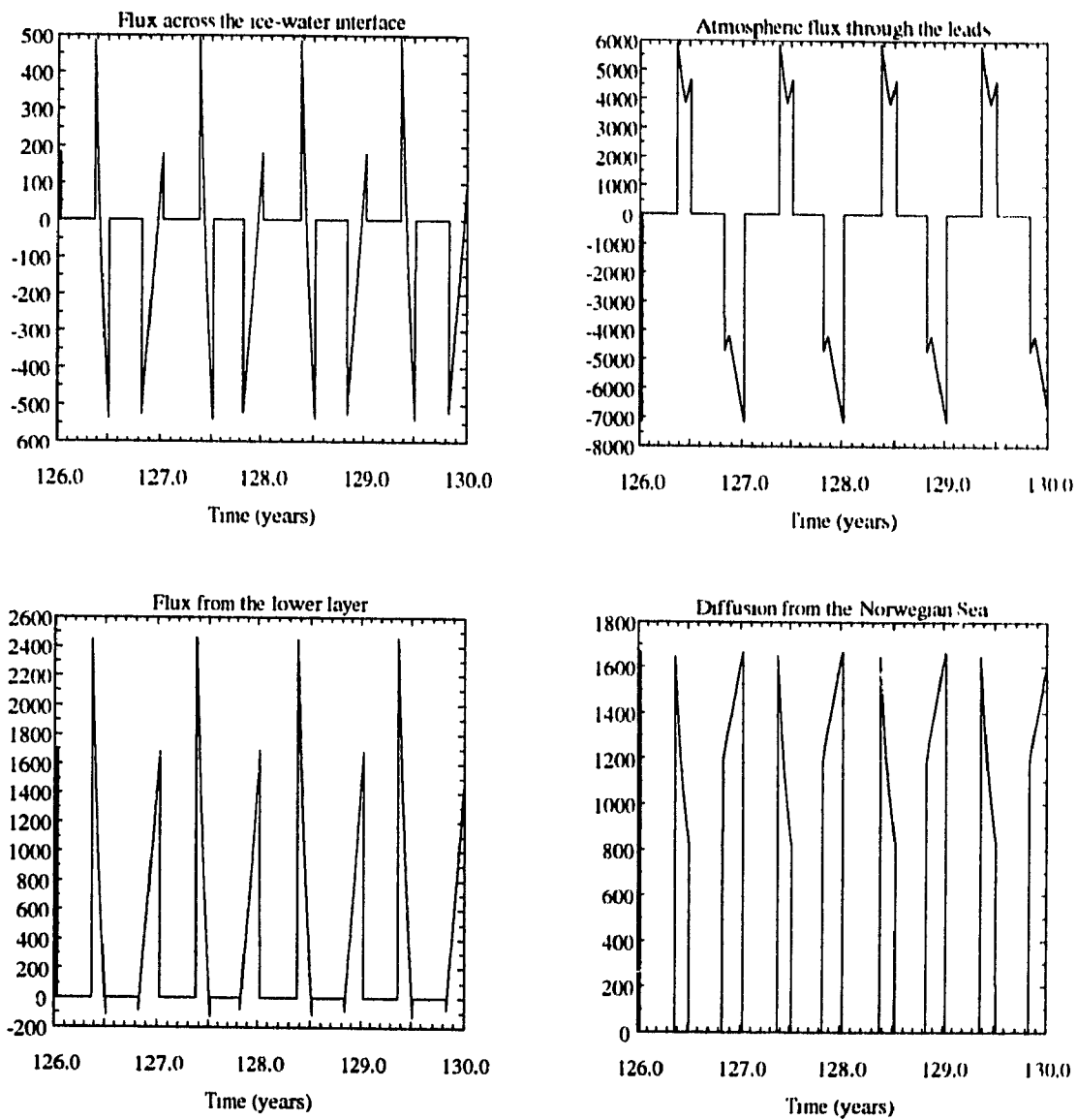


Fig. A-16. Numerical estimate of the temperature terms in the Greenland Gyre (State 4).

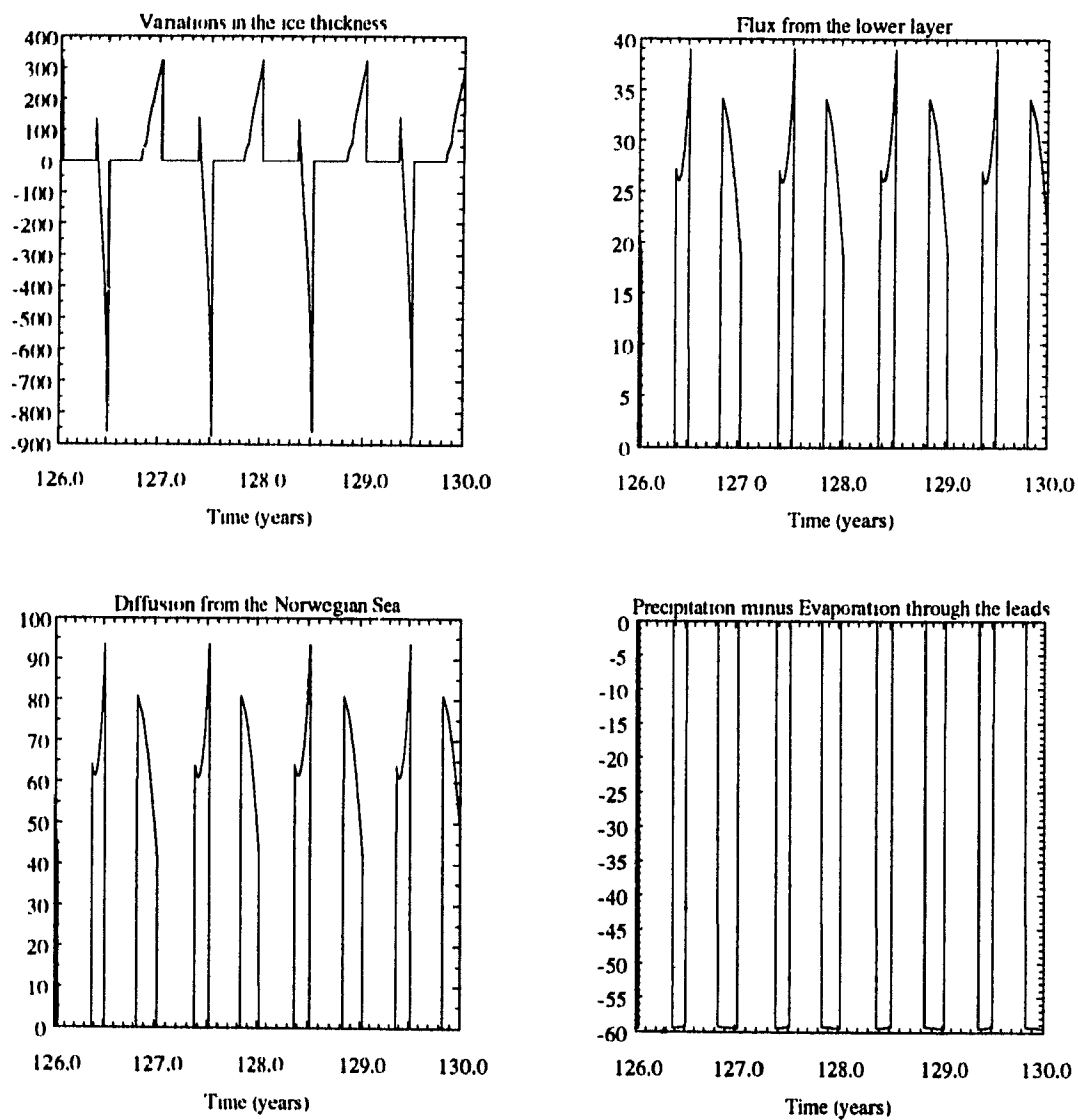


Fig. A-17. Numerical estimate of the salinity terms in the Greenland Gyre (State 4).

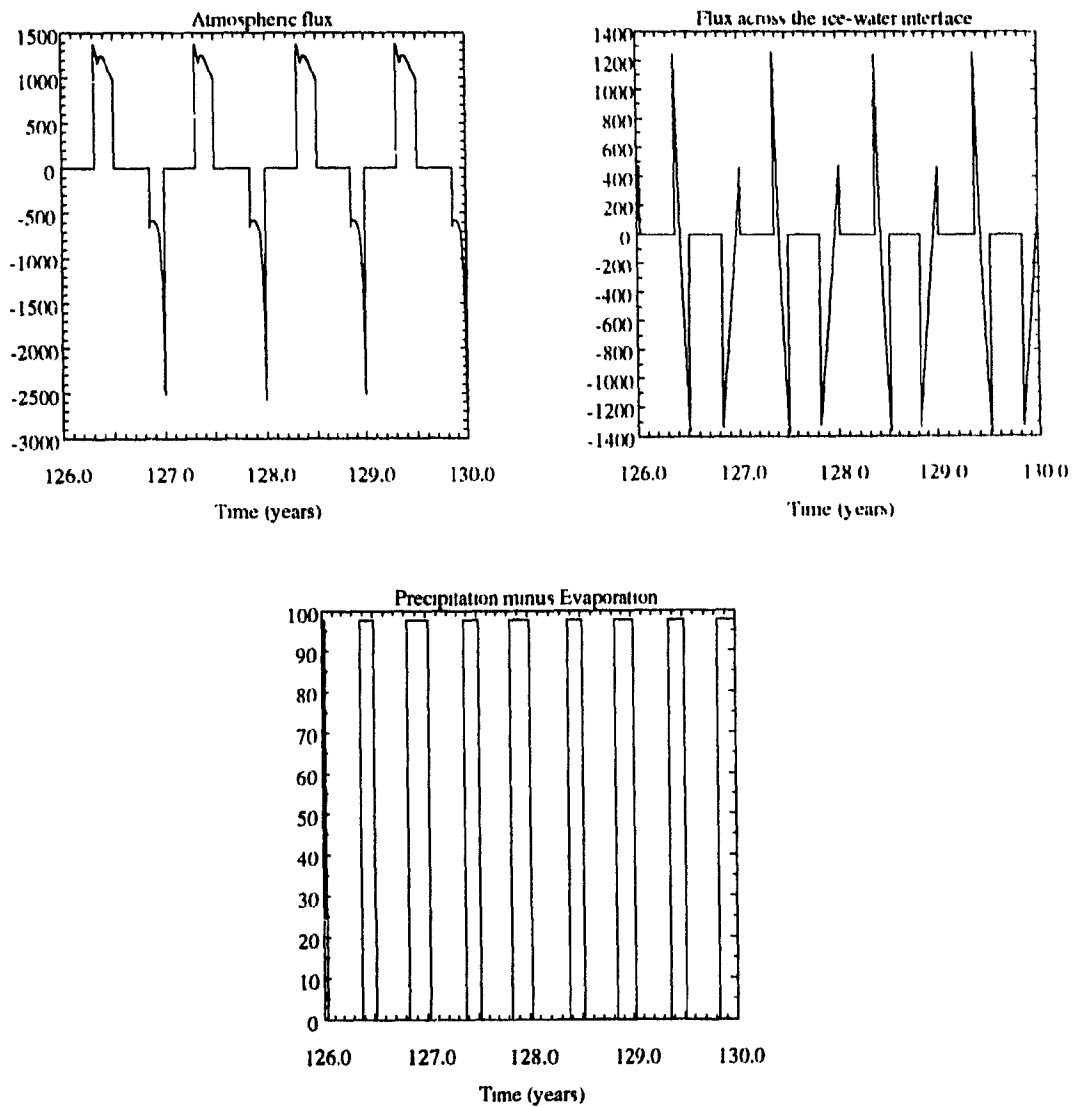


Fig. A-18. Numerical estimate of the ice thickness terms in the Greenland Gyre (State 4).

References

- Aagaard, K. and E.C. Carmack, 1989: The Role of Sea Ice and Other Fresh Water in the Arctic Circulation. *Journal of Geophysical Research*, **94**:14485-14498.
- Björk, G., 1989: A One-Dimensional Time-Dependent Model for the Vertical Stratification of the Upper Arctic Ocean. *Journal of Physical Oceanography*, **19**:52-67.
- Bourke, R.H. and R.P. Garrett, 1987: Sea Ice Thickness Distribution in the Arctic Ocean. *Cold Regions Science and Technology*, **13**:259-280.
- Carmack, E.C., 1990: Large-Scale Physical Oceanography of Polar Oceans, in Polar Oceanography, Part A: Physical Science. Academic Press, San Diego, p. 171-222.
- Carmack, E. and K. Aagaard, 1973: On the Deep Water of the Greenland Sea. *Deep-Sea Research*, **20**:687-715.
- Clarke, R.A., J.H. Swift, J.L. Reid and K.P. Koltermann, 1990: The formation of Greenland Sea Deep Water: double diffusion or deep convection? *Deep-Sea Research*, **37**:1385-1424.
- Coachman, L.K. and K. Aagaard, 1974: Physical Oceanography of Arctic and Subarctic Seas, in Marine Geology and Oceanography of the Arctic Seas. Springer-Verlag, New York, p. 1-72.
- Darby, M.S. and L.A. Mysak, 1992: A Boolean Delay Equation Model of an Interdecadal Arctic Climate Cycle. *Climate Dynamics*, in press.

Darby, M.S. and A.J. Willmott, 1993: A simple time-dependent couple ice-ocean model with application to the Greenland-Norwegian Sea. *Tellus*, in press.

Dickson, R.R., J. Meincke, S.A. Malmberg and A.J. Lee, 1988: The "Great Salinity Anomaly" in the Northern North Atlantic 1968-1982. *Progress in Oceanography*, **20**:103-151.

Holland, D.M., L.A. Mysak and J.M. Oberhuber, 1991: Simulation of the Seasonal Arctic Sea-Ice Cover with a Dynamic Thermodynamic Sea-Ice Model. Center for Climate and Global Change Research Report No. 91-17, McGill University, Montréal.

Jónsson, S., A. Foldvik and K. Aagaard, 1992: The Structure and Atmospheric Forcing of the Mesoscale Velocity Field in the Fram Strait. *Journal of Geophysical Research*, **97**:12585-12600.

Martinson, D.G., P.D. Killworth and A.L. Gordon, 1981: A Convective Model for the Weddell Polynya. *Journal of Physical Oceanography*, **11**:466-488.

McDougall, T.J., 1983: Greenland Sea Bottom Water formation: a balance between advection and double-diffusion. *Deep-Sea Research*, **30**:1109-1117.

Midttun, L., 1985: Formation of Dense Bottom Water in the Barents Sea. *Deep-Sea Research*, **32**:1233-1241.

Mysak, L.A., 1992: Decadal-Scale Variability of Ice Cover and Climate in the Arctic Ocean and Greenland Sea. To appear in proceedings (National Academy Press) of workshop on Decade-to-Century Time Scales of Natural Climate Variability, Irving, California, September 1992.

Mysak, L.A. and D.K. Manak, 1989: Arctic Sea-Ice Extent and Anomalies, 1953-1984. *Atmosphere-Ocean*, **27**:376-405.

Mysak, L.A. and S.B. Power, 1991: Greenland Sea Ice and Salinity Anomalies and Interdecadal Climate Variability. *Climatological Bulletin*, **25**:81-91.

Mysak, L.A. and S.B. Power, 1992: Sea-Ice anomalies in the western Arctic and Greenland-Iceland Sea and their relation to an interdecadal climate cycle. *Climatological Bulletin*, **26**: 147-176.

Mysak, L.A. and J. Wang, 1991: Climatic atlas of seasonal and annual Arctic sea-level pressures, SLP anomalies and sea-ice concentrations, 1953-88. Center for Climate and Global Change Research Report No. 91-14, McGill University, Montréal.

Mysak, L.A., D.K. Manak and R.F. Marsden, 1990: Sea-Ice anomalies observed in the Greenland and Labrador Seas during 1901-1984 and their relation to an interdecadal Arctic climate cycle. *Climate Dynamics*, **5**:111-133.

Press, W.H., B.P. Flannery, S.A. Teukolsky and W.T. Vetterling, 1989: Numerical Recipes: The Art of Scientific Computing (Fortran Version). Cambridge University Press, 702 pp.

R ed, L.P., 1984: A Thermodynamic Coupled Ice-Ocean Model of the Marginal Ice Zone. *Journal of Physical Oceanography*, **14**:1921-1929.

Serreze, M.C., J.A. Maslanik, R.G. Barry and T.L. Demaria, 1992: Winter Atmospheric Circulation in the Arctic Basin and Possible Relationships to the Great Salinity Anomaly in the Northern Atlantic. *Geophysical Research Letters*, **19-3**:293-296.

Shea, D.J., 1986: Climatological atlas: 1950-1979. Surface air temperature, precipitation, sea-level pressure and sea-surface temperature (45 S-90 N). NCAR Tech. Note-269+STR, Boulder, Colo.

Stigebrandt, A., 1981: A Model for the Thickness and Salinity of the Upper Layer in the Arctic Ocean and the Relationship between the Ice Thickness and Some External Parameters. *Journal of Physical Oceanography*, **11**:1407-1422.

Turner, J.S., 1973: Buoyancy Effects in Fluids. Cambridge University Press, London, 367 pp.

Welander, P., 1982: A Simple Heat-Salt Oscillator. *Dynamics of Atmospheres and Oceans*, **6**:233-242.

Welander, P. and J. Bauer, 1977: On a differentially heated saltwater-ice system. *Tellus*, **29**:462-469.

Willmott, A.J. and L.A. Mysak, 1989: A Simple Steady-State Coupled Ice-Ocean Model, with application to the Greenland-Norwegian Sea. *Journal of Physical Oceanography*, **19**:501-518.

Wood, R.G., and L.A. Mysak, 1989: A Simple Ice-Ocean Model for the Greenland Sea. *Journal of Physical Oceanography*, **19**:1865-1880.